Bates College
SCARAB

Honors Theses | Capstone Projects

Spring 5-2012

Using Sedimentary and Geochemical Proxies for Little Ice Age Climate Climate Change Reconstructions, South Mainland Shetland

Jennifer A. Lindelof
Bates College, jlindelo@bates.edu

Follow this and additional works at: http://scarab.bates.edu/honorstheses

Recommended Citation
Lindelof, Jennifer A., "Using Sedimentary and Geochemical Proxies for Little Ice Age Climate Climate Change Reconstructions, South Mainland Shetland" (2012). *Honors Theses*. 30.
http://scarab.bates.edu/honorstheses/30

This Open Access is brought to you for free and open access by the Capstone Projects at SCARAB. It has been accepted for inclusion in Honors Theses by an authorized administrator of SCARAB. For more information, please contact batesscarab@bates.edu.

Using Sedimentary and Geochemical Proxies for Little Ice Age Climate Change Reconstructions, South Mainland Shetland

An Honors Thesis

Presented to

The Faculty of the Department of Geology
Bates College

In partial fulfillment of the requirements for the
Degree of Bachelor of Science

by

Jennifer Ann Lindelof
Lewiston, Maine

March 23, 2012

Abstract

The Broo Site, located in South Mainland Shetland, is an archaeological site dated to the late 17th century that is believed to have been inhabited for a short period of time before massive sand blows completely buried the stone buildings. Previous investigations indicate deposition of thick sand layers in nearby lochs, potentially tied to Little Ice Age storminess; however the timing and mechanisms of deposition have yet to be determined. Analyses performed on eight cores from the nearby Lochs of Brow and Spiggie include bulk organic matter, stable isotope analysis, biogenic silica, grain size analysis, percent loss on ignition, magnetic susceptibility, and plutonium dating. The objectives of the study were to use sedimentary and geochemical proxies to examine changes in environmental conditions through the last few hundred years. Contiguous coarse-grained sediments were seen in the middle of most cores in the Loch of Brow. Confirmation of a minerogenic layer in the loch was identified through increases in magnetic susceptibility and sediment particle size within the unit, and visual identification. Bulk organic stable isotope analysis indicates a relatively stable carbon isotope signal with $\delta^{13}C$ values ranging between -27‰ and -30‰. Stable nitrogen isotope values increased from 1-2‰ at the bottom of the core to 5‰ at the top of the core. Elevated C/N ratios indicate a terrestrial origin of organic matter in organic layers. The proposed models of sand genesis include marine inundation, aeolian deposition, and anthropogenic activity on the landscape, in particular increased agricultural activity, in conjunction with increased storminess of the Little Ice Age.

Acknowledgements

I would first and foremost like to thank my advisors Professors Bev Johnson and Mike Retelle for their patience, unerring flexibility, and infectious love of science over the past year. Your support and enthusiasm for all of my endeavors has meant the world to me. I would also like to thank the entire Geology Department, especially Dyk Eusden, for their support and guidance. I feel like I have truly found my niche at Bates. Thank you for always saying yes and pushing me towards the finish line.

Special thanks to Professor Gerry Bigelow for providing me with the opportunity of a lifetime. Traveling to the Shetland Islands and partaking in the Shetland Islands Climate and Settlement Project was one of the most dynamic experiences I have ever had. I would like to acknowledge Amy Johnston and Will Ambrose for their support over the past year.

I would also like to thank Phil Dostie for instilling in me a "fix it" mentality. Whether in the field or lab, I know I can always count on you to help figure things out and have a good laugh. The help of Matt Duvall and Will Ash of the Bates College Imaging Center has also been an invaluable part of my Bates experience. Thank you for tolerating my presence over the years. I have definitely learned more sitting in Coram than in any classroom at Bates.

Finally, I need to acknowledge all of the geology students I have met over the course of my four years. You more than anyone have inspired a love of geology and the outdoors that I would have never dreamed possible. From the early morning van rides across New England, to the late night work sessions in Coram, I don't know how I would have made it through without you. Bridget, Colin, Ethan, Haley, Heather, Ian, Peter, and Sonshine thanks for listening to me chat my way through thesis and help maintain my sanity this year. Lastly, I would like to thank my family for providing me with the opportunity to attend Bates and supporting me in all of my crazy endeavors.

This study was made possible by the Bates College Department of Geology and funding from the National Science Foundation and the Bates College Student Research Fund.

Table of Figures

Table of Figures

Throughout this thesis the place names featured will be referred to in Scottish English. Loch is the equivalent of a lake, voe is synonymous with inlet, and burns are streams. Finally, it is important to note the difference in notation between the Old House of Broo and the Loch of Brow. For historical accuracy the house and former town will be referred to as Broo, while the loch due to its continued presence on contemporary maps will be referred to as the Loch of Brow.

Chapter 1:

Introduction

The climate of the late Holocene was particularly turbulent in the North Atlantic region. Fluctuations in temperature, ocean and air currents, and other factors associated with the Little Ice Age are said to have contributed to a period of increased storminess (Lamb, 1977, 1985, 1991; Grove, 2001; Mann et al., 2008). Great storms are well documented in the historical record and caused large-scale coastal flooding, the mobilization of sand-dunes in coastal areas, financial losses, and loss of human life (Lamb, 1991). However, despite being an era of increased storminess and variability in terms of regional climate, the area has a rich history of human occupation. First settled in the Mesolithic period, nearly 6,000 years ago, Shetland has since been occupied by a variety of different groups. Evidence for these settlements is provided through a wide assortment of well-preserved archaeological sites (Bigelow et al., 2005; McGovern, 1990).

Figure 1.1 Location map of the Shetland Islands. The red box highlights the Quendale and Dunrossness areas. Inset map shows the location of the Shetland Islands in relation to the rest of the United Kingdom. Data from USGS, 2010.

In the late seventeenth century, the Shetland Islands (Figure 1.1) experienced a number of intense storms and the coastal township of Broo was inundated by thick accumulations of sand. Several archaeological sites in the former township have been identified, including the Broo Site (Bigelow et al., 2005). In this study, the excavation site will be used in addition to sediment cores extracted from nearby lochs to develop an understanding of the mechanics of the sand blow and its relationship to the variable climate of the Little Ice Age. A multi-proxy approach using geochemical, sedimentological, and geochronological methods will allow for the paleoenvironmental reconstruction of the landscape.

1.1 Background

The Shetland Islands, located off the northeastern coast of Scotland, are a collection of islands that form the northernmost archipelago of the British Isles (Figure 1.1). Situated between 60 and 61° N latitude, Shetland sits at the same latitude as Alaska, southern Greenland, and Scandinavia, just south of the Arctic Circle. The islands sit on the boundary of the Atlantic Ocean (on the north and west coasts) and the North Sea (on the south and eastern coasts). Due to the close proximity of the ocean to any point on Shetland and warming by the North Atlantic Drift Current (NADC) and Gulf Stream, the climate is strongly affected by the ocean (Birnie et al., 1993). Hence, the climate is slightly milder than one would expect from such northerly latitude (Lamb, 1985). While there are close to 100 different islands that make up Shetland, only sixteen are inhabited today (Birnie et al., 1993). "Mainland", the largest and most southerly island, is the most populated and is the third largest island in Scotland (Johnston, 1999).

1.1.1 Bedrock Geology

Shetland bedrock consists of both old sedimentary rocks that were metamorphosed during the Caledonian Orogeny, in the early Devonian, and sedimentary and volcanic rocks that were deposited and folded during the later portion of that orogeny (Mykura, 1976). The Walls Boundary Fault, a Devonian transcurrent dextral fault, essentially divides the islands in half, creating a north-south elongation (Mykura, 1976; Flinn, 1967). East of the fault, rocks are generally metamorphic, recrystallized granites with strong north trending vertical foliations

(indicative of strain along the fault), or sedimentary members of the Colla Firth Group (Mykura, 1976). West of the fault, rocks include a mix of igneous units, part of the Northmaven Plutonic Complex, a series including granite, diorite, and gabbros, as well as Old Red Sandstone sediments.

On the southeastern tip of the Mainland, older rocks are overlain by Old Red Sandstone (ORS) sedimentary rocks. Rocks in the East Mainland Succession, estimated to be 22 to 27 m thick, are thought to comprise a complete stratigraphic sequence, with the oldest rocks in the west and youngest, the ORS, in the east. To the west of the fault, there is a much larger variety of lithologies including metamorphic bands, folded sandstones, volcanic rocks, and diorites. Included in this portion are the Lewisian gneisses, which form the Caledonian Foreland, as well as two major groups of metasedimentary rocks. This band of metasediments is found from the northern tip of the Mainland along the Walls Fault to Muckle Roe (Blackadder, 2003) and consists of an older quartzite, gneiss, muscovite schist layer, and a younger finer grained Greenschist Group (Mykura, 1976).

The Old Red Sandstone formation, a combination of clastic lithologies, is found in many parts of Shetland including southeastern Shetland and areas to the west including the island of Papa Stour. However, the Old Red Sandstone should be thought of in the context of time as much as a specific lithologic unit, as the age, tectonic development, and the degree to which the formation was altered by later igneous intrusions varies greatly (Blackadder, 2003). All localities of the sandstone overlie the metamorphic complex and it is assumed that the collection of rocks referred to as Old Red Sandstone is not a continuous sequence but the deposits of several different terrestrial basins (Mykura, 1976). The Old Red Sandstone roughly correlates to the Devonian time period, though it also deposited in the late Silurian and early Carboniferous periods.

The study area in Dunrossness lies east of the Walls Boundary Fault in a portion of the East Mainland Succession known as the Clift Hills Division. Three main lithologies dominate the area, including the Dunrossness Phyllitic Group, the Old Red Sandstone, and several igneous intrusions making up the Spiggie complex (Figure 1.2). Phyllites in the area are characterized by chlorite, muscovite, and in some areas staurolite or kyanite. According to Flinn (1967) only one

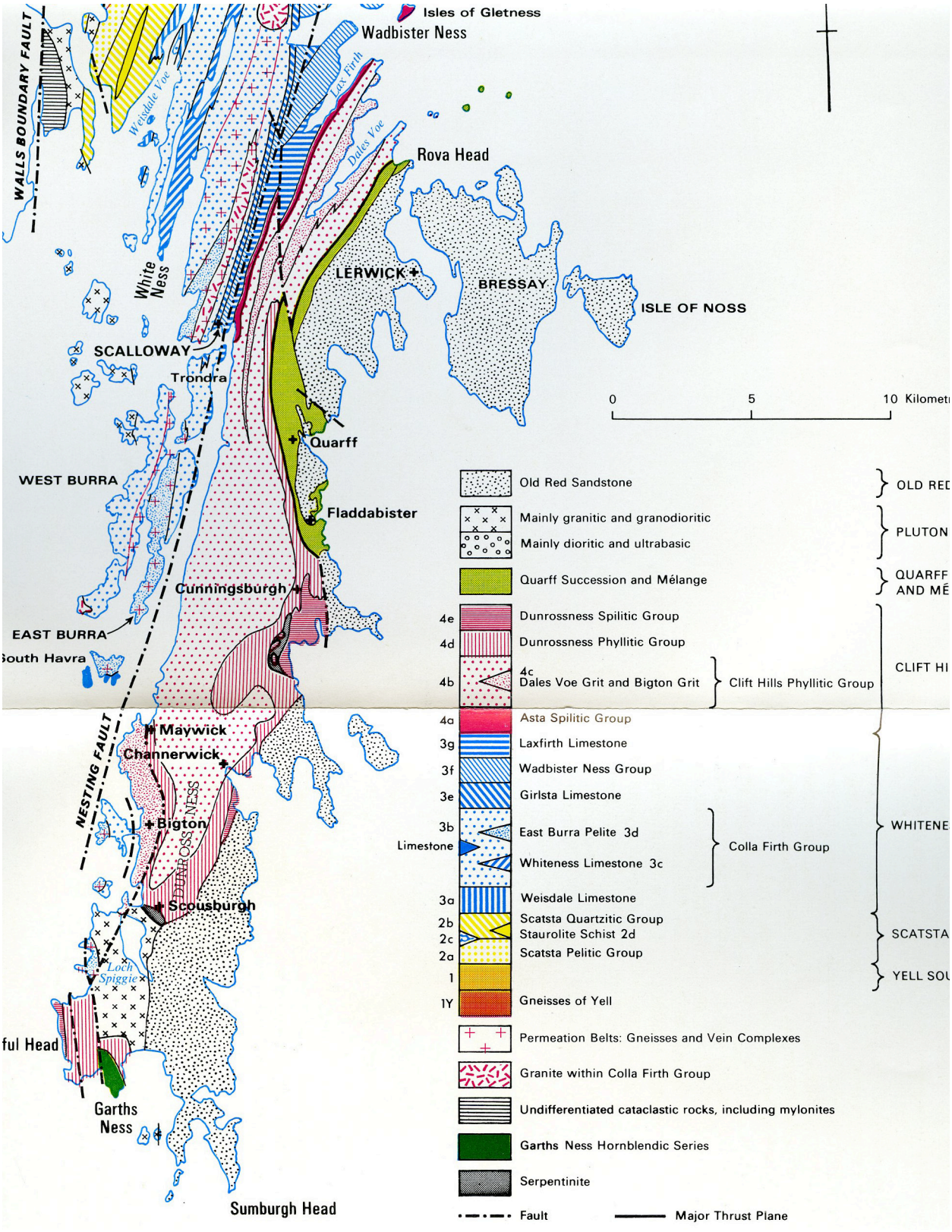

Figure 1.2. Bedrock map of the southern portion of Mainland Shetland. The study area includes three major lithologic groups and is highlighted in red (Mykura, 1976).

deformational event has affected the area. This deformation is responsible for shearing, creating either planar (s-tectonite) or linear (l-tectonite) fabrics depending on location. While there is no evidence of large scale folding in this region of Shetland, some areas show small isoclinal folds. The exception to this is a handful of open folds associated with the intrusion of the Spiggie granites, when the rocks were brittle (Mykura, 1976). The Walls Boundary Fault and the smaller parallel Nesting Fault also deformed the rocks in the study area. Displacement from these faults ranges from 60-80km (Mykura, 1976).

1.2 Quaternary in Shetland

The ice sheets of the Pleistocene and the rise in sea level that accompanied their melting, are major factors in shaping the present landscape; however there is much debate as to the origin and nature of the ice (Figure 1.3; Golledge et al., 2008). Earliest reports from Peach and Horne (1879) indicated an east to west flow, as ice from Scandinavia crossed the North Sea. Later, Hoppe (1965) suggested a local ice cap that radiated outward from its center on Mainland. Mykura (1976) then employed a hybrid of the two previous reconstructions, citing evidence for a late stage Pleistocene ice cap, which flowed radially over the landscape and evidence for local ice flow merging with the larger Scandinavian sheet. Evidence for this model includes a wide variety of inconsistently oriented striation sets. In southern Mainland, Mykura (1976) supports the idea of eastward flowing ice, with evidence of an earlier westward flow. The most recent analysis of Shetland glaciation (Golledge et al., 2008) suggests 3 discrete stages of glaciation on the

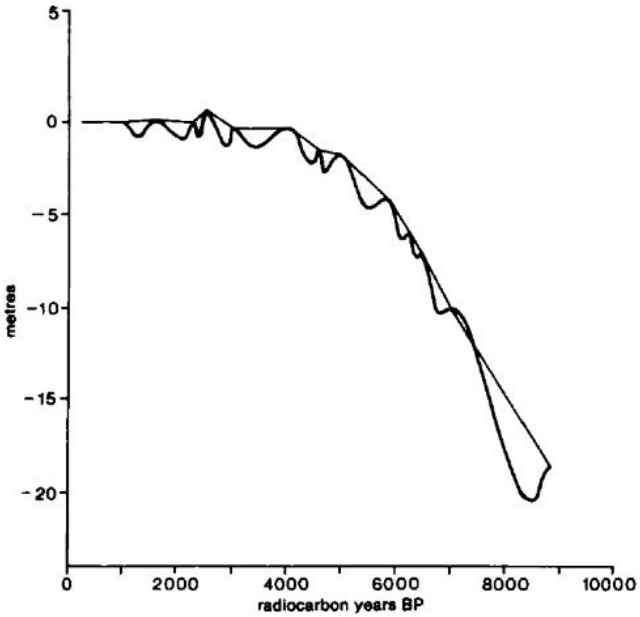

Figure 1.4 A model of the regional eustatic sea level curve for the Shetland Islands (Shennan, 1989).

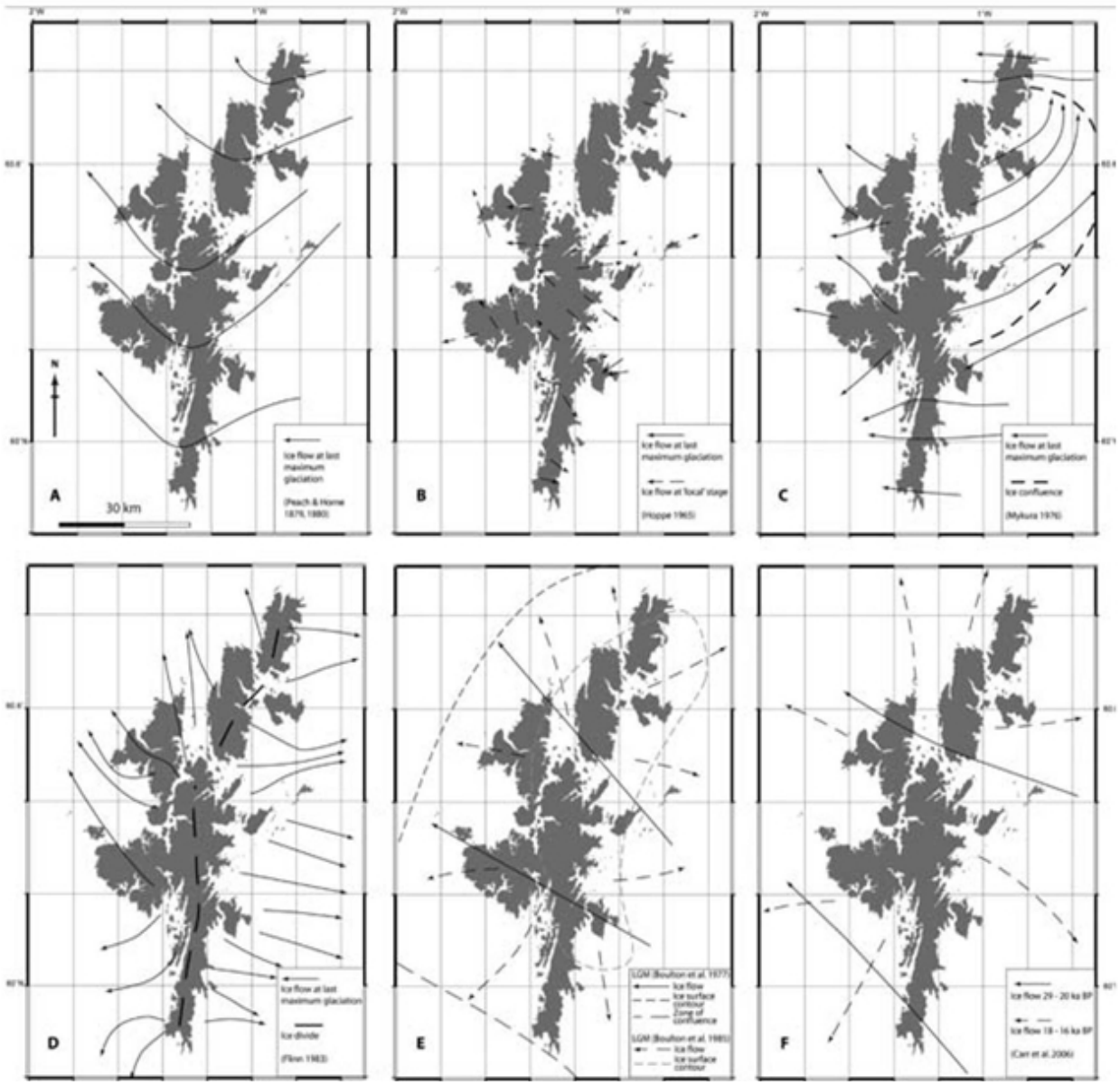

Figure 1.3 Different reconstructions of glacial ice flow over the Shetland Islands. Frame A: Peach and Horne (1879), Frame B: Hoppe (1965), Frame C: Mykura (1976), Frame D: Flinn (1983), Frame E: Boulton et al. (1977, 1985), and Frame F: Car et al., (2006). From Golledge et al. (2008).

archipelago. Evidence presented show late Devensian ice flow of the Fennoscandian ice sheet, which crosses the islands from east to west. This was followed by a more subdued second stage, featuring rounded moraines, sub-glacial streams, and ice marginal drainage features (Golledge et al., 2008). Finally, the Younger Dryas glaciation is characterized by a localized ice cap centered on Mainland.

Postglacial sea level rise in the Holocene has submerged much of the former glacial topography of Shetland. The lack of raised beaches and other marine landforms indicate that eustatic rise outpaced isostatic rebound and that sea level has risen since the decay of the last ice sheet (Figure 1.4) (Lambeck, 1993; Shennan, 1989; Mykura, 1976). Radiocarbon ages from submerged peat samples at Symbister harbor, located on the island of Whalsay just north of Lerwick, indicate that at 5,500 years BP sea level was at a minimum 9 meters below modern (Hoppe, 1965). It is due to this rise in sea level that the former U-shaped valleys of the Devensian became the elongate inlets and voes that are seen on most of Shetland's coastline (Birnie et al., 1993).

1.3 Climate of the Shetland Islands

The Shetland Islands are located at 60° N latitude and experience a wet maritime climate. Average annual rainfall approximates 1,220 mm (~48 in), the bulk of which falls between October and January (~100 mm / month) (Wheeler and Mays, 1997). Additionally, the influence of the surrounding ocean allows the Shetland Islands to experience long mild winters and short cool summers (Wheeler and Mays, 1997). In the winter months, temperatures averages close to 6°C (~42°F). Temperature values for the summer months are not much higher, with an average temperature of approximately 13.5°C (~55°C) (Wheeler and Mays, 1997). The archipelago is among the windiest regions of the British Isles; with an average of 45 days a year where winds are considered to be gale force (sustained wind speeds exceed 33 knots, i.e. 61 km/hr). Wind generally comes from the southwest. The absence of trees and tall plants on Shetland is primarily attributed to a combination of topography and windiness (Wheeler and Mays, 1997). Because of its location at 60° N latitude sunlight hours are extremely variable throughout the year (Wheeler and Mays, 1997).

Due to the close proximity of the ocean to almost all points in Shetland, ocean currents play a significant role in regulating climate (Figure 1.5). The North Atlantic Drift Current (NADC) is a shallow, warm, wind-driven surface current that covers much of the North Atlantic. It originates in the Gulf Stream and slowly travels northwest of Shetland (Rossby, 1996). Due

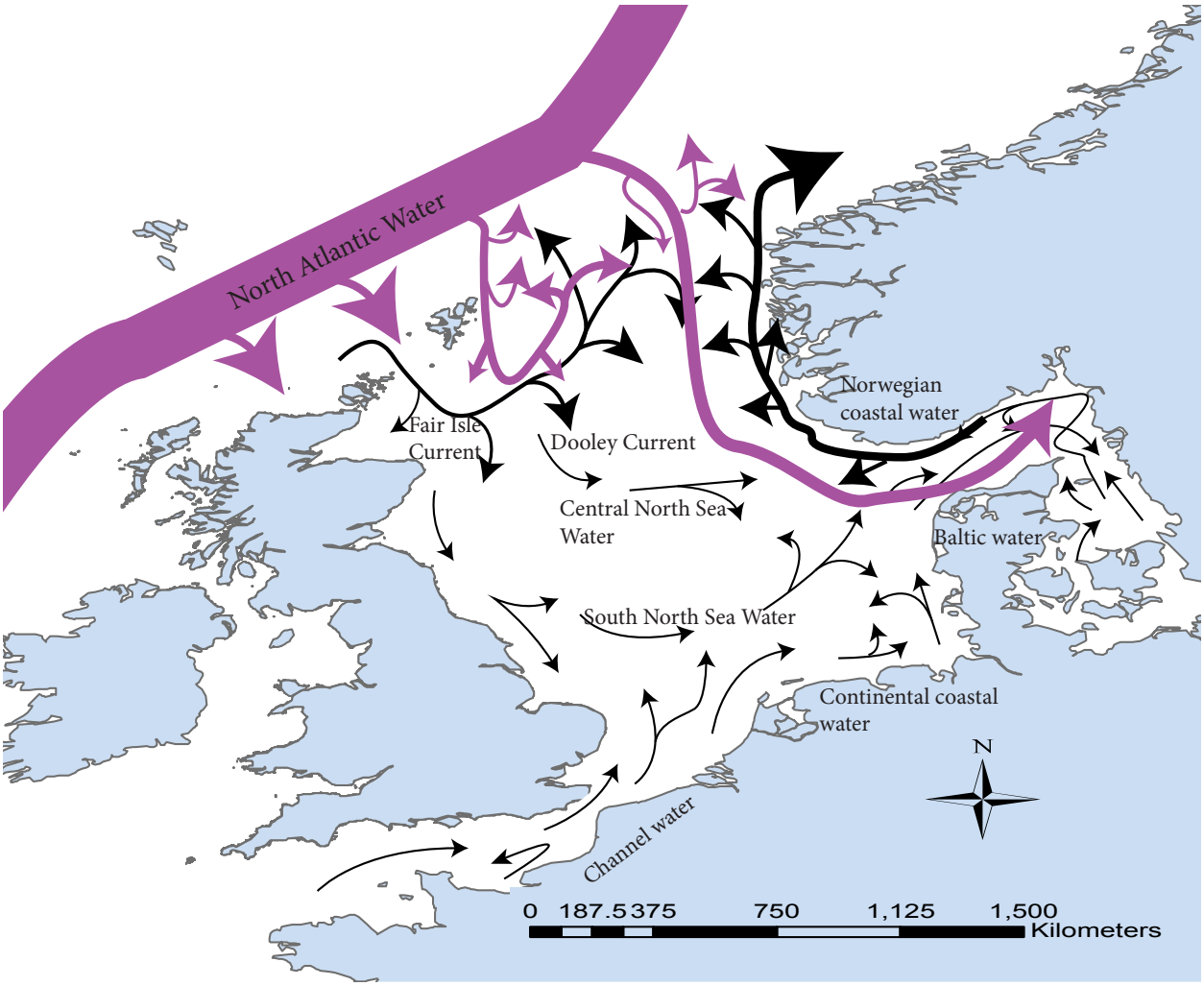

Figure 1.5 Circulation patterns of ocean currents in the northern North Atlantic. Purple arrows indicate water of Atlantic origin, while black arrows indicate locally sourced water. The width of arrows is reflective of the quantity of water transported via the current.

to its supply of warm surface water, the NADC has been shown to be the primary forcing in moderating climates of Western Europe and the United Kingdom (Little et al., 1997). The NADC is not a new phenomenon, modeling based on diatom records show that the current was probably first established 13,400 years BP (Little et al., 1997). The waters near Shetland also serve as a mixing zone for colder Arctic currents including the East Greenland Current and the Subpolar Front.

In addition to water currents, air circulation patterns including the North Atlantic Oscillation (NAO), contribute significantly to weather patterns observed in the islands (Figure 1.6; Hurrell, 1995). The NAO is a cyclical fluctuation of atmospheric pressure zones in the North Atlantic due to shifts in the Azores high and Iceland low. High pressure cells, from sub-tropical latitudes, and low-pressure cells, from the Icelandic low, balance from year to year creating different weather patterns. When the NAO is in its positive mode, the high-pressure cell from the sub-tropics migrates further north dominating over the low-pressure cells from the polar areas. In years when the NAO is in its positive mode (Figure 1.6) the climate of the British Isles is milder than usual. By the same token, when the NAO is in negative mode, both pressure cells are relatively weak and cold fronts from the north leave Britain with a colder winter (Hurrell, 1995).

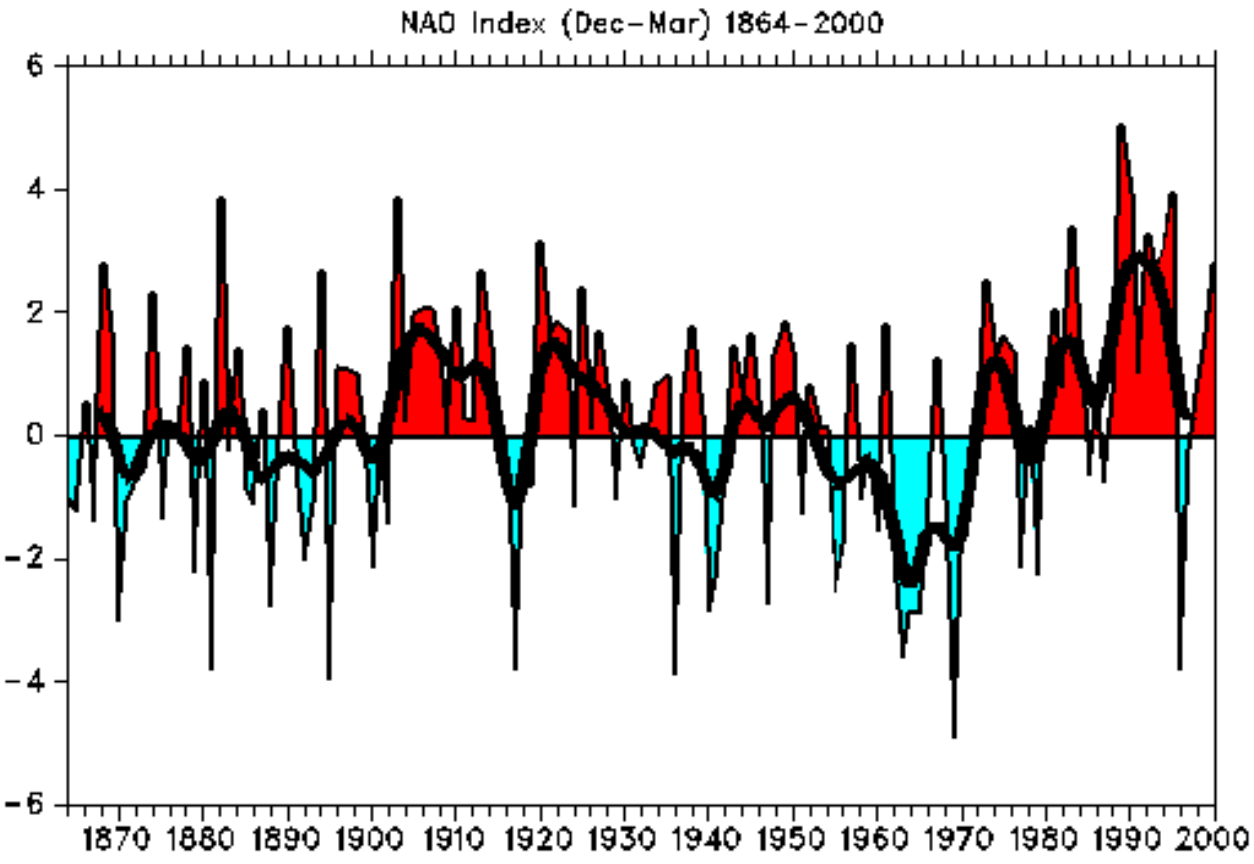

Figure 1.6 Hurrell (1995) shows an averaged December through March value of the NAO index. Bars illustrated in red highlight the NAO in its positive phase, while the blue illustrates its negative phase. Figure from updates to Hurrell (1995).

1.4 The Little Ice Age

The Little Ice Age is a period when temperatures and weather conditions in Europe were cooler than usual (Mann et al., 2008; Grove, 2001; Lamb, 1985). Generally attributed to the time period between 1300 and 1850 AD, the Little Ice Age (LIA) is well documented in historical records, through mention of failed crops, general decreases in temperature, and increased presence of sea ice in the North Sea, as well as an increase in storminess (Lamb, 1977; Lamb, 1985; Grove, 2001; Grove, 1988). In addition to the historical record, scientific evidence for the LIA is seen in lacustrine varve thickness, ice cores (Fischer et al., 1999), sclerochronology (Schone et al., 2005), and dendrochronology (Beltrami et al., 1995). The LIA was a period when temperatures weren't consistently colder, but fluctuated fairly rapidly. Europe experienced severe droughts, excessive heat, unusually cold winters, and heavy rains every few years (Fagan, 2000).

The effects of the Little Ice Age were felt across much of Europe, yet no singular cause for the cooling period has been identified. One theory on the cause of the Little Ice Age is that a decrease in radiation from the Holocene Climatic Optimum in conjunction with a variety of other forcings including increased volcanic activity (Schindel et al., 2003; Crowley, 2000; Fagan, 2000; Robock, 2000), long term changes in solar forcing (Schindel et al., 2003), and Milankovich orbital cycles (Campbell et al., 1998) led to a period of decreased temperatures between about 1600 and 1850. Kaufman et al. (2009) discuss long term drivers of climate change in the Arctic through a multi-proxy analysis and find that a millennial-scale cooling trend is consistent with evidence showing that peak summer temperatures reached their maximum during the first half of the current interglacial period, and then cooled into neoglaciation. Rather than a consistent 1900 year cooling trend (Mann et al., 2008), temperature trends in the Arctic show variability on a centennial scale (Kaufman, 2009). Kaufman et al. (2009) state that, "the timing of the Holocene thermal maximum (HTM) transgressed from west to east across the North American Arctic, but generally peaked around 7500 years ago, suggesting a post-HTM cooling rate between -0.11°C and -0.32°C per 1000 years"(pg.1237). Volcanic eruptions may have also played a part, though the influence of volcanic activity is dependent on the year (Schindel et al, 2003). The eruption

of Mt. Tambora in 1815 and the resulting release of sulfate aerosols into the stratosphere, for example, was described as one of the main contributors to the "year without a summer" (Fagan, 2000; Crowley, 2000). In addition, eruption events were shown to lead to freshening and vertical stratification of the North Atlantic subpolar gyre, reducing ocean convection and consequently reducing basal sea-ice melt (Zhong et al., 2011). Furthermore, Miller et al. (2012) show through simulations that in addition to long-term orbital forcing, repeated explosive volcanism may have led to the expansion of sea ice during the LIA. Finally, the Maunder minimum, a period of decreased sunspots, occurred between 1645 and 1715 and could have contributed to lower than average temperatures (Eddy, 1976).

Another one of the major theories is that the Little Ice Age is the result of a thermohaline circulation system shutdown and is proposed by Prof. Wallace Broecker (1985, 1989, 1997, and 1999). Broecker et al. (1985) describes an increase in the amount of freshwater in the North Atlantic, resulting in the slowing of the Meridional Overturning Circulation (i.e. thermohaline conveyor belt) and/or shift the location of sinking leading to an increase in sea ice growth. In addition, strong feedback loops in the North Atlantic contribute to rapid changes in climate. These are tied to changes to Dansgaard-Oeschger events, millennial changes in climate that begin and end abruptly. In particular, a connection is made to the most recent Dansgaard-Oeschger oscillation to warming in the Allerod, followed by cooling into the Younger Dryas, and finally warming during the Holocene (Broecker et al., 1985).

The North Atlantic Oscillation, which in its negative stage has been associated with increased sea ice cover, could have also potentially played a role (Grove, 1988). In addition, Nesje and Dahl (2002) write that increased winter precipitation associated with the positive phase of the NAO could contribute to fluctuations in climate. Reichert et al. (2001) suggest that low summer temperatures alone cannot explain the rapid advance of glaciers during this period. Data from Scandinavian glaciers show that precipitation is the dominant factor over temperature, in the relationship between increased mass balance of glaciers and the NAO index (Reichert et al., 2001).

While the specific causes of the LIA are unclear, it is clear that this period was one with great storms. Intense winter storms and gales are recorded in naval logs and weather reports (Lamb, 1991). Forced closure of shipping lanes, coastal flooding, and reports of wrecked ships and loss of property help to pin down December to March as the period with the most intense storms (Lamb, 1991). Lamb (1985) identifies the potential of these storms to create intense winds and thus potentially destabilize coastal dunes creating large sand blows.

1.5 Storms of the Little Ice Age

Large storms generated during the Little Ice Age, instigated by shifts in the NADC, as well as the NAO, were recorded as early as 1316 (Lamb, 1991). In particular, severe storms were noted in coastal communities by their propensity to cause sand-dune movement and disruptions to stable landscapes (Lamb, 1991). In 1413, the medieval township of Forvie, located in northeastern Scotland near Aberdeen, was completely buried by sand dunes, which now exceed 30 meters in height. While multiple storm events have occurred since the initial 1413 storm, destabilizing the landscape even further, in the storm of 1413, sand dunes advanced between 50 and 250 meters (Lamb, 1991). Destabilization of the landscape in the wake of a storm is triggered by the result of vegetation death, burial, wash over, and sometimes is the result of a combination of these factors. Ritchie (2000) also documents sand blows in other nearby regions, including Denmark, the Faeroe Islands, and other parts of the Shetland Islands. Stories of the abandonment of villages, the narrowing and destruction of harbors, and the general destruction of fertile land are fairly commonplace during the late 17th c. In addition to the mobilization of sand, some storms generated large-scale flooding that contributed to financial losses and loss of human life. For example, in the case of the Christmas Day flood of 1717, the North Sea rose along the German coast killing 11,000 people (Lamb, 1991).

1.6 The Storegga Landslide and associated tsunamis

The Storegga landslide, one of the largest submarine slides known in the world, occurred off the coast of Norway approximately 8,100 calendar years ago and is responsible for the generation of a large tsunami that inundated many countries bordering the North/Norwegian Sea (Bondevik et al., 2005b). Evidence for the tsunami is abundant and characteristic sand deposits are observed interbedded within peat units in several adjacent land areas including the Shetland Islands, western Norway, the Faeroe Islands, and northern Scotland (Dawson and Smith, 2000). Approximately 3,500 km^3 of material slid from the shelf break in the area referred to as the Storegga Slide depression or North Sea Fan, generating a huge tsunami in the north Atlantic approximately 7,300 ^{14}C years or 8,150 calendar years (Haflidason et al., 2005; Bondevik et al., 2003). There are several hypotheses concerning the triggering mechanism for the slide, among them are the effect of gravity on unstable sediments and the release of methane gas from biogenic activity (Bugge et al., 1988). However, most scholars believe that sliding is likely due to seismic activity in the region (Bondevik et al., 1997; Bugge et al., 1988; Haflidason et al., 2005). Evidence for waves as high as 20 meters above the sea level of the time exists in Shetland, as tsunami waves eroded surficial peat and deposited a wide spread sand layer that is identified in the stratigraphy (Figure 1.7; Bondevik et al., 2003).

The tsunami also inundated fresh water lakes where the record is best preserved by the presence of marine diatoms, fossils, gyttja, and disturbed bedding within the lake's stratigraphy (Bondevik et al., 2005a). There is additional evidence of two later tsunamis, also generated from submarine slides in the Storegga area, including the Garth tsunami which occurred 5500 cal yr BP (~4800 yr ^{14}C yr BP) and the youngest Dury Voe event, which occurred about 1500 years old (Bondevik et al., 2005b). While there is abundant evidence for this tsunami throughout the Shetland Islands it is unlikely that it occurs in the stratigraphy of the Loch of Brow or the Loch of Spiggie, as tsunami deposits are generally seen at greater depths in the sediment record (seen at ~900 cm in the northern area of the Mainland, as per Bondevik et al., 2005a) than recovered in the surface cores from the two study lochs.

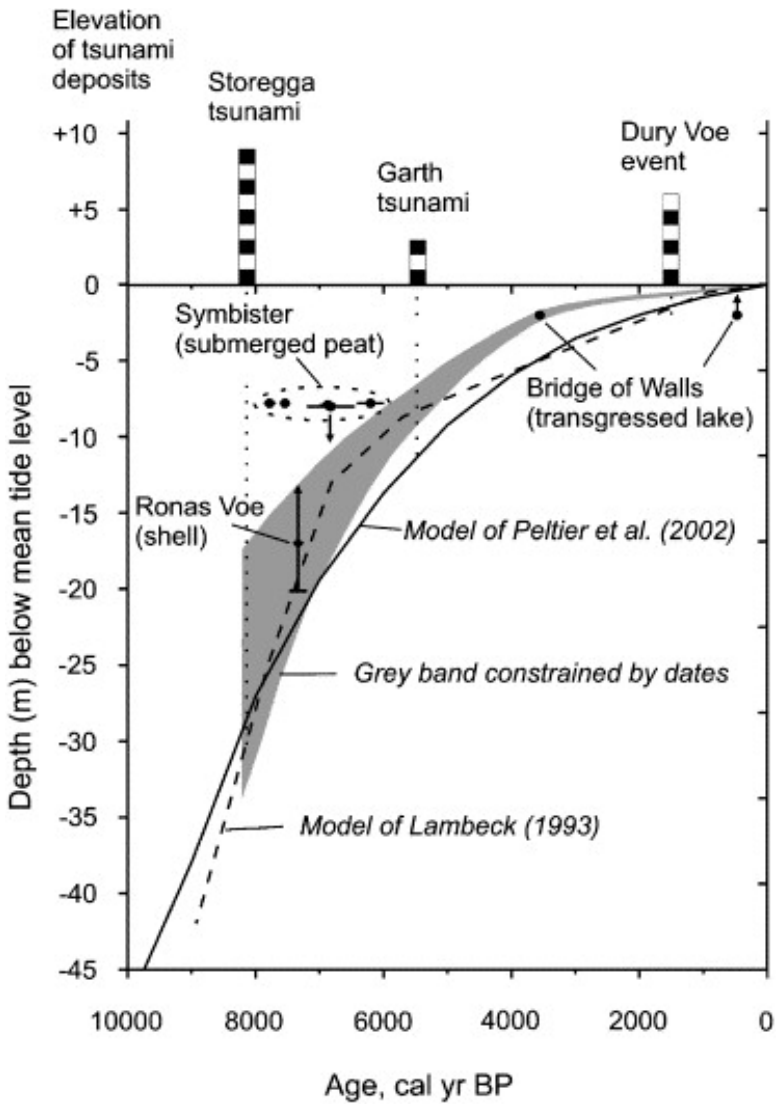

Figure 1.7 Illustration of the height of runup associated with various tsunamis on Shetland between 8000 and 1500 calendar years BP from Bondevik et al. (2005b). Sea level estimates constrained by 14C dating, seen in the grey wedge are drawn from Lambeck (1993) and Peltier et al. (2002).

Tsunami run-up is strongly influenced by topography and bathymetry and is highly localized (Dawson and Smith, 2000). Physical evidence of an historic tsunami is also influenced by the availability of a sediment source (Bondevik et al., 2005b). While in some cases the lack of available sediment leaves a minor record onshore, in the case of Shetland there is ample evidence that the wave reached heights between 20 and 25 meters above the sea level at the time (Bondevik et al., 2005a). The characteristic layer of sand associated with the Storegga tsunami was found in 4 lakes in northeastern Shetland, as well as a 1-5 cm thick wide spread sand layer resting on top of

30-40 cm of peat on land (Bondevik et al., 2005b). This layer, continuously traced for 150 meters, shows characteristic properties of a tsunami, specifically the fact that there is a decrease in the bed layer thickness and a decrease in grain size inland (Bondevik et al., 2003). These proximal/distal portions of the wave allow for a rough approximation of the extent of the waves. Additionally, the elevation of sand beds in conjunction (9.2 meters above present high tide mark) with estimates of sea level indicates that the height of the tsunami waves must have reached a minimum of 20-25 meters. This value is a minimum number due to the fact that all of the measurements are recorded relative to high tide. The addition of low tide would increase the range of values by approximately 2-3 meters (Lambeck, 1993; Bondevik et al., 2005a).

1.7 Archaeology

Humans have lived in the Shetland Islands since the Mesolithic time, as determined from the discovery of a shell midden on the southern tip of the Mainland that dates to over 6,000 years ago (Bigelow, 2005). While limited information is available on the earliest arrivals, there is much more evidence of Neolithic settlement by farmers and herders between 4,000-5,000 years ago (Bigelow et al., 2005). Shetland has a very high density of known archaeological sites, many of which are close to the study location including Jarlshof, Old Scatness, and the Broch of Mousa. Jarlshof was initially settled by Bronze Age settlers 4,500 years BP, but contains relics from the Iron Age, Pictish period, as well as from the Norwegian immigrants who arrived 1,200 years ago and Scottish immigrants who arrived in the late medieval period (Bigelow, 2005). However despite the multitude of established archaeological sites, Shetland is relatively unexplored in comparison to other localities in the North Atlantic (Bigelow et al., 2005).

The Shetland Islands Climate and Settlement Project

The Broo Site, located in South Mainland Shetland, was selected as the excavation site for the Shetland Islands Climate and Settlement Project (SICSP), which aims to study the settlement history of coastal sand environments to evaluate how settlers adapted to shifts in climate and land use. One of the focal sites for the SICSP is the Broo site. Located adjacent to Quendale Links, Dunrossness (Figure 1.8), it was selected because of its coastal location and it is well

documented that sand blows buried the historic Broo Township in the late 17th century (Bigelow et al., 2005). It is known that the sand blows were both abrupt and that the value of the township's land was quickly degraded from highly profitable to near worthless over the course of a few years. Rev. George Low, a minister from Orkney who visited the island in 1774 writes of the Broo estate stating, " it is now a mere wilderness, occasioned by the blowing of a small dusty kind of sand which never possibly can rest… this spot is an Arabian desert in miniature" (Bigelow et al., 2005).

Figure 1.8 This structure is known as Site 2. This portion of the house was the area was the last to be abandoned, with residents living in the back portion before moving to higher ground. Aerial photo courtesy of Prof. Gerry Bigelow.

The Broo Site, consisting of two excavation sites, is one of potentially many structures in the area covered by the sand blows. Excavations of the site, now located beneath a sheep pasture, began in 1997 by Professor Gerald Bigelow and team. The building currently being excavated is Site 2 (Figure 1.8). This building, once owned by the Sinclair family in the 1600s, appears to be a farm building that was occupied once the sand blows intensified. The patterns of deposition (i.e. sedimentary structures) on the exterior walls of this structure indicate that sand was deposited very quickly, as cross bedding is seen in the stratigraphy. The structure was initially larger, but an interior wall was erected during the height of the sand blows strengthening the structure. In addition to creating this structural wall, the residents of the Broo House apparently needed to dig themselves out of the sand on a regular basis. This is deduced from ground penetrating radar, which shows that the pathways the occupants were traversing were located higher than the depth of the sub-floor. It is unclear however, how long the residents lived like this and how long it took for them to abandon the site. Currently the structure resides beneath two meters of sand (Bigelow, 2011, personal communication).

1.8 Study Area and Previous Works

This study is focused in the southern part of Mainland known as the Quendale and Dunrossness area (Figure 1.1). This area, which contains the historic township of Broo, also contains two lochs that will be the primary focus for this investigation. The Loch of Spiggie, and the Loch of Brow are located approximately 1 km north of the excavation site. The Loch of Brow is a smaller and shallower loch than the Loch of Spiggie with an average depth of roughly 1.5 meters, compared to the deep hole at Spiggie, which is 12 meters (Figure 1.9; George and Maitland, 1984). Spiggie Loch is an interesting loch to study because it is recorded that what is now a loch used to be a voe, that was subsequently impounded by blown sand. The exact age of the closure of this former marine inlet is not known though there is evidence that it was open in the time of the Hanseatic League, roughly 1300 A.D. (Bigelow, 2011, personal communication).

Analysis of the Broo site began in 1997 and is currently ongoing. Previous studies of the site include a wide spectrum of archaeological, biological, and geologic analyses, aiming to understand how climate affected settlement patterns in Shetland. Anderson (1998) conducted preliminary research linking the sand environments of the Quendale region to storminess during the Little Ice Age. Mazur (2006) conducted a sedimentological study of the sands surrounding the site and worked with sediment cores from the Loch of Brow to confirm the presence of a minerogenic layer in the stratigraphy. Mazur's work in particular, served as a framework for this investigation as it provided background information on the Loch of Brow, which was cored and analyzed. Mazur's work with geochemical and sedimentary proxies tied the sand blows of the Broo Site to the sand unit within the Loch of Brow. This study was also able to identify a terrestrial source of organic matter in the Loch of Brow. While much has been uncovered about the nature of the sand movement , the timing and mechanisms for the deposition of sand are not yet well understood.

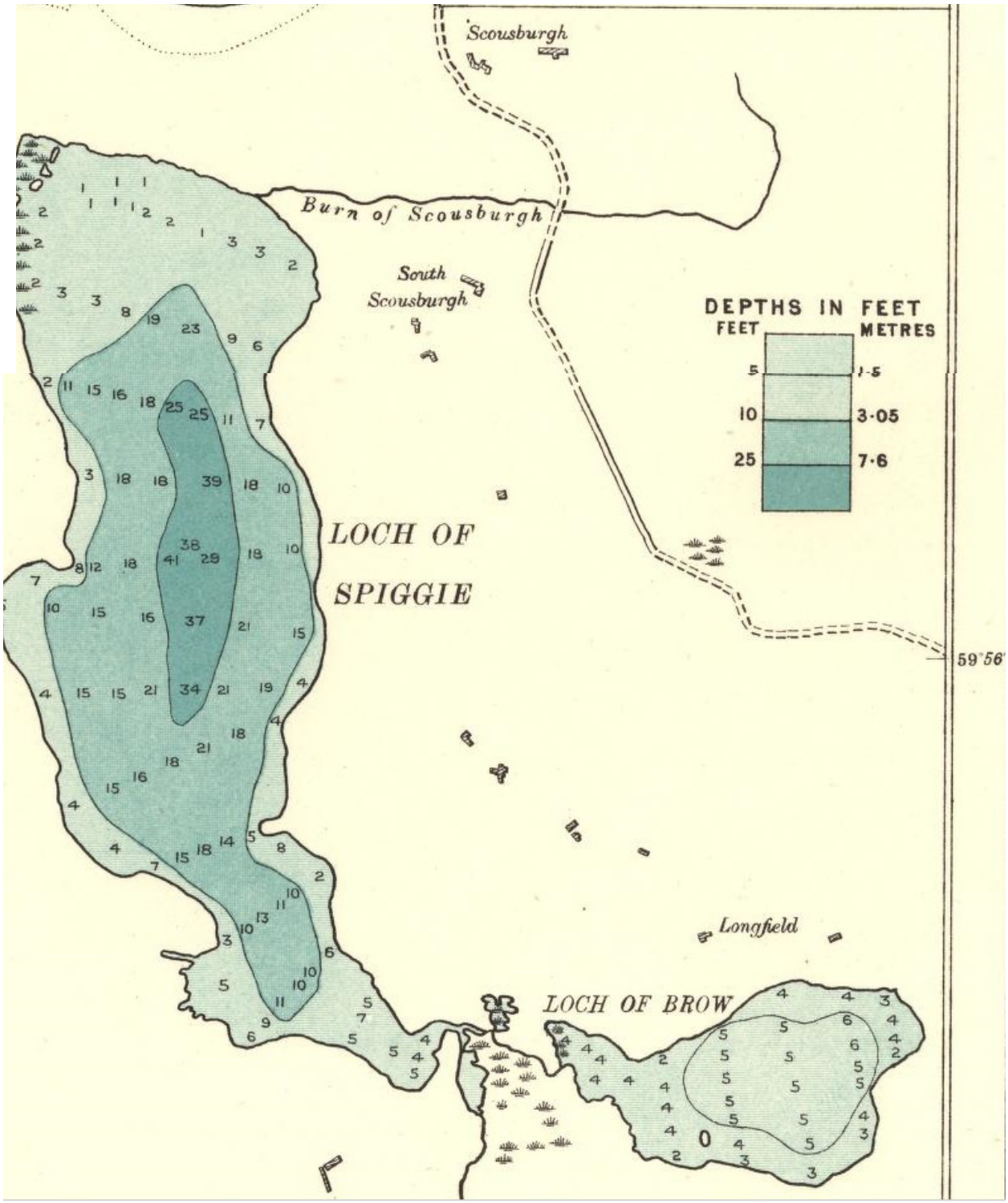

Figure 1.9 Bathymetric map of the Lochs of Spiggie and Brow. Units visible on the map are in feet. From Johnston et al. (1903).

1.9 Scope and Objectives

The Broo Site is believed to have been inhabited for a short period of time before massive sand blows completely buried the stone buildings in the late 17th century. It is currently hypothesized that the massive sand blows are connected to shifts in the oceanic climate that Shetland experiences, in particular climatic variability associated with the Little Ice Age (Lamb and Woodruffe, 1970). However, overgrazing of the landscape and increased agricultural activity have also likely contributed to the mobilization of sand. Previous investigations indicate deposition of thick sand layers sandwiched between organic sediments in nearby lochs, but the timing and mechanisms of deposition have yet to be determined. It is hypothesized the wind-blown sand that disrupted the settlement of Broo in the late 17th century is deposited in adjacent lochs as a distinctive, discrete minerogenic layers. The purpose of this study is to determine the genesis and timing of the sand blows, and to evaluate shifts in climate and land use in the area, prior to and beyond the period of occupation at Broo. Eight cores retrieved from the Loch of Spiggie and the Loch of Brow, both in close proximity to the Broo site were studied using a suite of geochemical, sedimentological, and geochronological analyses that serve as proxies to evaluate environmental shifts through time. Analyses performed include, bulk organic matter stable isotope analysis, biogenic silica, grain size analysis, percent loss on ignition, magnetic susceptibility, and plutonium dating. The objectives of this study are to: (1) compare sedimentary proxies to examine changes in land cover, (2) identify changes in terrestrial production inputs over the last several hundred years, and (3) develop a chronology that will be used to establish the relative age of the minerogenic layer found within the basin of the Loch of Brow. The combination of sedimentary and geochemical data will allow for a reconstruction of past land use and speculation as to the degree to which climate was responsible for the mobilization of sand that buried the Broo house.

Chapter 2:

Methods

2.1 Field Methods

Field work for this investigation was completed between May 25 and June 3, 2011 in the South Mainland area of the Shetland Islands. Lochs analyzed were chosen based on proximity to the Old House of Brow dig site, depth, proximity to aeolian sand deposits, and accessibility. The Loch of Brow and the Loch of Spiggie are the primary lochs studied in this thesis; however sediment cores were also recovered from the Loch of Tingwall and the Loch of Clumlie (Figure 2.1) and are stored at 4°C in the Department of Geology, Bates College.

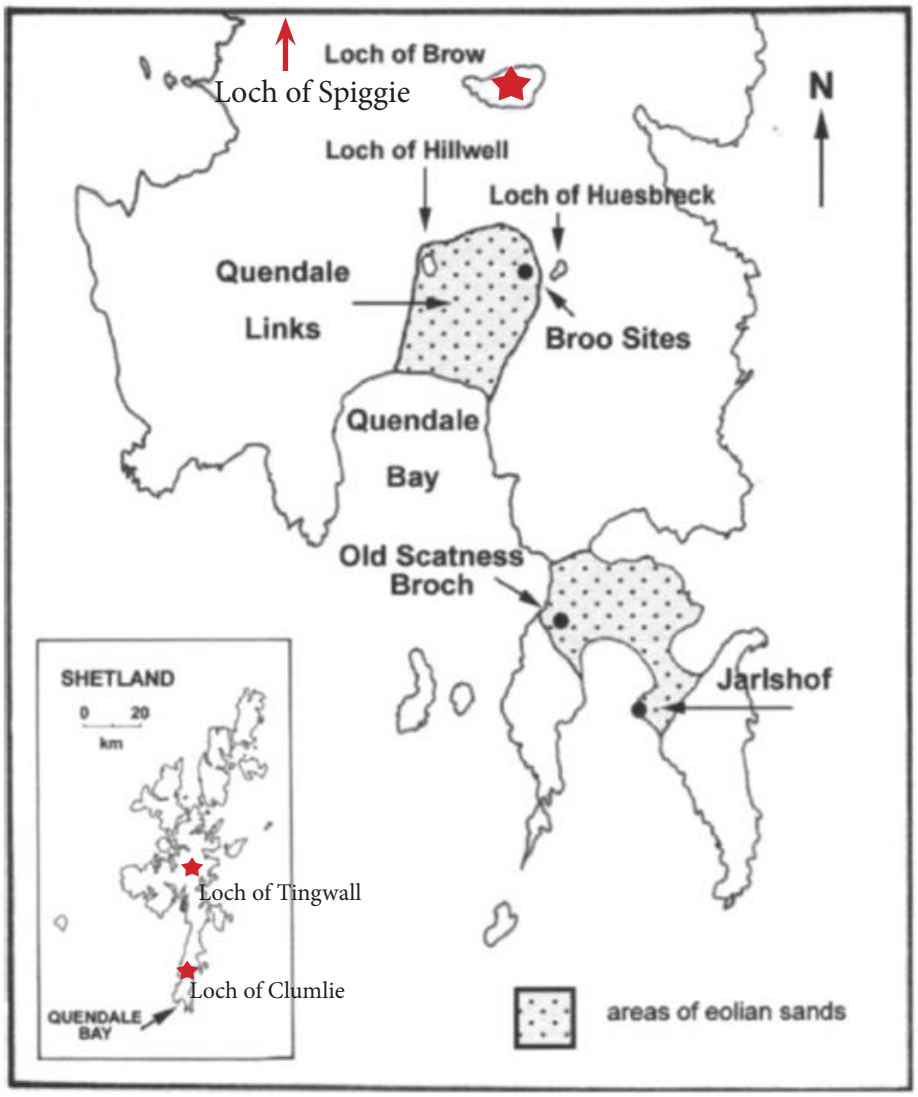

Figure 2.1 Modified illustration from Bigelow et al. (2005) highlighting the position of each of the cored lochs. In addition, Aeolian sand deposits and beach localities are noted.

Figure 2.2 Coring localities in the Loch of Spiggie and the Loch of Brow (Google Earth, 2010).

2.1.1 Sediment Coring

All cores taken were extracted using a universal gravity corer, fitted with a hammer, from the side of an anchored boat (Figure 2.3). Due to high wind conditions that make coring extremely difficult in Shetland, two Danforth anchors were used to secure the boat on station. Sampling locations of all cores were logged using a Garmin® eTrex Venture HC GPS device set to the British National Grid projected coordinate system.

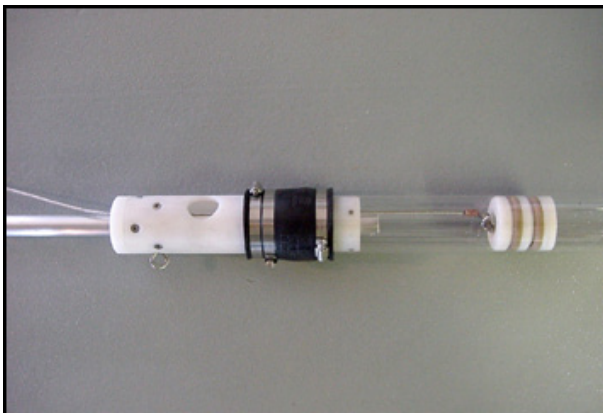

Figure 2.3 A universal gravity corer similar to the one used to extract sediment cores from the side of a row boat (Aquatic Research Instruments, 2006).

Cores were extracted across the basin from the deepest section of each loch, which was determined using bathymetry maps obtained from the British Ordnance Survey and an electronic Humminbird echosounding fish finder. Replicate cores were taken in each loch, with five cores taken across the basin of Brow and three in Spiggie Loch (Figure 2.2). To extract each core the universal gravity corer was fitted with a 76 mm diameter polycarbonate tube. Core tubes were cut to be approximately 1 meter in length. Great care was taken to ensure that the coring device entered the sediment vertically. In instances where it took multiple attempts to extract a core, an effort was made to avoid coring in an area where the top layer of sediment had been disturbed by previous attempts.

Immediately after extraction, cores were capped, labeled, and taped shut using electrical tape. Back on shore, water was siphoned off the top of the core with rubber tubing. Cores were then left uncapped and upright to remove as much additional water as possible before being packed with sterilized sand and foam noodles to prepare for shipping. Tightly packed cores were then placed horizontally in a large plastic container and shipped back to the United States, where they arrived approximately a month after coring occurred.

2.1.2 Water Sampling and Hydrolab Profiling

Water samples and Hydrolab data were collected once in every loch at the deepest point. A 50 meter Hach® Hydromet Hydrolab was used to collect depth, pH, specific conductivity, temperature, and dissolved oxygen measurements at half meter intervals down the water column. Water samples were collected in 1 liter brown (light-proof) Nalgene plastic bottles from just below the surface. Additionally, water samples were taken from all inlets and outlets of each loch. Three liters of water were collected from each sampling location. Water was collected for later analyses to establish chlorophyll levels, isotopic analysis of particulate organic matter, and major cation concentrations at various points of interest. These analyses will not be included in this thesis, but data can be viewed in Appendix A.

2.2 Lab Methods

2.2.1 Sediment Cores

Core Preparation

All 12 sediment cores were split approximately one month after coring. A table saw was used to score the outside of the plastic core tube and a circular saw on a large Dremel® tool was used to finish the cut. A length of monofilament fishing line was then used to create a clean slice through the middle, splitting the core in two, a working half and an archive half. Split cores were then visually logged noting changes in color, composition, grain size, and texture to distinguish stratigraphic units. The archived half of each core was photographed the day of splitting. Both halves of the core were then wrapped in plastic wrap and stored in D tubes at 4°C in the core storage room in Carnegie Science Hall.

Subsampling Procedure

All cores from the Loch of Spiggie and the Loch of Brow were subsampled for chronologic, sedimentological, and geochemical analysis (Figure 2.4). Subsampling locations in each core were chosen based on the stratigraphy, ideally obtaining a sample at the top, middle, and bottom of each stratigraphic unit making sure to straddle boundaries between units. In some cases this was not possible as the unit was too narrow to allow for 3 samples. In these cases as many samples as possible were obtained. All samples were obtained using stainless steel samplers from the top of the split surface of the core and away from the core walls, where there was greatest control on stratigraphy. For geochemical bulk isotopic analysis 2 cubic cm were removed, for chronology two 0.5 cubic cm samples were removed (only for the upper 10cm of Brow2011_2, Brow 2011_3, Brow2011_5, and Spiggie2011_1), and for sedimentary analysis 1 cubic cm (0.5 for LOI and 0.5 for grain size analysis) was removed from the core at each subsampling location as seen in Figure 2.2.

An additional 2cc was removed for geochemical analysis in the stratigraphic centimeter below the above sampling scheme in the middle of stratigraphic units when possible to be used later for other analyses. Other analyses undertaken with sediment from the green 2 cc section include analysis of lipid biomarkers for higher plant leaf waxes. These data will not be presented however, due to a failure to effectively isolate the compounds.

Core	Total Depth	# of Subsampling Depths	# of Additional 2ccSampling Depths
Brow2011_1	50	18	4
Brow2011_2	67.5	9	3
Brow2011_3	68	16	5
Brow2011_4	81	15	5
Brow2011_5	48	15	3
Spiggie2011_1	42	17	4
Spiggie2011_2	81.5	15	5
Spiggie2011_3	61	15	5

Table 2.1 Summary of subsamples extracted from the eight analyzed sediment cores.

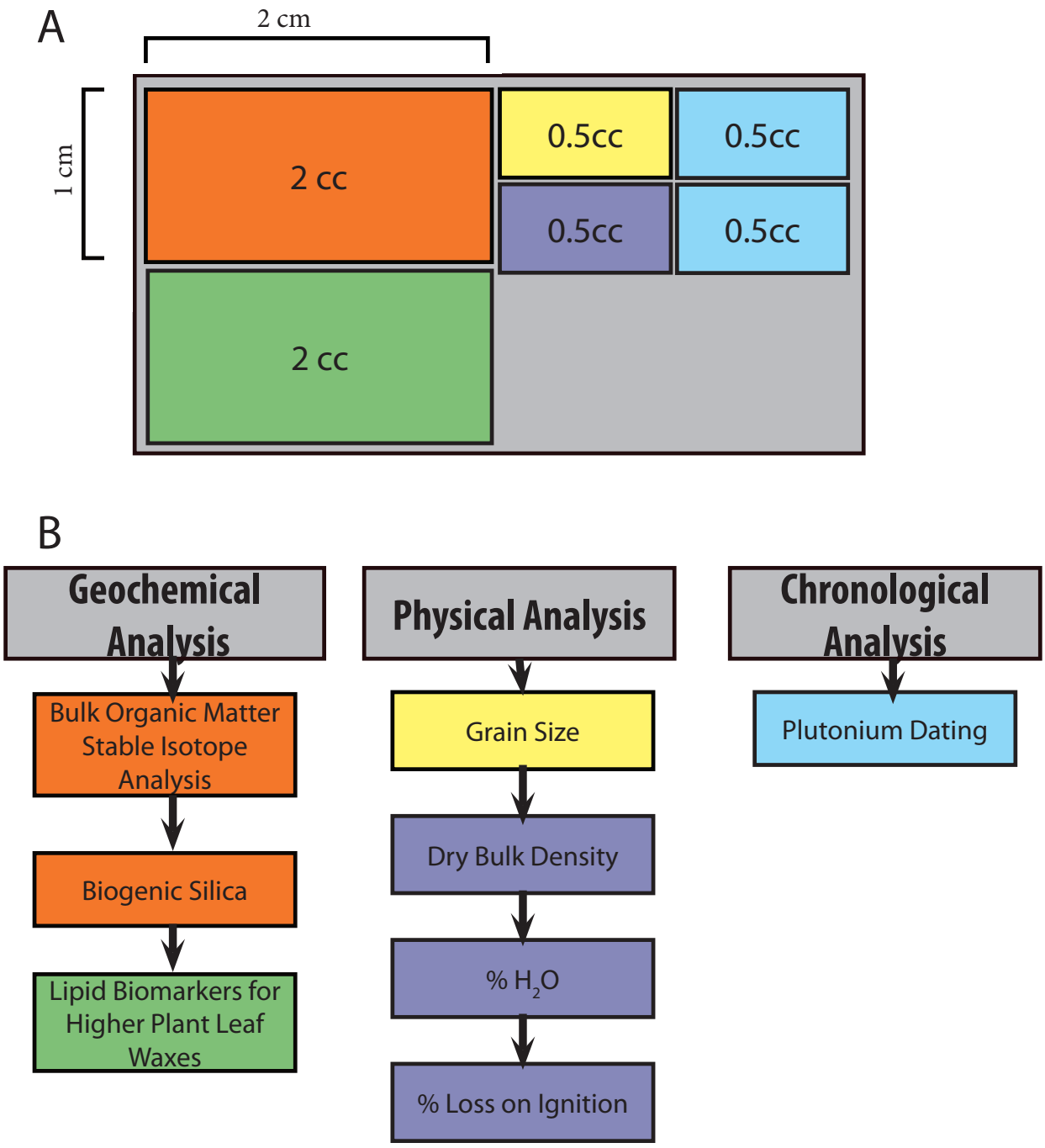

Figure 2.4 Sampling strategies from sediment cores. Upper block A illustrates sample location from each core level. In B, subsamples are grouped together based on color, for example the blue 0.5 cc section of the core was later analyzed for plutonium dating.

2.2.2 Plutonium Dating

The upper 10 cm of Brow2011_2, Brow2011_3, Brow2011_5, and Spiggie2011_3 were subsampled at 0.5cm increments using a 0.5 cc constant volume sampler, yielding 20 samples per core. Samples were placed in crucibles and dried for 18 hours at 100°C in the Precision® 511221132 drying oven in the Bates College Environmental Geochemistry Lab. Dry samples were then pulverized using a mortar and pestle and placed into 20mL pre-massed glass vials. Samples were weighed, yielding masses between 0.05-0.42 g, and sent to Prof. Michael Ketterer, Department of Chemistry and Biochemistry at Northern Arizona University, for analysis (Ketterer et al., 2004).

2.2.3 Percent Loss on Ignition

Each 0.5cc subsample was dried in a pre-weighed porcelain crucible in the Fisher Isotemp® 500 Series drying oven in the Quaternary Sedimentology Lab at 60°C for 48 hours. Samples were allowed to cool in the oven before weighing again to calculate the dry mass of sediment. Samples were then transferred to the Thermolyne® 6000 muffle furnace in the EGL and heated for 4 hours at 550°C. Crucibles containing the samples were allowed to cool in the oven before being reweighed in the crucibles. The dry bulk density and %LOI were then calculated using the formulas:

$$Dry\ Bulk\ Density = \frac{dry\ mass}{0.5\ cc} \qquad \%LOI = \left(\frac{(dry\ mass - muffled\ mass)}{dry\ mass}\right)*100$$

2.2.4 Magnetic Susceptibility

Core images were acquired and magnetic susceptibility measurements were made using a Geotek Multiscan Core Analysis System, from the Geosciences Department at the University of Massachusetts-Amherst. The magnetic susceptibility measurements are made on the Geotek system using a Bartington® MS2E High Resolution Surface Sensor, at 0.5cm increments continuously down the length of the archived half of each core.

2.2.5 Grain Size Analysis

A Beckman Coulter LS13 320 Particle Size Analyzer was used in the Sedimentology Lab at Bates College for grain size analysis (Figure 2.5). Before analysis could occur, organic matter from each subsampled unit was digested in H_2O_2. Due to the high content of organic matter in the Shetland cores, a test was run on a sample core from Profile Lake in New Hampshire, USA to determine the ideal amount of sediment needed for each sample as well as the ideal time and methodology for disintegrating organic matter. Profile Lake was selected as an ideal test core due to the fact that it mimics Shetland cores in both high organic content in some stratigraphic horizons and high concentrations of terrigenous sediment and lithic fragments in others. After testing a variety of preparation methods it was determined that the ideal amount of sediment was 0.5cc. A hybrid of two different organic matter digestion techniques from Wool (2011) and Rodbell (pers. comm. to M. Retelle, 2009) was used to completely disintegrate organic matter.

For the digestion, 0.5cc of subsampled material from each stratigraphic unit was dried in a pre-weighed porcelain crucible in the Fisher Isotemp® 500 Series drying oven in the Quaternary Lab at 60°C for 24 hours. Upon removal from the oven the dry mass of each sample was then obtained. Thirty mL of 40% hydrogen peroxide and the sample were placed in 47 mL Oak Ridge plastic centrifuge tubes. Samples were mixed in capped centrifuge tubes for 2 minutes using the Vortex Genie 2. Additionally samples were sonicated for 1 minute using a Fisher Scientific 60 Sonic Dismembrator to re-suspend dried sediment in solution. Samples were then heated in the centrifuge tubes on a hot plate at 75°C for 5 hours. Samples were then left for a variable amount of time, up to overnight at room temperature in the peroxide until the sample was ready to be run. Upon removal from the heat, samples were centrifuged for 5 minutes at 2500 rpm in a Damon IEC Division CU 5000 centrifuge. The supernatant was decanted and the samples were rinsed with DI water and centrifuged 3 additional times to remove any residual peroxide.

After removal of organic matter, 20 mL of deionized water and 17 mL of dispersant solution (0.7g/L sodium metaphosphate) was added to each sample. Samples were again mixed for 1 minute using the vibrating Vortex Genie 2 mixer and sonicated for 2 minutes using the Fisher Scientific 60 Sonic Dismembrator to deflocculate and re-suspend any particles that had adhered together over the course of the previous steps. This step eliminates aggregates of small grains and helps to prevent subsequent development of flocs (Arnold, 2009).

After preparing a sample, it was dumped manually into the sample chamber of the Coulter LS 13 320 to insure that the entire subsample was processed for grain size analysis. The Coulter LS 13 320 has capabilities of measuring grain size variability from 0.4 to 2000 microns, by projecting a laser through a water filled chamber that contains the sample solution and inferring grain size based on the scattering of light particles. The Coulter continuously sonicates the sample solution while in the chamber, preventing any flocculation. Three runs were conducted for each sample, along with an auto-rinse at the end of each sample run. Mean and median grain size as well as % obscurance was recorded for each sample run, with the mean and median of all three runs calculated after analysis. A schematic of the Beckman-Coulter LS 13 320 can be seen in the image below. Mean and median grain size processed with the Fraunhofer correction to take into consideration particle shape and surface area were used instead of the manually calculated average that was obtained from the unprocessed three runs.

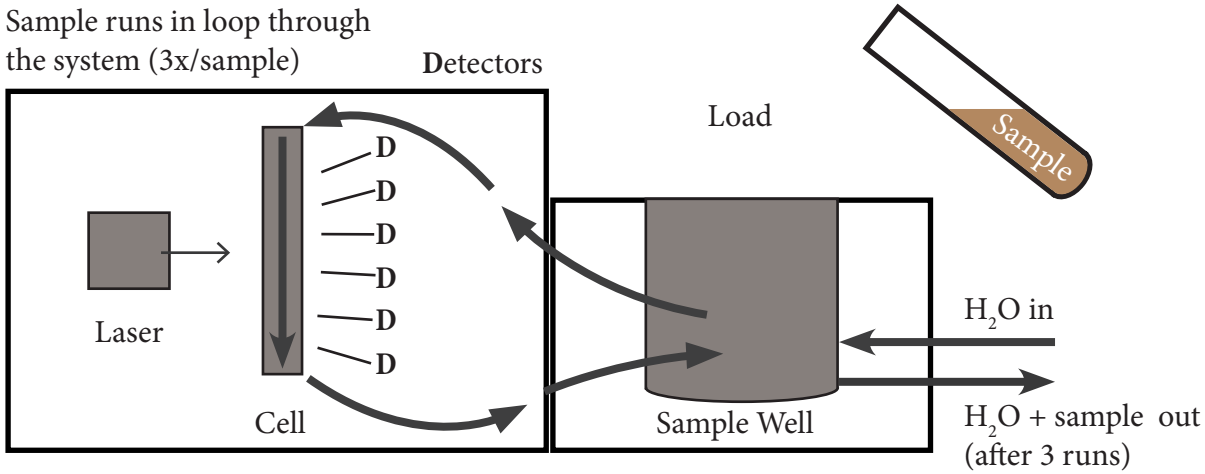

Figure 2.5 The diagram is a simplified illustration of the interior mechanics of a Beckman Coulter Counter.

2.2.6 Dry Bulk Density and %H_2O

2 cc of sediment was removed from each core using a 2 cc constant volume sampler for geochemical analysis. Samples were placed in pre-massed bags and weighed again to determine the wet mass of sediment. Samples were then freeze dried using a Labconco Freezone 6 Freeze Dry System. Dried samples were then weighed again to determine a dry mass. Dry bulk density and % H_2O were calculated using the following formulas:

$$\%H_2O = \left(\frac{(wet\ mass - dry\ mass)}{wet\ mass}\right) * 100$$

2.2.7 Decalcification

Due to high concentrations of inorganic carbon (i.e. carbonate) in the study area, before biogenic silica determination or bulk isotope analysis could occur, samples needed to be decalcified. For this procedure, 300-500 mg of dried, ground sediment obtained in 2.2.3 was added to a 250 mL Erlenmeyer flask along with 80 mL of 1 N H_3PO_4. Samples were sonicated using a VWR Scientific® Aquasonic 250 T for 15 minutes and left for 18-24 hours at 25°C. After sitting at room temperature for 24 hours, 40 additional mL of 1 N H_3PO_4 were added to the sample solution and sonicated for 15 minutes. Samples were then filtered onto 47 mm diameter 0.4 µm pore size Isopore® polycarbonate, track etched filters using a filtration device pictured below. Filters were then placed in covered plastic petri dishes and dried at 60°C in the EGL drying oven overnight (Precision® 51221132). Percent calcium carbonate and consequently an estimate of inorganic carbon present in solution were determined using the formula:

$$\%CaCO_3 = \left(\frac{Original\ Dry\ Sample\ Weight - Dried\ Decalcified\ Sample\ Weight}{Original\ Dry\ Sample\ Weight}\right) 100$$

2.2.8 Biogenic Silica

Samples for biogenic silica (SiO_2) were obtained from the 2 cc subsection of the core for geochemical analysis (2.2.3). The first step of the process, decalcification (2.2.9), is necessary to prepare sediments to run for samples for bulk organic stable isotopes as well as biogenic silica. In addition to analysis of sample sediments, a procedural blank was created using identical methodology to track baseline contamination to serve as the "zero point" on a calibration curve. It should be noted that for this entire procedure only plastic containers were used. Plastic containers are necessary due to the high silica content in glassware which would skew sample concentrations. Rather than apply a correction for the interference from non-amorphous silica phases, plastic containers were used.

Dissolution of Silica

Approximately 5 mg of decalcified, dried sediment was weighed out and transferred to a 30 mL polycarbonate centrifuge tube, along with 15 mL of 1.0 M Na_2CO_3. Na_2CO_3 was used for leaching, rather than HCl or NaOH, due to the fact that it allows for accurate estimates of amorphous silica over the whole spectrum of sedimentary silica/clay ratios (Eggimen et al., 1980). A solution of 1.0 M Na_2CO_3 allows for the complete dissolution of most silica sources despite the nature of the material, aging, water content and incipient crystallinity, surface coatings and potentially other factors (Eggimen et al., 1980). Samples were sonicated for 10 minutes using a VWR Scientific Aquasonic 250T sonicator and then heated for 3 hours in a 90°C Forma Scientific orbital shaker in the EGL. After cooling, samples were filtered through a 0.45µm pore size Tuffryn filter using a plastic filtration apparatus. A squirt bottle of 1 M Na_2CO_3 was used to rinse the centrifuge tube, tower, and frit three times. Filtrate was then transferred to a 60 mL plastic screw-cap bottle, along with 1 drop of methyl orange pH indicator solution and approximately 10 mL of 6 N HCl until the pH was approximately 3.4 and the color of the solution changed from yellow to pink. The final sample volume of the extract was then measured using a plastic 50 mL graduated cylinder.

Spectrophotometric Analysis

After the dissolution of silica, 0.1 mL of sample solution was transferred to plastic scintillation vials with 2.9 mL of deionized water and 0.1 mL of molybdate solution ($(NH_4)6Mo_7O_{24}\bullet 4H_2O$). In this reaction, the sample solution reacts with the molybdate solution yielding silicomolybdates, phosphomolybdates, and arsenomolybdates. After sitting for 10 minutes, 0.1 mL of oxalic acid ($H_2C_2O_4$) was added and thoroughly mixed, this was followed by 0.05 mL of ascorbic acid ($C_6H_8O_6$). The addition of acid serves to reduce the silicomolydbdate generating a blue color that should develop between 30 minutes and 1 hour, depending on the concentration of silica present within solution. While reducing the silicomolybdate solution, the oxalic acid simultaneously decomposes any phosphomolybdate or arsenomolybdate formed in the first reaction. 1 mL of the final solution was then transferred to a 1 cm path length quartz cuvette and measured for absorbance spectrophotometrically at 810-820 nm in the Beckman DU 800 in Dana Chemistry Hall at Bates College. Sample absorbance was corrected by subtracting the procedural blank absorbance prior to calculating silica concentrations using a 2 ppm silica standard. Samples were plotted on a standard curve of absorbance vs. concentration to determine the silica concentration of the extract solution for each individual sample. The percent silica in the sediment and the percent opal (SiO_2) in total sample were then calculated.

$$\%\, Si = \frac{silica\ concentration * 10^{-6}}{initial\ sample\ weight} * (dilution\ factor * sample\ volume) * 100$$

$$\%\, Opal\ in\ total\ sample = \frac{\%\, Si}{0.468} * (1 - \%\, CaCO_3\ /100\ )$$

$$Opal\ Flux = \frac{\%opal}{100} * mass\ flux$$

Where [Si] are measured in mg/l, sample weight is recorded in mg, and sample volume is measured in mL.

2.2.9 Stable Isotope Analysis

Elemental Analyzer-Isotope Ratio Mass Spectrometer (EA-IRMS)

Homogenized samples obtained through decalcification (2.2.9) were again used for this portion of the analysis. Between 2 and 20 mg of sample were weighed out into 5.0 x 9.0mm tin cups using a Mettler-Toledo microbalance. Samples greater than 7 mg of sediment were weighed out into a second tin cup to compact the material further. In addition to samples, three sets of standards (acetanilide (BC 2991), caffeine (BC 2992), and cod muscle (BC 5676)) were run with each batch of samples. Samples were then run through the Elemental Analyzer (EA) interfaced with the ThermoFinnigan Delta V Advantage Stable Isotope Ratio Mass Spectrometer (IRMS) via the Conflo II interface, in the Bates College EGL (Figure 2.6). Isotopic values are reported using δ- notation, where:

$$\delta^{13}C_{PDB}=[\ \frac{(13C/12C)sample-(13C/12C)standard}{(13C/12C)standard}\ x\ 1000\ ]$$

and

$$\delta^{15}N_{air}=[\ \frac{(15N/14N)sample-(15N/14N)standard}{(15N/14N)standard}\ x\ 1000\ ].$$

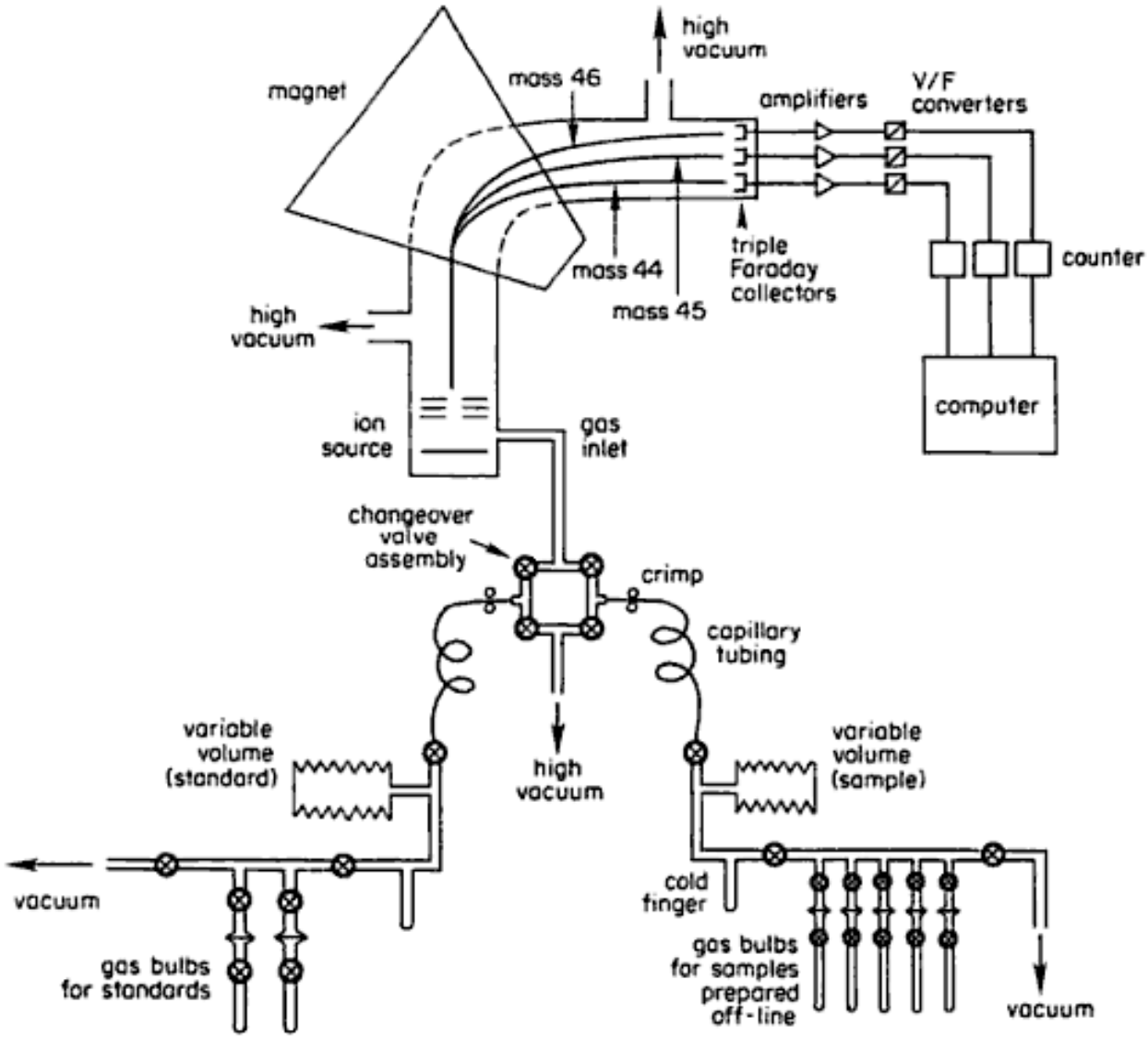

Figure 2.6 Schematic diagram of an Isotope Ratio Mass Spectrometer (IRMS) (Coleman and Fry, 1991). In the Bates College EGL set up, an elemental analyzer, not pictured here, uses a gas chromatography column to separate compounds before entering the IRMS.

Chapter 3:

Results

3.1 Limnology

3.1.1 Loch Bathymetry and Watershed Profile

The Loch of Brow is located at WGS 84 Coordinates of 59.9232, -1.31128 (BNG coordinates HU3815 (438500, 1115500)) and is approximately 600 meters x 300 meters, with a max depth of 1.5-1.8m. The loch is located within 1-2 meters of sea level and is surrounded by agricultural fields (Figure 3.1). There are three small inlets into the loch, all found along the northeastern segment. These were observed to be low flow streams that are relatively shallow and travel through the upland fields. There is only one outlet from the loch, a boggy area that connects the Loch of Spiggie to the Loch of Brow. Local residents have described frequent flooding of the lowland between the lochs during large winter storms.

The Loch of Spiggie, is larger than the Loch of Brow and is located at WGS 84 coordinates of 59.9323, -1.32898 (BNG coordinates HU3716 (437500, 1116500)). The deep hole ranges in depth between 9 and 12 meters (30-40 feet). A shallow shelf, only a meter in depth, extends around the perimeter of the loch with the largest section occurring in the northern portion, where it extends out nearly 300 meters. The loch drops off steeply at the edge of this shelf and water depth quickly increases to 3 and 4 meters as it steadily decreases out to the deep hole. The Loch of Spiggie is approximately 2,000 meters x 300 meters at its widest point. Two inlets have been identified as sources of fresh water to the loch. These include the previously mentioned connection to the Loch of Brow and the Burn of Scousburgh, a stream that connects to the loch in the northeastern corner of the loch. There is only 1 outflow from the loch, a stream of water that exits the loch in the northwest corner and enters into the Bay of Scousburgh near the small island of Colsay (Figure 2.1). It is also known that the Loch of Spiggie was once connected to the Bay of Scousburgh and thereforemarine sediments can be viewed below the recent lacustrine record.

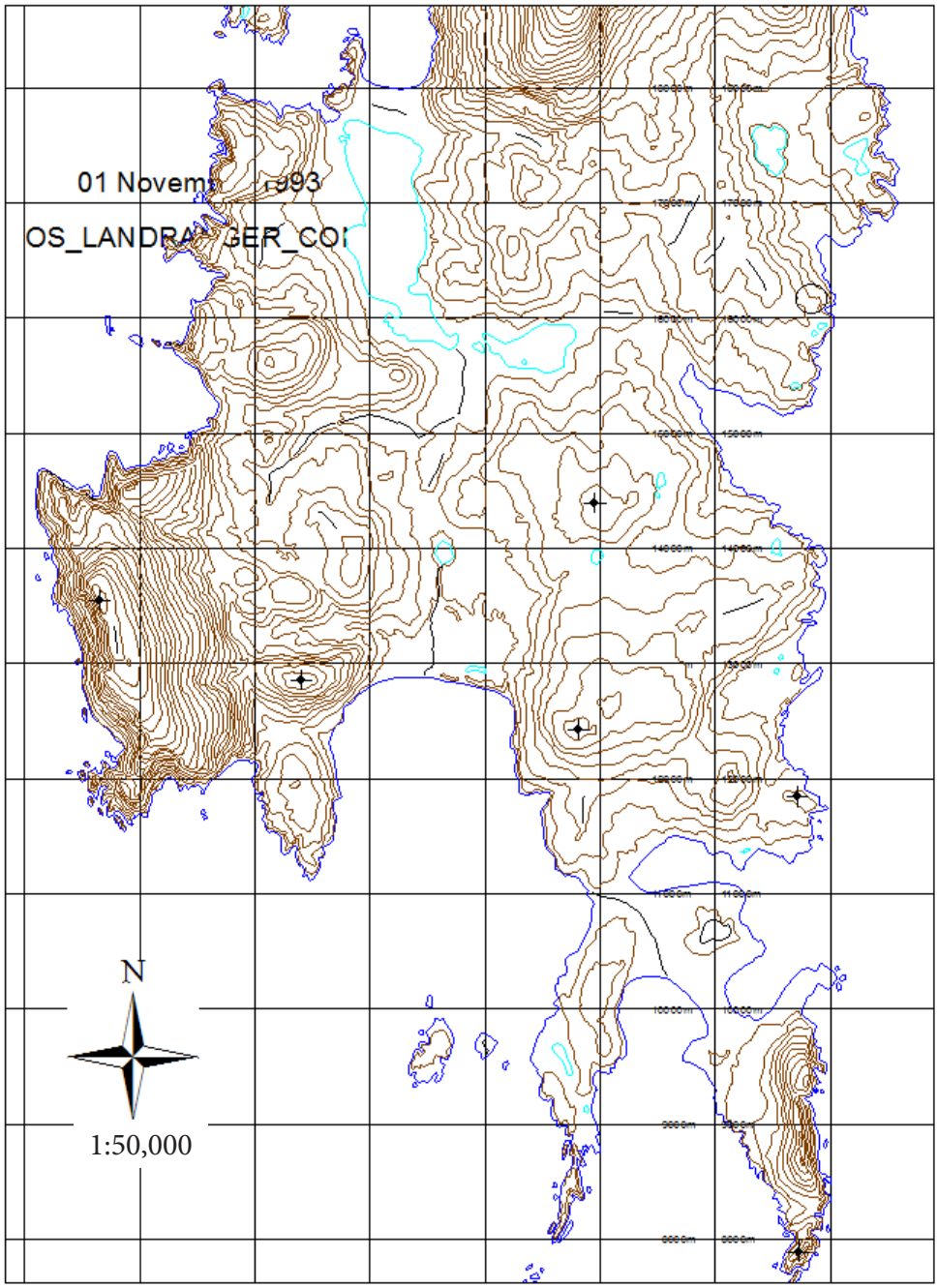

Figure 3.1 Topographic map of the south Mainland Shetland, focusing on the Quendale and Dunrossness areas. Contour interval,10 m. Modified from data obtained from the British Ordnance Survey (2010).

3.1.2 Water Quality Analysis

Water Column Profiles

Water column profiling was conducted on May 30, 2011 at one coring location in each of the sampled lochs (Figure 3.2). In the Loch of Brow, water sampling occurred at the same coordinates as the Brow2011_3 core. In the Loch of Spiggie, the profile was taken at the same location as Spiggie2011_1. pH data were intended to be collected, however the sensor on the Hydrolab fell off during one analysis and subsequent measurements could not be taken.

In the Loch of Brow, values for all analyses remained fairly constant throughout the water column. Temperature values remained constant at ~12.7°C. Specific conductivity also remained at a constant value of 0.395-0.397 mS/cm. Dissolved oxygen was the only parameter that decreased slightly at the deepest sampling location. Average dissolved oxygen values for the entire loch were 10.6 ppm, with a slight decrease to 10.1 ppm at the bottom of the loch. These values indicate that the loch is thoroughly mixed and oxygenated throughout the water column.

The Loch of Spiggie, showed more variability throughout the water column. Temperatures at the surface averaged 12.7°C, while temperatures below gradually decreased averaging 11.2°C at the bottom of the deep hole. The thermocline can clearly be seen in Figure 3.2. Unlike temperature values, specific conductivity remained relatively constant ranging between 0.626 and 0.631 mS/cm, two times that seen in the Loch of Brow, likely due to the influence of saline groundwater or sea spray. Finally, dissolved oxygen also showed a slight decrease in values at the base of the water column, though it still remained thoroughly oxygenated. Values for dissolved oxygen averaged 11.3 ppm in the upper surface water and gradually decreased with depth to 9.6 ppm.

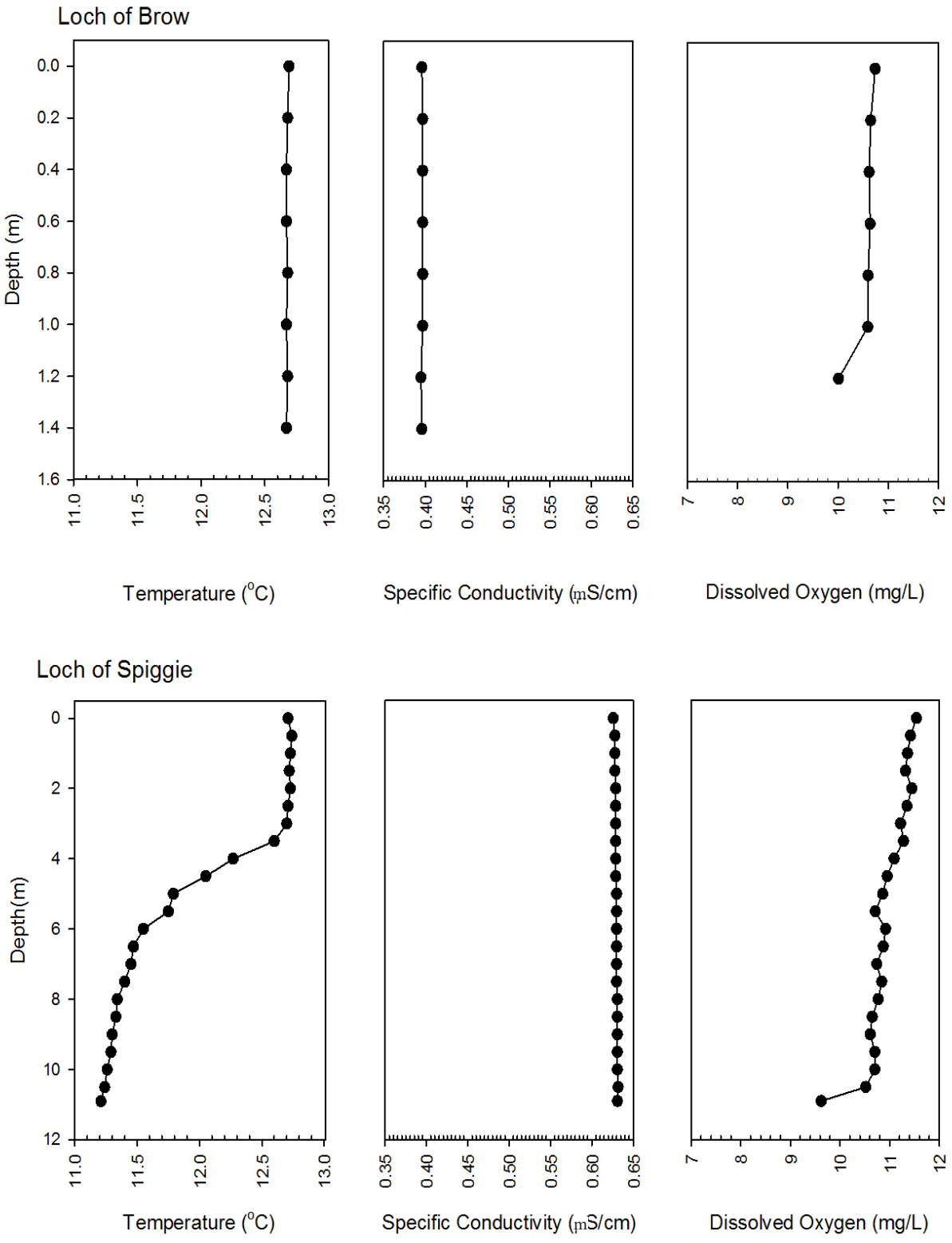

Figure 3.2 Water column profiles generated from Hach Hydrolab. Data collection occurred on 5/31/11.

3.2 Sedimentary Analysis

3.2.1 Core Descriptions

Five cores were extracted from the Loch of Brow over a two day period. Brow2011_1 and Brow 2011_2 were extracted on May 30, 2011, while the remaining three cores were extracted on May 31, 2011. All cores taken from the Loch of Brow were in areas where the water depth ranged from 1.2-1.5 m. The three cores extracted from the Loch of Spiggie were removed on May 31, 2011. Water depth at the location of these three cores varied and is noted in the following section.

Loch of Brow

Brow2011_1 (Figure 3.3) is 50 cm in length. The top unit (0-14cm) is an organic rich dark grayish brown layer with minor macrophytes and rootlets dispersed throughout. These macrophytes are fine and fibrous, with average length of 0.5 cm. Beneath this top silty layer is a tan fine grained sand unit (14- 30.5 cm) with some interbedded bands of organic rich sediment. The organic bands seen within the sand unit are very narrow and are a minor constituent. Deeper in the core, from 30.5-35.5 cm depth, is a transitional unit, between sand and gyttja, where an olive brown inorganic layer with very narrow bands of darker black silt is visible. Finally, the bottom unit of the core is a very fine black organic gyttja layer (35.5- 49cm) with small to very small macrophytes and rootlets, similar in size and composition to the macrophytes seen in the upper most units.

Brow2011_2 (Figure 3.4) was extracted from the eastern side of the Loch of Brow (Figure 2.2), and measured 67.5 cm. The upper unit (0-18.5 cm) consists of a dark brown loosely compacted organic unit. Small fibrous macrophytes less than 1 cm were present throughout. The underlying unit consists of a silty sand layer (18.5-34 cm) where very few macrophytes are identified. Below this, a very fine black organic gyttja unit (34-67 cm) is seen, containing several large macrophytes up to 3 cm in length. Macrophytes identified are hollow reeds and are not salt marsh plants.

Brow2011_3 (Figure 3.5) was extracted from the center of the loch and was the most heavily subsampled of all cores. Units present in this core include a dark greyish brown organic layer (0-17.25 cm) with small macrophytes. Below this is the fine grained tan sand (17.25-36 cm). Like the sediments from Brow2011_1, several narrow bands of organic sediment (~0.25-1 cm) can be seen within the silty sand unit. A transitional unit (36-44cm) can also be seen in this core, where the tan sand grades into the lower gyttja unit. Finally, macrophytes ranging in size from 2-3 cm were observed in the lower gyttja unit (44-67.5cm).

The longest core extracted from the Loch of Brow was Brow2011_4 (Figure 3.6) and was 81.5 cm long. This core, taken the closest to the outlet into the Loch of Spiggie on the western side of the loch, does not contain a sand unit. Here, the upper dark greyish brown organic unit (0-37 cm) overlays the bottom gyttja unit. The lower gyttja unit (37-81.5 cm) contained the largest macrophytes seen in the entire loch, with the largest measuring 5.5 cm in length.

Brow2011_5 (Figure 3.7) was the shortest core extracted from the Loch of Brow with a total length of 48 cm. This core resembles the other 4 cores in stratigraphy, including an upper dark greyish brown unit (0-16 cm) with a few small macrophytes. Also contained in this upper layer were a few minor lithic fragments. Underlying this unit is a fine grained sand unit (16-23 cm) that contains a narrow, yet pronounced black organic unit from 17-19 cm. Beneath the sand, is the dark brown organic gyttja unit (23-48 cm). The dark brown gelatinous gyttja layer is loosely compacted and is mottled with several patches of darker black colored mud, potentially related to bacterial decomposition. These dark spots were not viewed in any of the other Loch of Brow cores.

Loch of Spiggie

Spiggie2011_1 (Figure 3.8), is a short core, 42 cm in length, that was recovered from a water depth of 12.19 m. Stratigraphic units contained within this core are very different in appearance from the Loch of Brow sediments. Here, the upper unit (0-11 cm) is a very dark brown to olive gray sand unit with narrowly interbedded organic units and some shell fragments, most of which were smaller than 1 cm in length. Underlying this unit is a fine-grained very dark gray sand unit (11-27.5 cm) with very few shell fragments, that transitions downcore into coarser grained dark gray sand with shell fragments up to 0.5 cm in length (27.5-31 cm). Finally, the bottom unit (31-42 cm) is a dark grey pebbly diamicton with a medium to coarse grained sand matrix.

Spiggie2011_2 (Figure 3.9), extracted at a water depth of 10.67m, also had a very different appearance. Here the upper unit (0-14.5 cm) was a very dark gray silty sand layer. The upper silt unit is underlain by a black organic rich unit with very fine, fibrous material (14.5-20 cm), which transitioned into a very dark grey fine grained sand layer (20-33 cm). Finally, the lowest unit seen in Spiggie2011_2 was a black silt/mud matrix with minor fine macrophytes present in the bottom 5 cm of the core.

Spiggie2011_3 (Figure 3.10), is 61 cm long and was taken from a shallower depth of 9.14 m in an attempt to avoid the diamicton unit seen in Spiggie2011_1. The upper unit (0-12 cm) is a faintly laminated dark olive gray unit with the most pronounced dark bands at 2, 4, and 8.5 cm depth. Below this unit (12-26.5 cm) is a black organic unit with faint lamination. At the base of this unit there is a sharp contact under which lies a dark gray medium to coarse grained sand unit (26.5-41 cm) with small (0.5-1 cm) shell fragments. Following this is an additional very dark gray fine grained sand to silt unit with no shells present (41-46 cm). Finally, the basal unit of the core is a very dark grey coarse grained gravel/ diamicton (46-61 cm) with lithic fragments up to 5 cm in diameter.

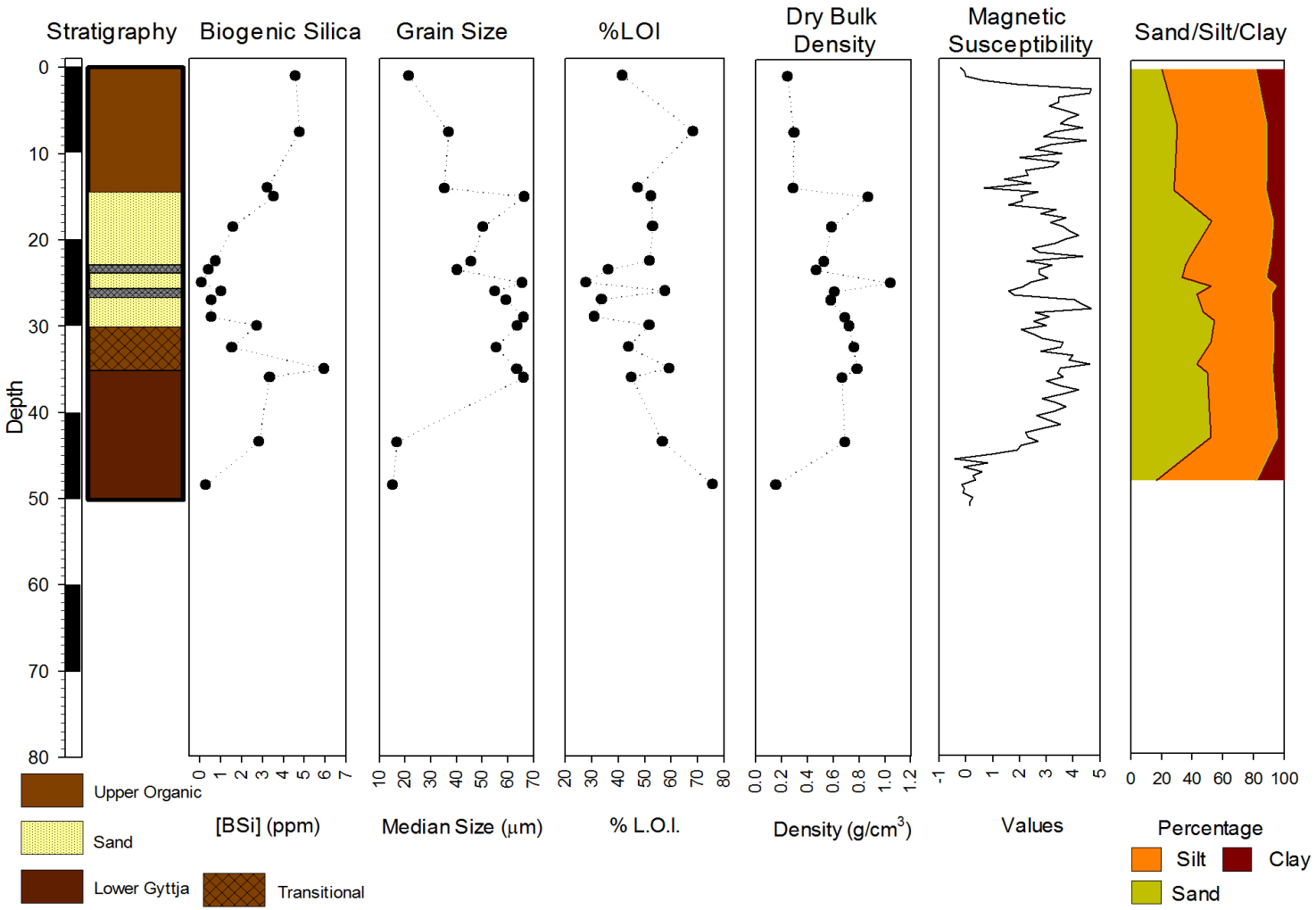

Figure 3.3 Summary figure of sedimentary analyses conducted on subsamples from Brow2011_1.

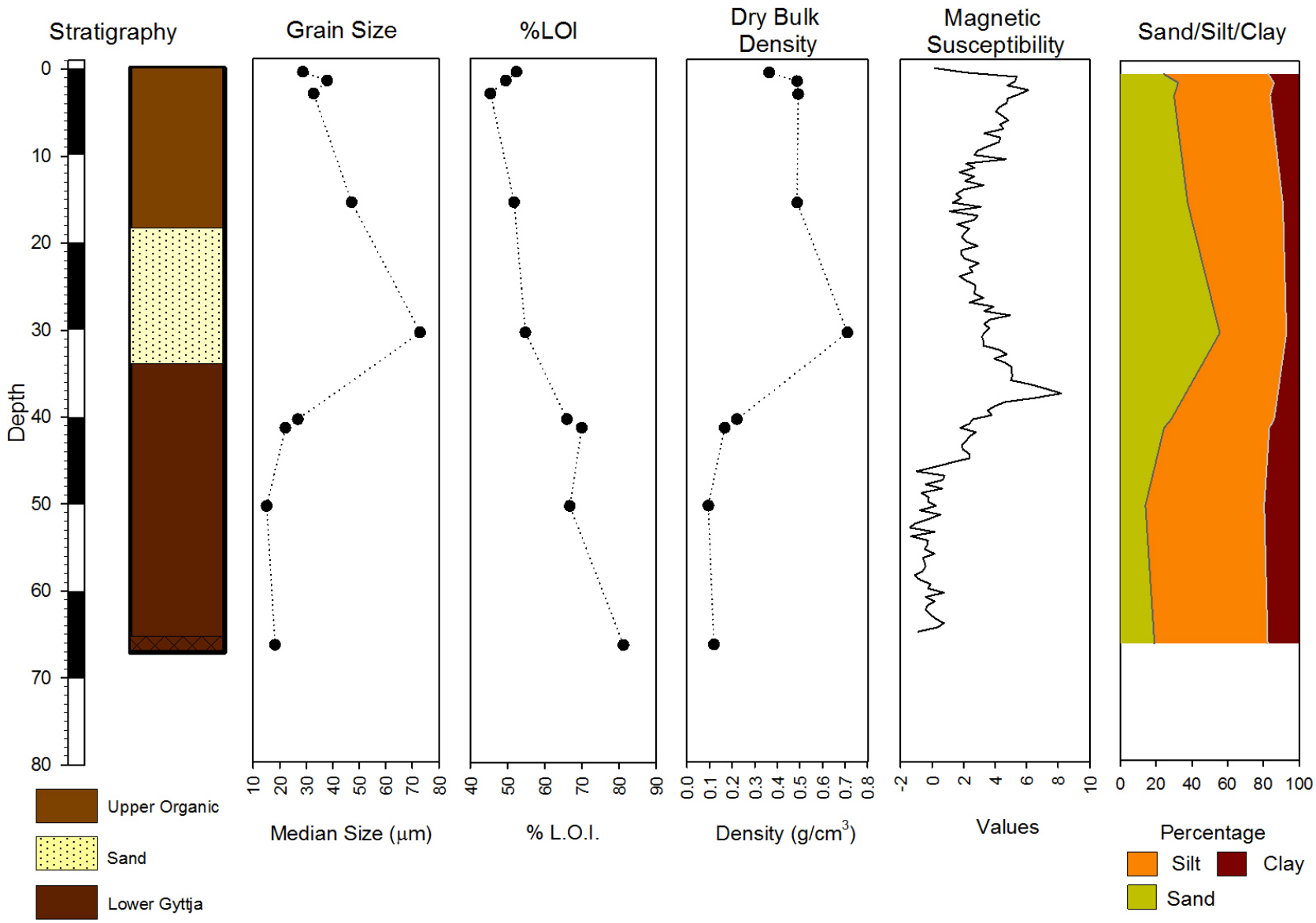

Figure 3.4 Summary figure of sedimentary analyses conducted on subsamples from Brow2011_2.

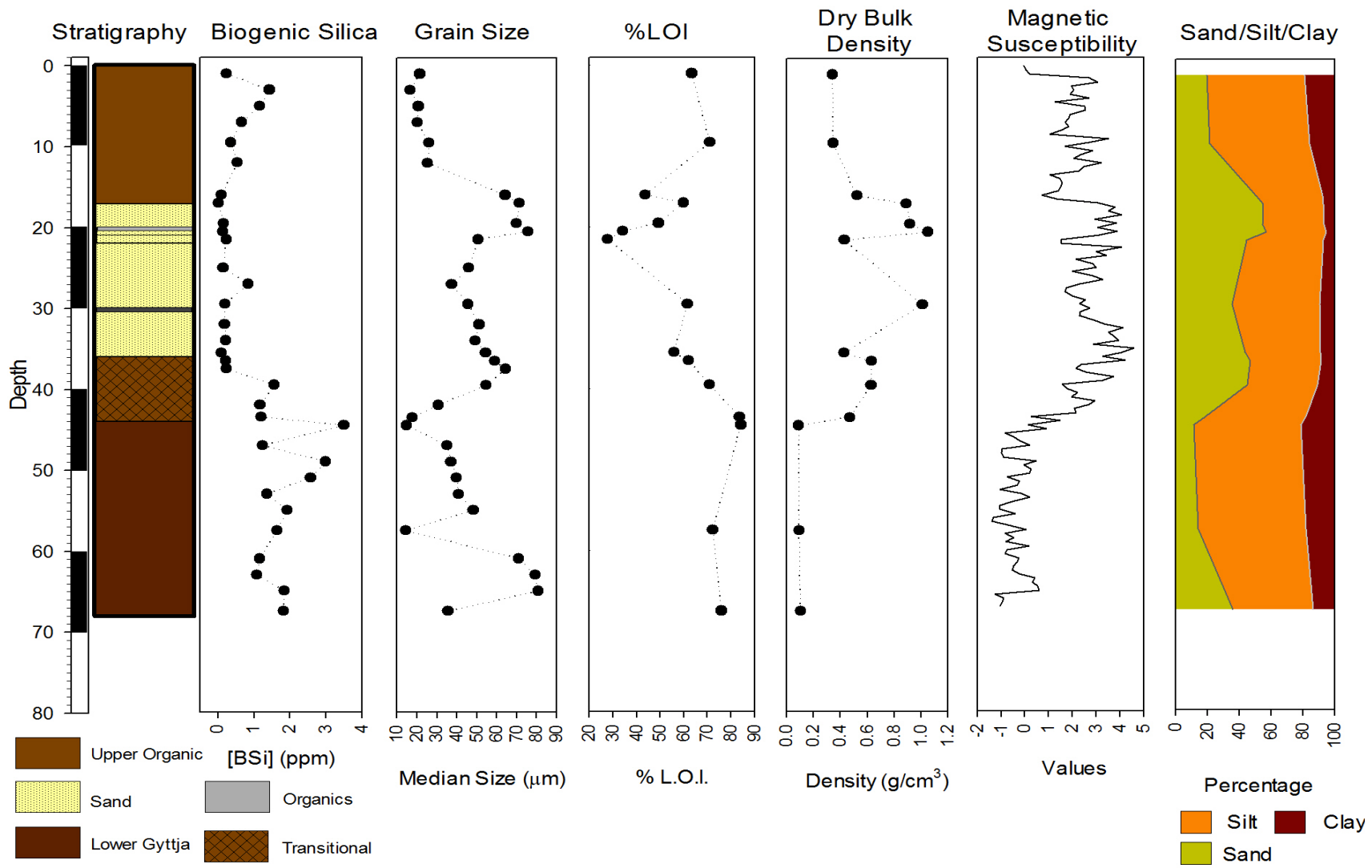

Figure 3.5 Summary figure of sedimentary analyses conducted on subsamples from Brow2011_3.

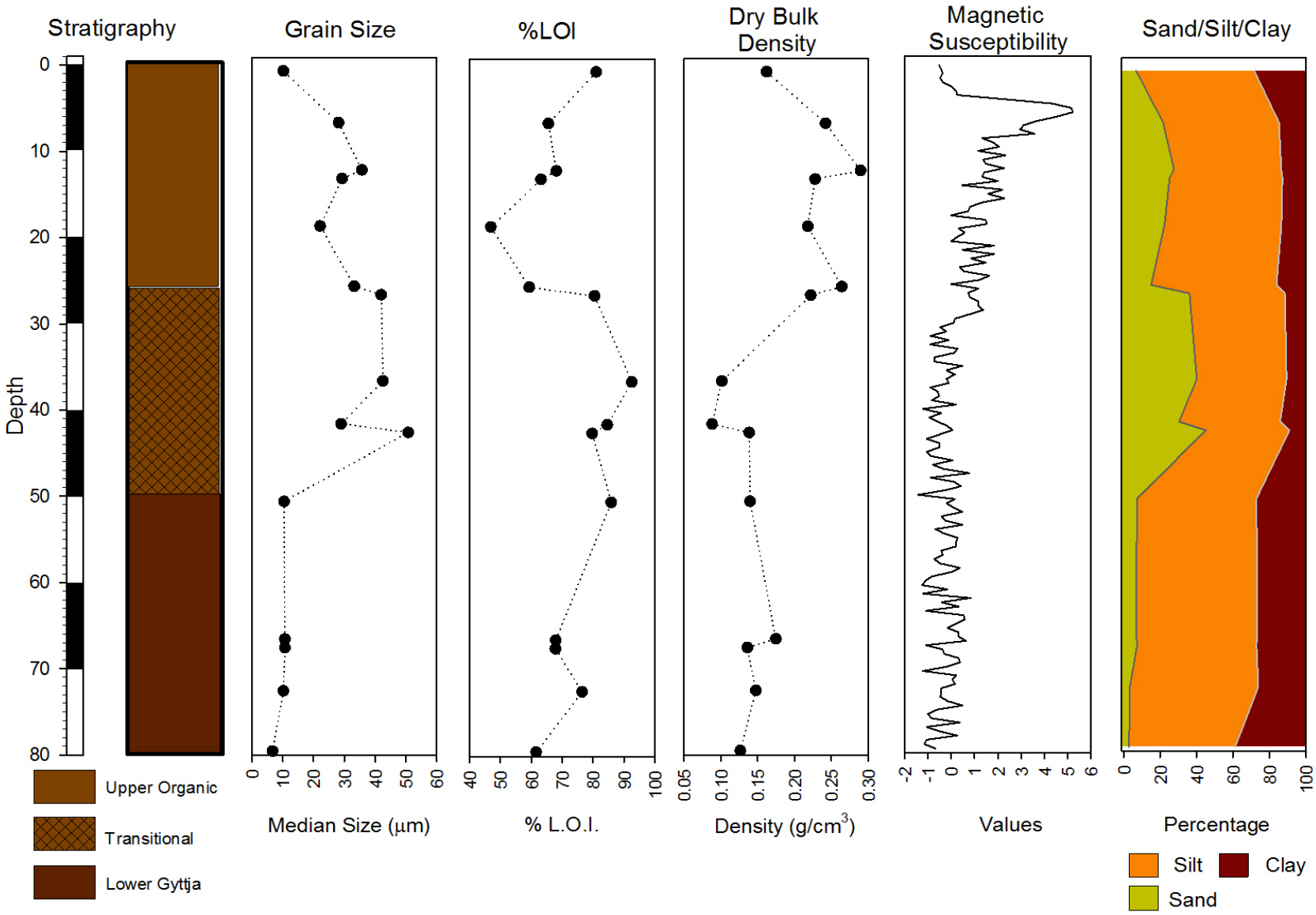

Figure 3.6 Summary figure of sedimentary analyses conducted on subsamples from Brow2011_4.

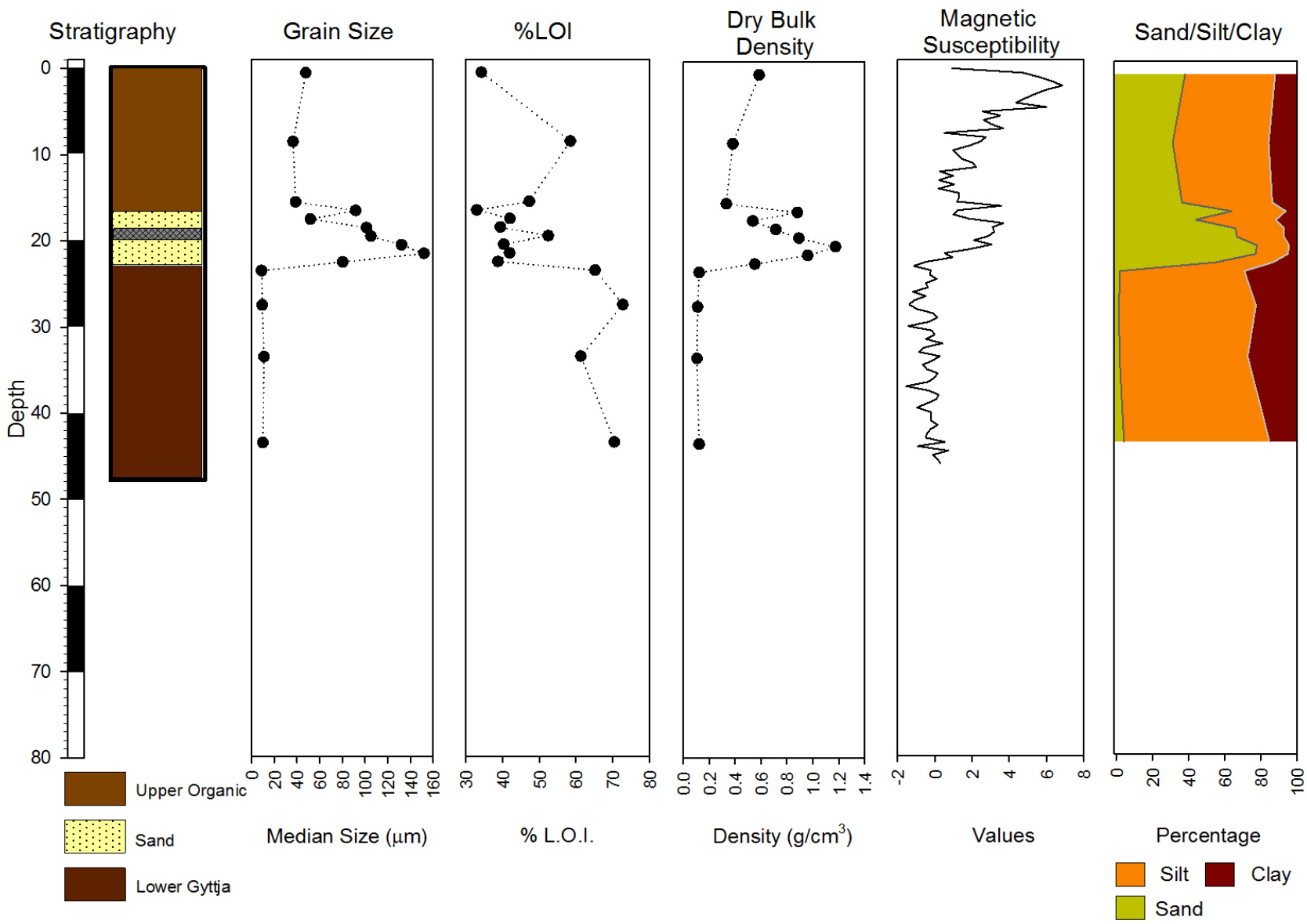

Figure 3.7 Summary figure of sedimentary analyses conducted on subsamples from Brow2011_5.

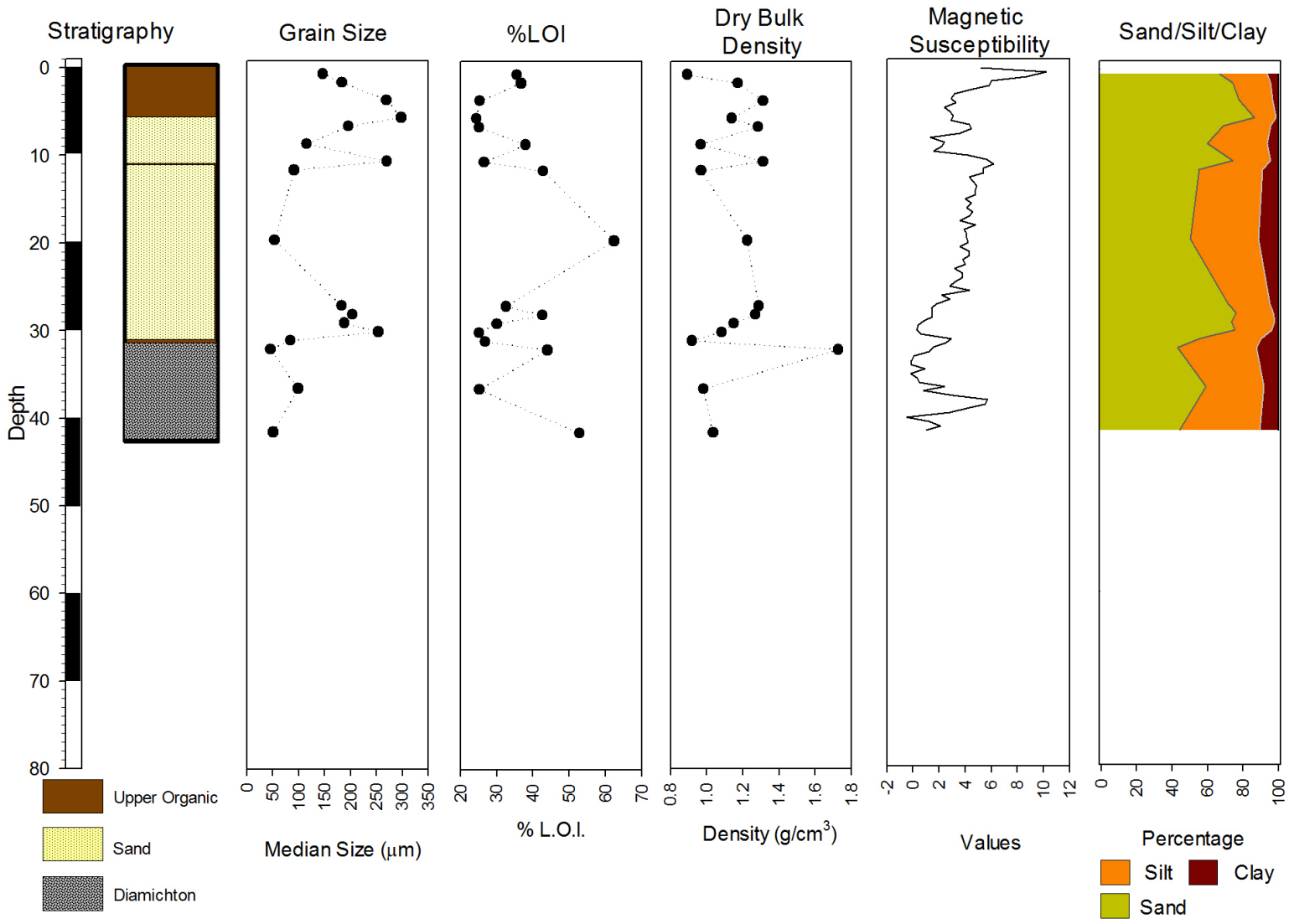

Figure 3.8 Summary figure of sedimentary analyses conducted on subsamples from Spiggie2011_1.

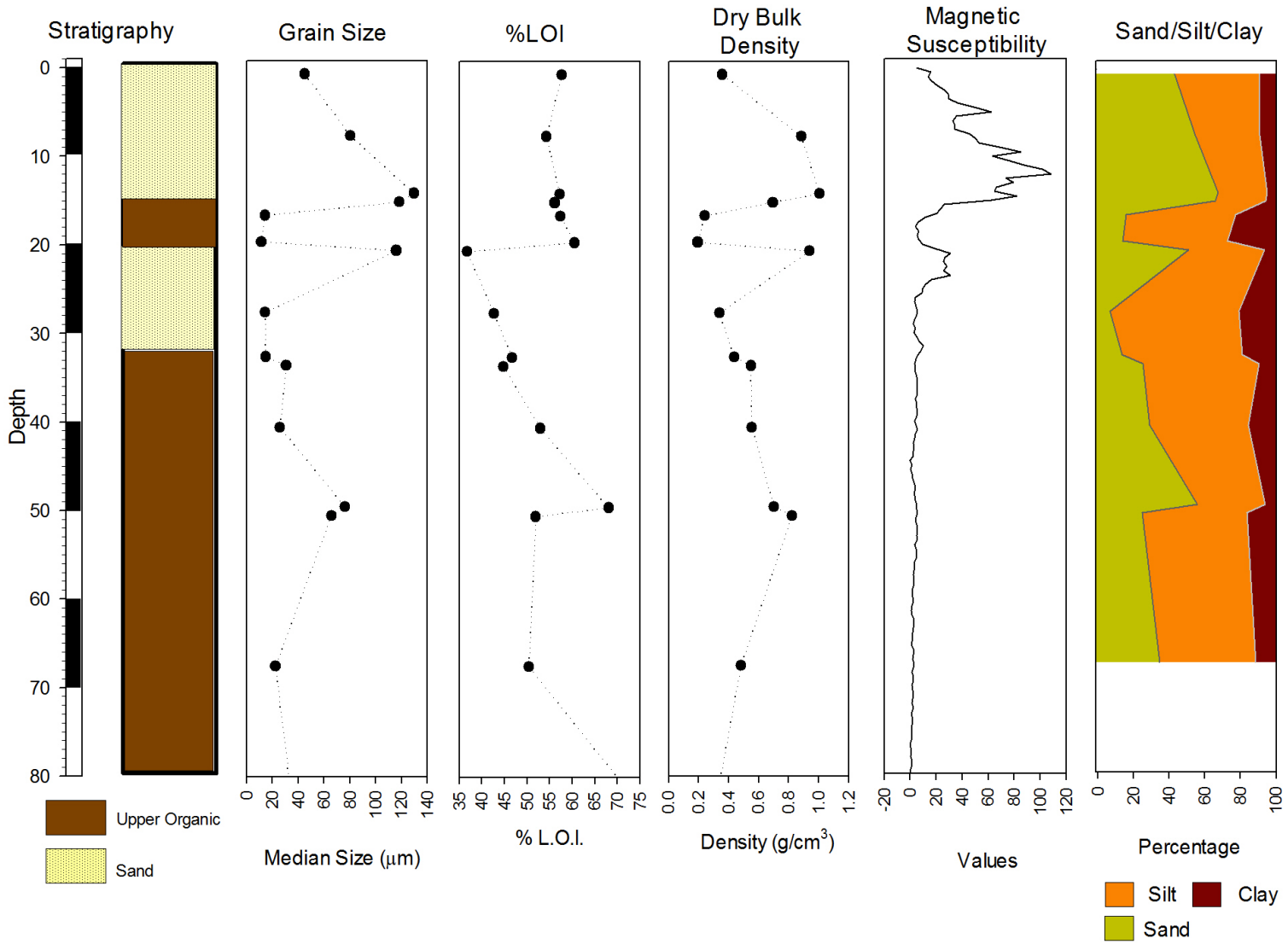

Figure 3.9 Summary figure of sedimentary analyses conducted on subsamples from Spiggie2011_2.

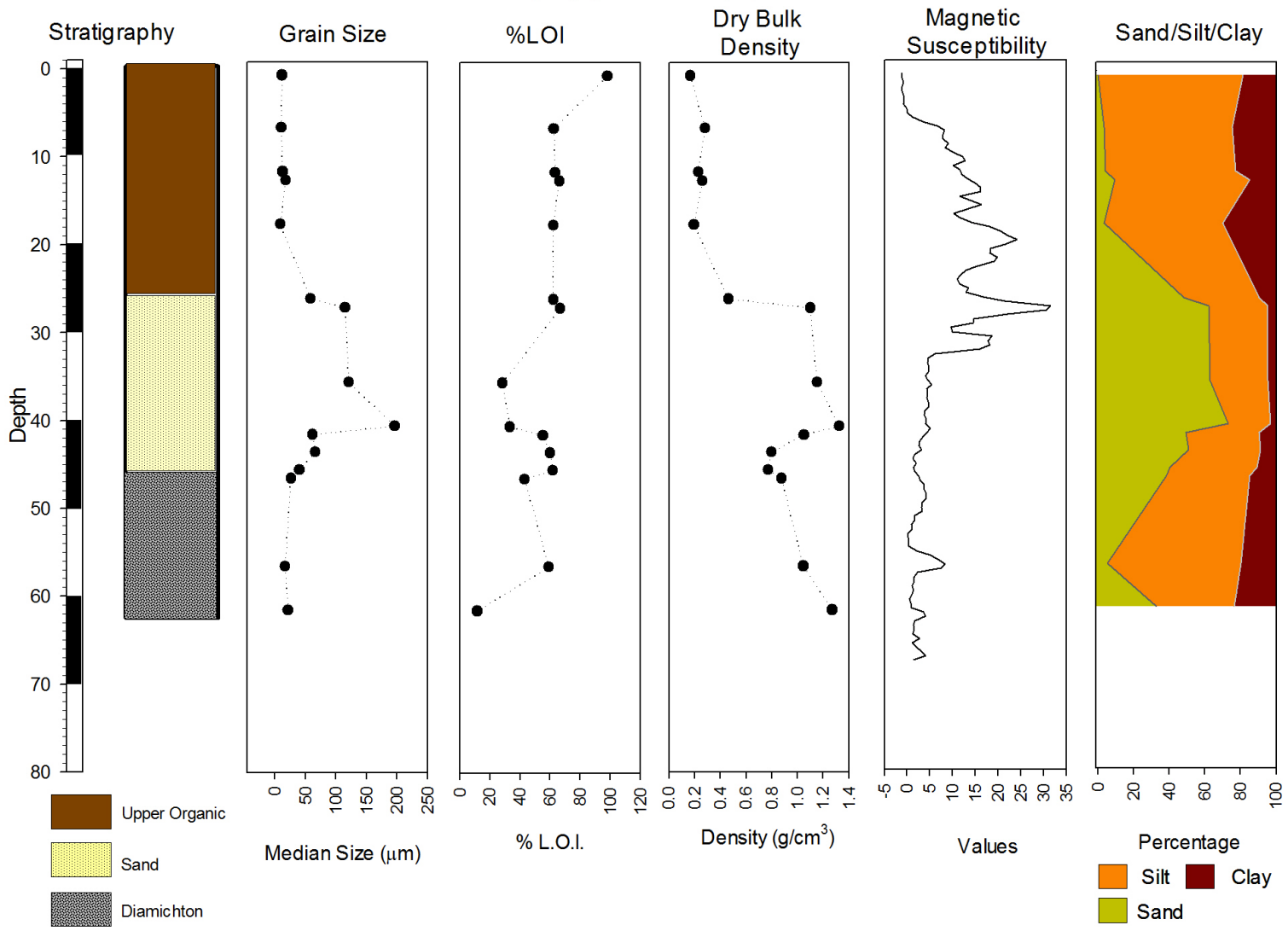

Figure 3.10 Summary figure of sedimentary analyses conducted on subsamples from Spiggie2011_3.

3.2.2 Correlation of Stratigraphic Units

Within the Loch of Brow, four different consistent stratigraphic units were identified across the basin (Figure 3.11). An upper organic rich unit can be seen in all five of the cores. This unit contains densely packed organic sediments and intermittently contains plant fibers and small macrophytes (>.25cm in length). Below this unit lies a minerogenic unit, a tan to greyish brown fine to very fine silty sand, which is varies in thickness across the basin. This sand unit is seen in every core except Brow2011_4, which was extracted closest to the eastern boggy area between the lochs. The next lower unit is a transitional unit between the previously mentioned minerogenic unit and the lower organic unit. The transitional unit is seen in Brow2011_1, Brow2011_2, and Brow2011_3, cores that were recovered from the central portion of the loch. Finally, a lower organic gyttja unit is seen in all five of the cores. This layer is loosely compacted and contains slightly large scale macrophytes fragments, ranging from 0.25 cm to 5 cm in length.

Cores from the Loch of Spiggie are also correlated loosely based on stratigraphy. Figure 3.11 illustrates similarities in units along a north – south transect. Spiggie2011_1 and Spiggie2011_3 show similar similarities, with 3 main units. The upper unit is an organic rich layer, similar to the Loch of Brow upper organic rich unit. Underlying this unit is dark grey sand, with shell fragments, and below this is a coarse diamicton. It is unclear based on the units present where Spiggie2011_2, taken from the deep hole, fits into the stratigraphy.

3.2.3 Biogenic Silica

Brow2011_1 and Brow2011_3 were the only two cores that were analyzed for biogenic silica, an indicator of aquatic productivity (Figures 3.3 and 3.5). Brow2011_3 was chosen for this analysis because it was taken from the center of the loch and subsampled the most extensively. Brow2011_1 was selected to have a comparable set of data points. Silica concentrations in the Brow2011_3 are consistent for the upper two units of the core, with values ranging from .01 ppm to 0.45 ppm. Concentrations of biogenic silica increased in the lower gyttja unit, with values ranging from 1.20 ppm to 3.49 ppm. In Brow2011_1, biogenic silica concentrations peak at 35.5cm depth with a concentration of 5.93 ppm. Unlike

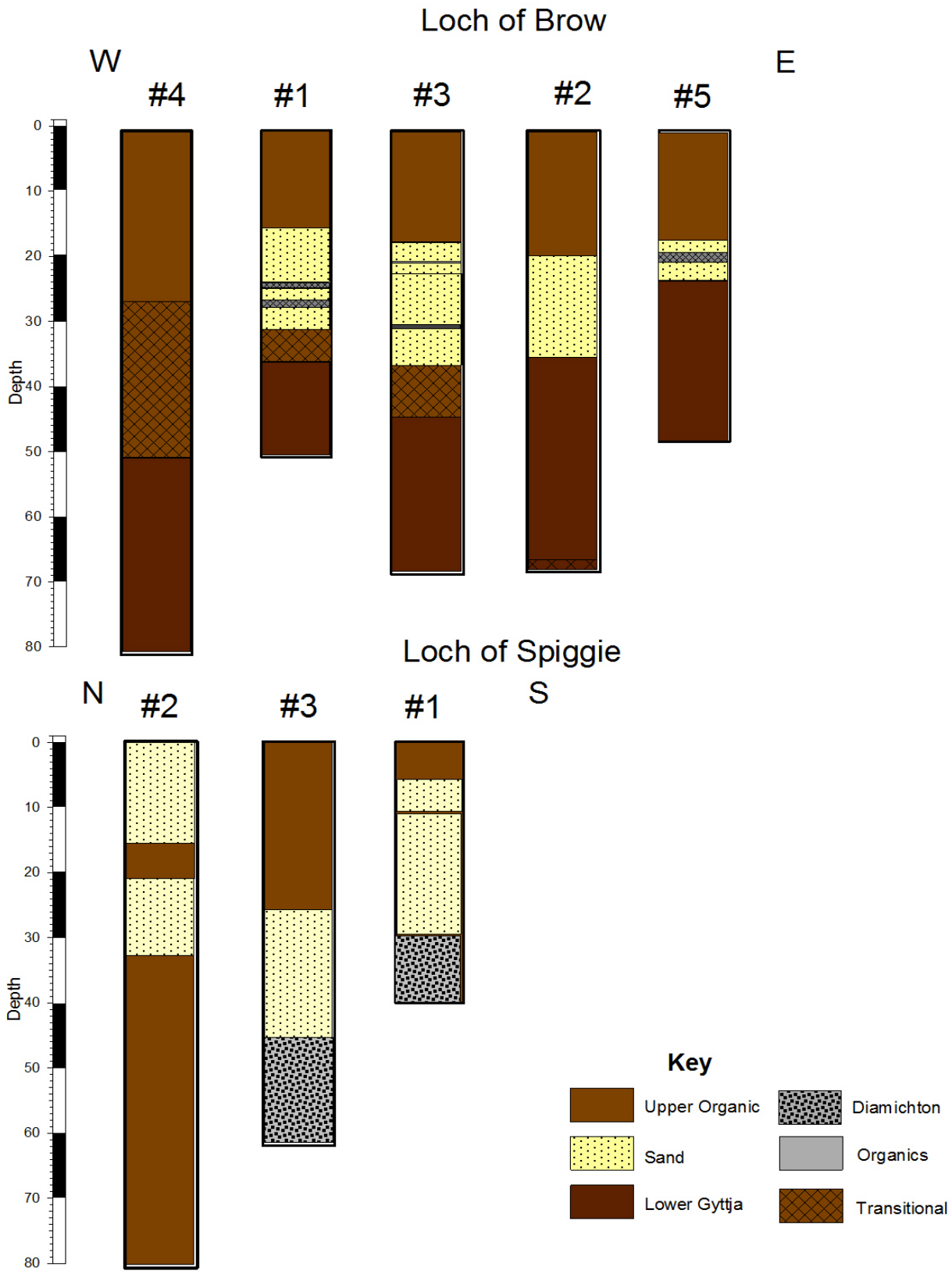

Figure 3.11 Correlation of stratigraphic units within the Loch of Brow. Three primary units have been identified, an upper organic unit, a middle sand unit, and a bottom gyttja unit.

Brow2011_1, a distinction in silica content can be seen between the upper organic unit and the minerogenic unit. A decrease of roughly 2 ppm can be seen on average throughout the minerogenic unit.

3.2.4 Grain Size and Sand/Silt/Clay Percentages

Loch of Brow

The stratigraphy in the Loch of Brow lines up well across the transect of cores extracted and is divided into 3 units, the upper organic unit, the silty/sand unit, and the lower gyttja unit. Grain size and the ratios of sand to silt to clay were variable across the five cores; however they were consistent within stratigraphic units. Average median grain size within the upper organic unit of Brow2011_1 was 51.01 ± 15.4μm. This varied slightly within the corresponding unit in the other 4 cores in the Loch of Brow. Grain size for Brow2011_2 yielded median values of 36.60 ± 7.9 μm; Brow2011_3 yielded an average median value of 33.20 ± 16.4 μm, Brow2011_4 30.37 ± 10.7 μm, and Brow2011_5 yielded a median value of 41.09 ± 5.9 μm. The average median grain size for the upper organic unit across the basin is 38.46 ±11.3 μm, classifying the inorganic component of the unit as silt. The underlying sand unit, absent in Brow2011_4, yields an average grain size of 38.46 ± 11.3 μm (Brow2011_1: 51.02 ± 15.4 μm, Brow2011_2: 36.62 ±7.9 μm, Brow2011_3: 33.21 ± 16.4 μm, Brow2011_4: 30.37± 10.7 μm, Brow2011_5: 41.10 ± 5.9 μm). Finally, the lower gyttja unit had an average median grain size of 27.10 ± 16.8 μm (Brow2011_1: 32.66 ±25.3 μm, Brow2011_2: 31.04 ±23.8 μm, Brow2011_3: 41.93 ± 29.7 μm, Brow2011_4: 18.32 ± 1.7 μm, Brow2011_5: 11.35 ± 3.5 μm). Sand, silt, clay percentages generally varied throughout each core depending on stratigraphy, with the vast majority of particles falling in the silt range.

Loch of Spiggie

Median grain size values for subsamples from Spiggie2011_1 ranged from 45.15 μm to 297.77 μm. In Spiggie2011_2, median grain size ranged from 129.75 μm to 11.33 μm. In Spiggie2011_3, median grain size ranged from 196.2 μm to 10.54 μm. The coarse grained diamicton unit found at the bottom of Spiggie2011_1 and Spiggie2011_3 was not run through the Coulter Counter and was not specifically analyzed for grain size.

3.2.5 Percent Loss on Ignition

Percent Loss on Ignition (%LOI) varied greatly throughout the cores, with an average value within the Loch of Brow of 58.04 ± 16.0 %, spanning a range of values from 27% to 92%. Average % LOI for the organic rich upper unit was 54.23 ± 17.7%, 47.87 ± 9.0% for the minerogenic sand layer, and 70.86 ± 8.6% for the lower gyttja unit. A comparison of %LOI with % organic carbon determined by EA-IRMS analysis should reveal a positive correlation with a slope of 0.4 (Meyer, 1999), given that % organic carbon contributes roughly 40% of all organic matter present within a sample is attributed to carbon. The correlation between these two factors however in the Loch of Spiggie and the Loch of Brow cores was not consistent (Figure 3.12), with low R^2 values seen in all 5 of cores (Brow2011_1 R2= 0.296; Brow2011_2 R2= 0.824; Brow2011_3 R2= 0.480; Brow2011_4 R2= 0.175; Brow2011_1 R2= 0.631). Similar inconsistencies, indicated by low R2 values were seen within the Loch of Spiggie (Spiggie2011_1 R2=0.162, in Spiggie2011_2 R2=0.226, and in Spiggie2011_3 R2= 0.3997).

Poor correlation between %LOI and % bulk organic carbon determined by the EA-IRMS indicates that one of the two factors is not functioning properly. Due to the fact that appropriate % organic carbon yields were recovered from standards on all runs of the EA-IRMS, it is assumed that the %LOI analysis is flawed. Variations in methodology for identifying %LOI in different muffle furnaces on campus, absorption of water between drying sessions, and perhaps even the dewatering of clay minerals at high temperatures may have contributed to the flaws in the analysis (Bengtsson and Enell, 1986; Heiri et al., 2001).

3.2.6 Dry Bulk Density

Dry bulk density values determined from all five cores extracted from the Loch of Brow ranged between 0.08 and 1.17 g/cm3. Density values fell within distinctive ranges within each stratigraphic unit, with average dry bulk density of the upper organic unit 0.44 g/cm3 ± 0.2. Density of the minerogenic middle sand unit yielded a higher average value of 0.76 g/cm3 ± 0.2. Dry bulk density values for the lower organic rich gyttja unit were the lowest of all three units, yielding an average value of 0.18 g/cm3 ± 0.2, where density decreases with depth.

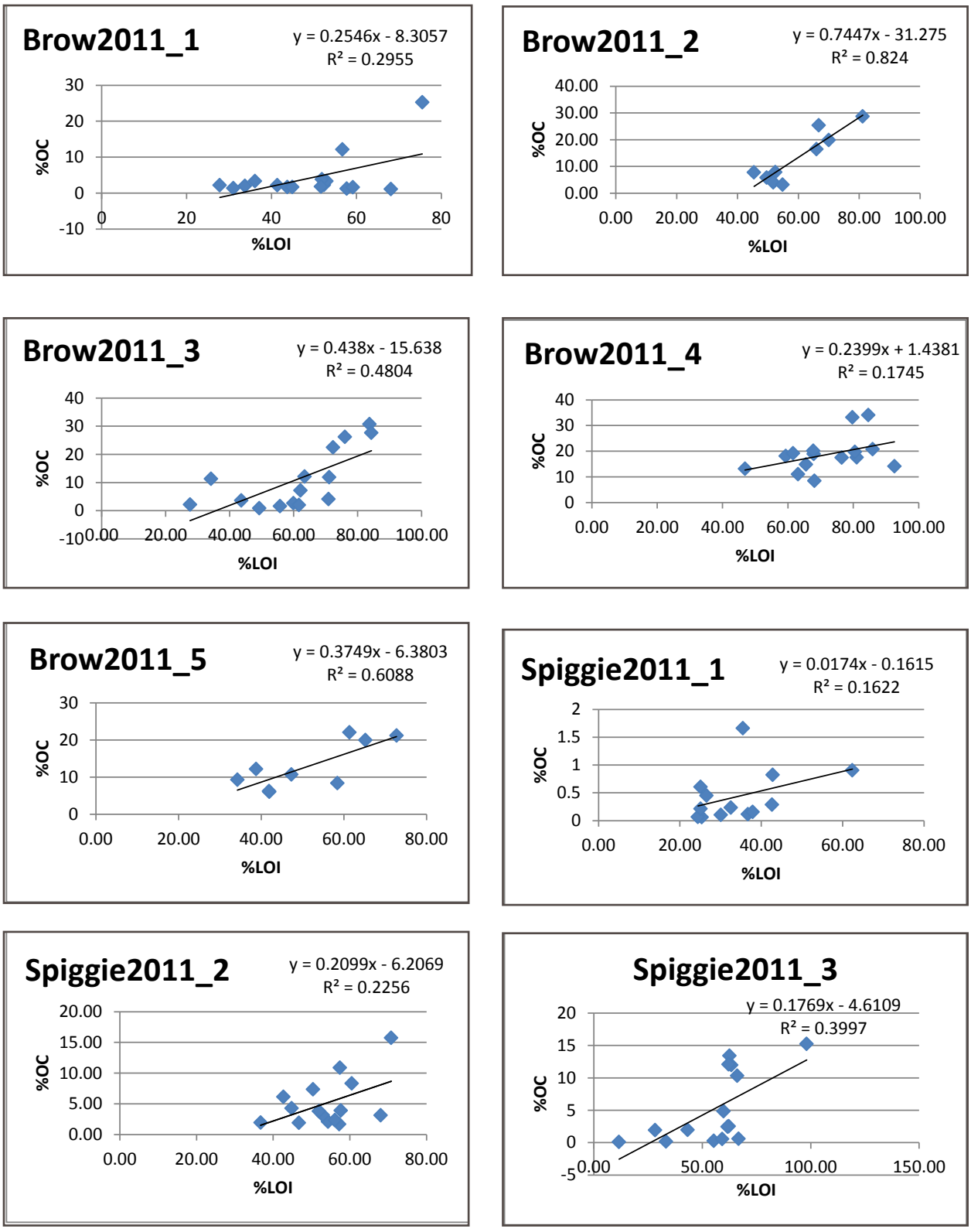

Figure 3.12 Plots of %LOI vs. %OC in all eight cores analyzed. Due to lack of correlation, LOI data will no longer be presented.

Values from the Loch of Spiggie also showed some consistency with stratigraphy. Similarities between the Spiggie2011_1 and Spiggie2011_3 can be seen in the lower diamichton unit. In the lower diamicton unit, an increase in bulk density down core can be observed with values increasing to greater than 1.00 and peaking at 1.72 g/cm3 in the lower unit of Spiggie2011_1. Generally speaking, dry bulk density values were slightly higher on average in the Loch of Spiggie than the Loch of Brow. Measured values for Spiggie2011_1 ranged from 0.892 g/cm3 to 1.729 g/cm3, from 0.194 g/cm3 to 1.019 g/cm3 in Spiggie2011_2, and from 0.166 g/cm3 to 1.325 g/cm3.

3.2.7 Magnetic Susceptibility

A maximum value of 8.2 cgs was measured at 37.5 cm in Brow2011_2. Spikes in magnetic susceptibility were also seen at similar depths in Brow2011_1 (4.68 at 28cm) and Brow2011_3 (4.580 at 35 cm). Increases were also observed in the other two Brow cores in the upper most portion of the stratigraphy, where values peak at 5.21 at 5.5 cm depth in Brow2011_4 and a value of 6.84 at 2.0 cm depth in Brow2011_5. Both of these cores also show a gradual decrease in susceptibility with depth.

Data collected from the Loch of Spiggie show higher bulk magnetic susceptibility within the cores. Core Spiggie2011_1 shows a general decrease in magnetic susceptibility with depth, with the highest value of 10.2 seen at 0.5cm depth in the upper organic unit. There is an additional spike in susceptibility that can be seen at 38 cm, where values increase to 5.7. A decrease in values with depth can also be seen in Spiggie2011_2, where after a spike in susceptibility, where values peak at 12 cm with a value of 108.4, values stabilize close to 0 from depths greater than 26 cm. In Spiggie2011_3, magnetic susceptibility values peaked at 31.52 at a depth of 27 cm. At depths greater than 27 cm, values stabilize close to zero.

3.3 Geochronology

3.3.1 Plutonium Dating

Four sediment cores, Brow2011_2, Brow2011_3, Brow2011_5, and Spiggie2011_3 , were analyzed for 239+240Pu activity(Figure 3.13). None of the cores analyzed yielded a classic rise and sharp Pu peak that can be correlated to the period between 1952 and maximum bomb testing in 1963 (Ketterer, 2004). Instead there are several spikes in Pu concentrations within the sampled section of the cores. A maximum age of sediments can however be obtained, as Pu concentrations do return to pre-bomb levels in all four of the sampled cores. The main Pu peak, signaling the period between 1952 and 1963, is variable in all four cores with a maximum age depth in Brow2011_2 occurring at ~7.5 - 8.0 cm depth, occurring between 1.5-7.0 cm in Brow2011_3, in Brow2011_5 between 1.5- 5.5 cm, and in Spiggie2011_3 between 2.5-6.5 cm. Unfortunately though, the depths at which concentrations of plutonium return to pre-bomb levels is not consistent amongst the Brow cores. Due to inconclusive Pu dates, units will from here on be referenced in terms of depth and stratigraphy rather than age, as no appropriate model could be constructed from the available data.

3.4 Geochemical Analysis

The following sections will present data from geochemical analyses conducted on sediment cores from Brow2011_1 (Figure 3.14), Brow2011-2 (Figure3.15), Brow2011_3 (Figure 3.16), Brow2011_4 (Figure 3.17), Brow2011_5 (Figure 3.18). Data from the Loch of Spiggie will be presented briefly (Figures 3.19-3.21).

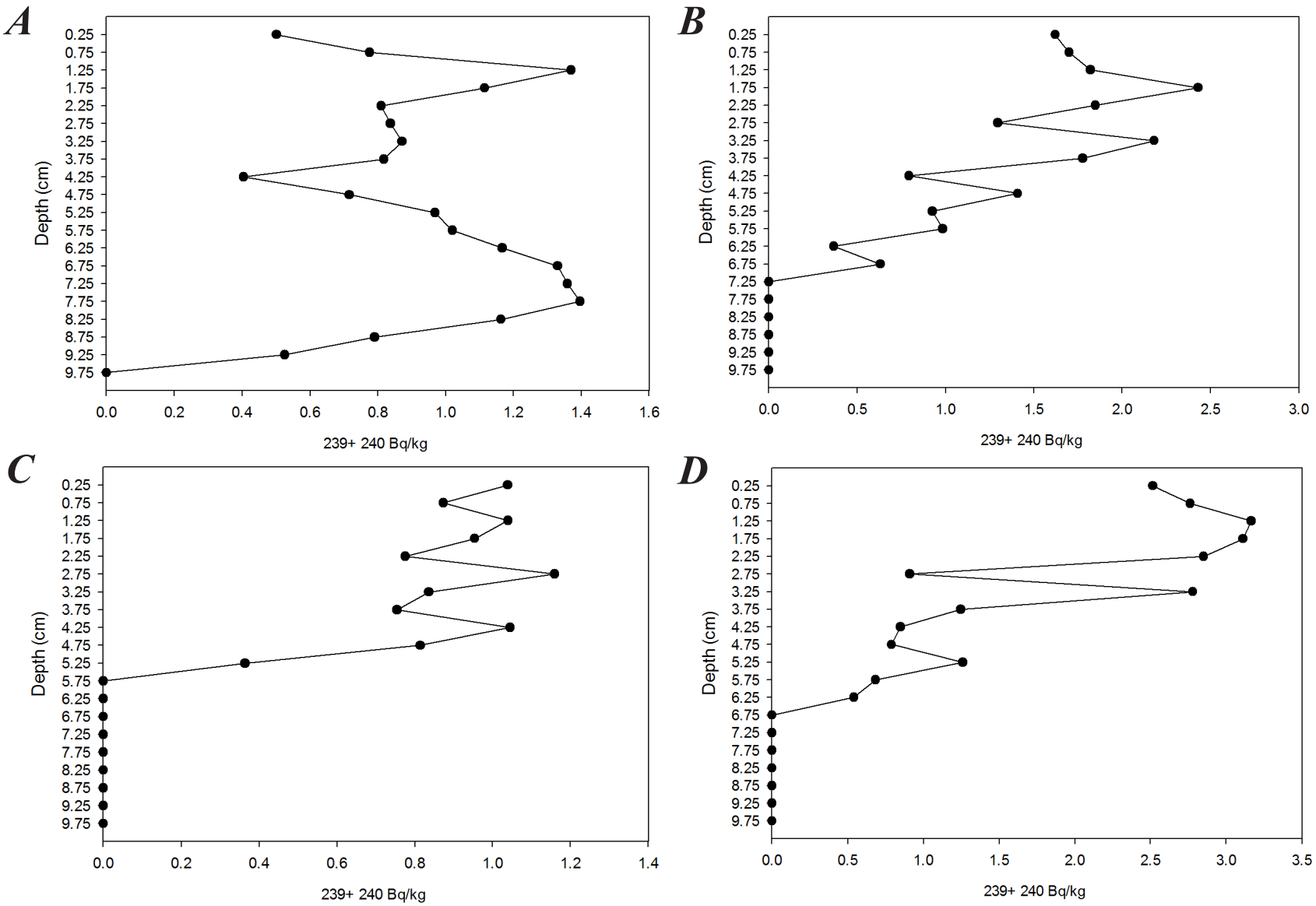

Figure 3.13 Plot of Pu concentrations versus depth for the top 10 centimeters of Brow2011_2 (A), Brow2011_3 (B), Brow2011_5 (C), and Spiggie2011_3 (D). Data plotted are reflective of samples taken at 0.5 cm intervals.

3.4.1 $\delta^{13}C$

$\delta^{13}C$ values remained relatively consistent throughout the 5 cores, yielding an average value of -27 to -28.5‰. In Brow2011_1, $\delta^{13}C$ ranged from -25.9‰ to -28.3‰. Values were generally consistent around -27‰, with the exception of a slight enrichment at 7.5 cm, where a δ13C value of -25.9‰ was measured. In Brow2011_2, values remained relatively homogenous throughout the core with measured values ranging from -27.4‰ to -28.5‰ throughout the core. Brow2011_3 values ranged from -26.7‰ to -28.5‰, with a slight enrichment seen in the lower gyttja unit. Brow2011_4 was slightly anomalous ranging in values from -24.8‰ to -31.3‰, with a noticeable depletion at 50.5 cm followed by a sharp enrichment peak at 67.5cm. Values for the rest of the core remain homogenous. Brow2011_5 also spans a slightly larger range of values from -27.6‰ to -31.5‰, with a $\delta^{13}C$ depletion seen between 27.5-33.5 cm.

3.4.2 δ^{15} N

Generally speaking $\delta^{15}N$ values gradually increased up core independent of stratigraphy. The highest recorded values of 4.5- 5.5‰ were seen at the top of all cores. In Brow2011_1 $\delta^{15}N$ values ranged from 1.5‰ at the base of the core to 5.1‰ at the top, in Brow2011_2 from 1.4‰ to 5.0‰, in Brow2011_4 data points ranged from -0.4‰ to 4.9‰, and in Brow2011_5 values ranged from 0.5 to 4.7‰. Brow2011_3 illustrated a slightly smaller enrichment up core, with values peaking at 3.1.

3.4.3 Percent Organic Carbon

Organic carbon concentrations seen within the Loch of Brow are dependent on both stratigraphy and location within the loch. In Brow2011_1, an increase in %OC in the lower gyttja unit paralleled increases in %N at equivalent depths. Brow2011_2, showed %OC increasing in the lower gyttja unit with values averaging 24%, a similar trend can be observed in Brow 2011_3, where %OC peaked at 30.7% at 43.5 cm depth. In Brow2011_4, %OC values spiked at 41.5 cm and decreased at 12 cm. Finally, in Brow2011_5 %OC values obtain indicate a significant decrease within the minerogenic units between 18-23 cm.

3.4.4 Percent Nitrogen

In general, very low nitrogen values were seen throughout the Loch of Brow. In Brow2011_1 values displayed a slight increase in the amount of nitrogen with depth. This increase at the base of the core mirrors an increase in organic carbon content. Brow2011_2 showed similar trends, with a slight increase in nitrogen content in the lower gyttja unit. Values obtained from Brow2011_3, Brow2011_4, and Brow2011_5 show noticeable correlations between nitrogen content and stratigraphy.

3.4.5 C/N Ratios

C/N ratios in the Loch of Brow range between 12.6 and 27.9 across the basin. In Brow2011_1, data points were not plotted at depths of 7.5 cm and 43.5 cm due to the fact that the isotopic data presented for these depths is a composite of two different runs through the EA-IRMS. Ratios in Brow2011_2 ranged display a slight increase at the top of the core. Values in Brow2011_3, Brow2011_4, and Brow2011_5 spanned a wide range of values.

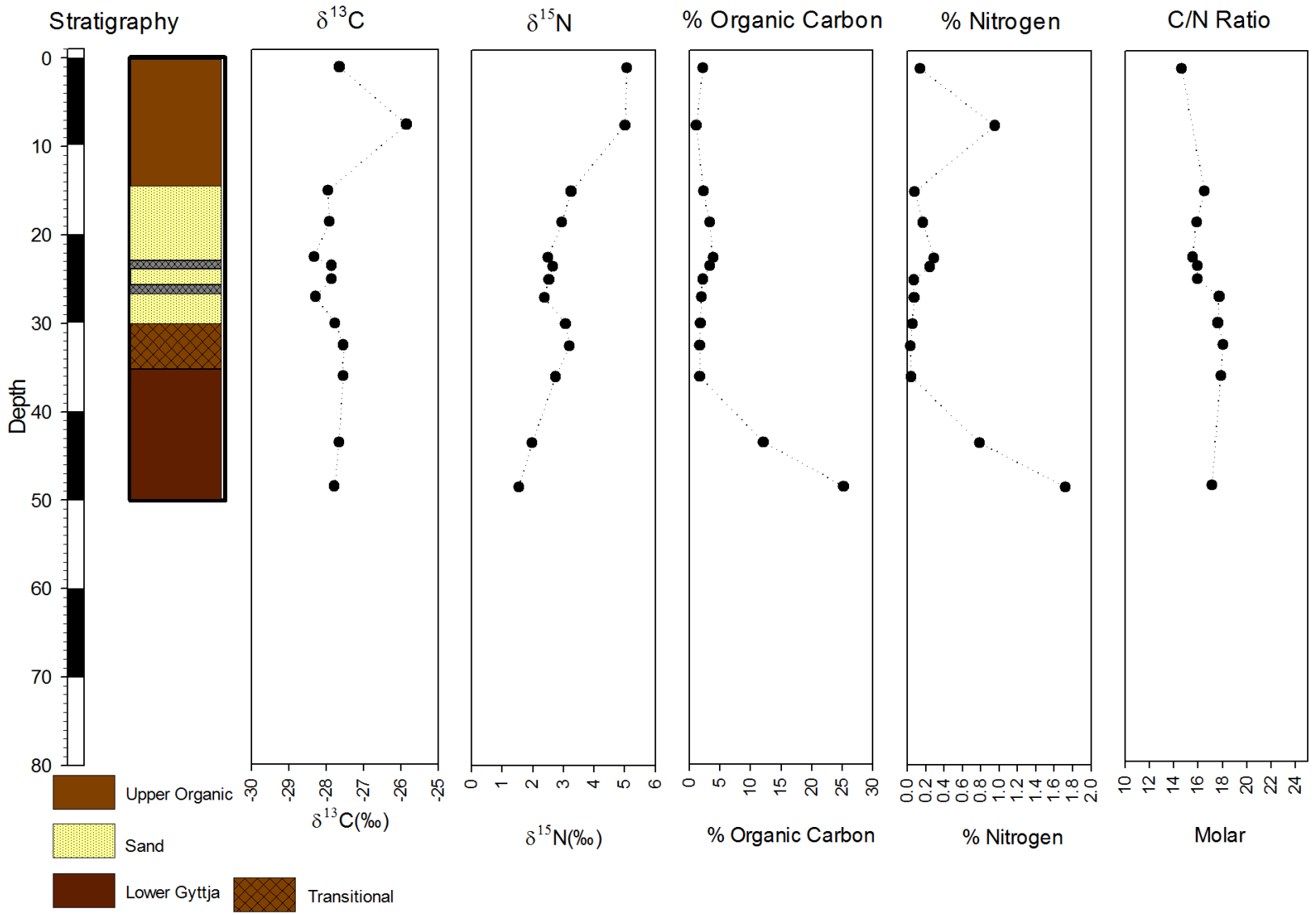

Figure 3.14 Summary figure of geochemical analyses conducted on Brow2011_1.

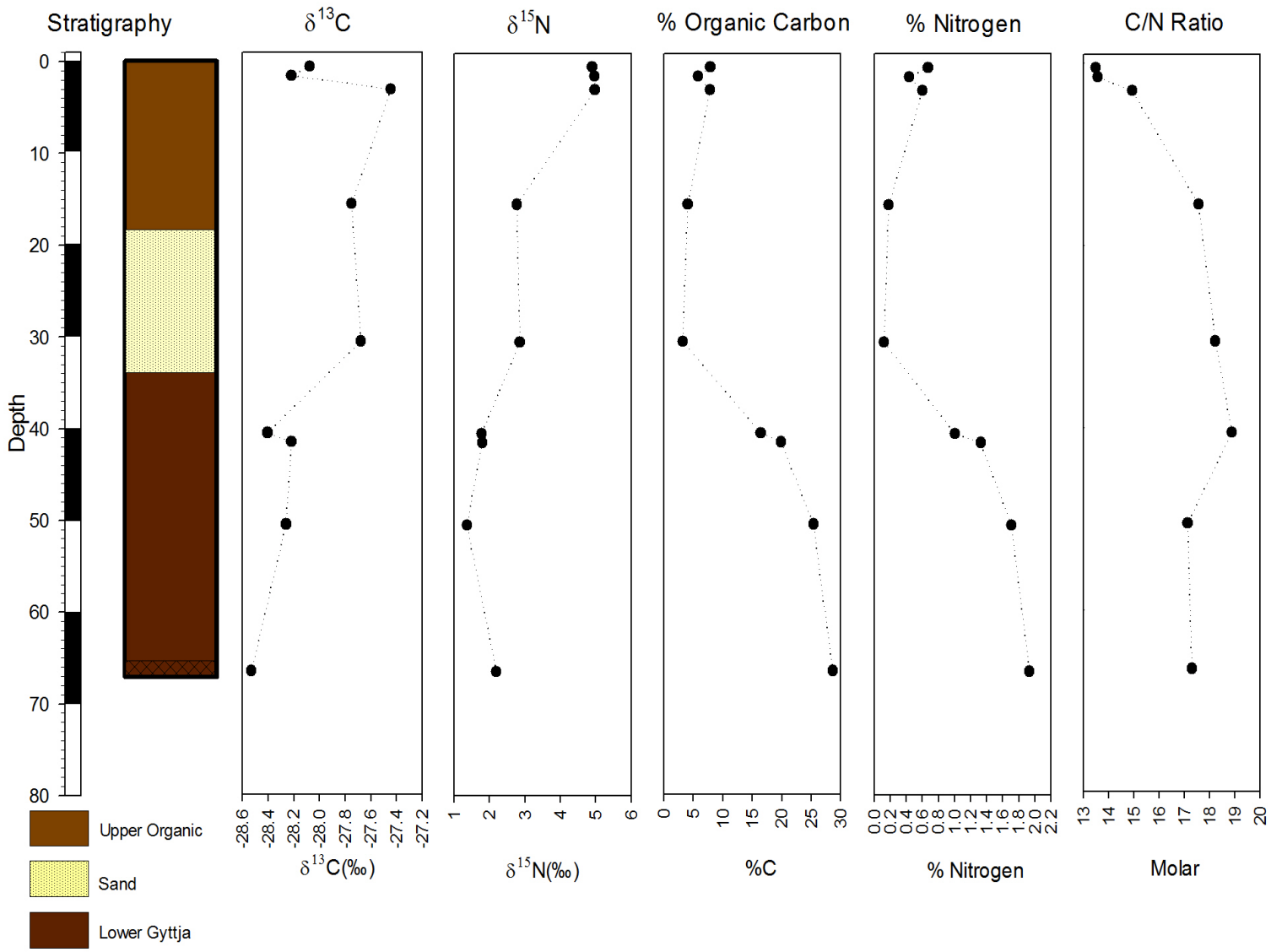

Figure 3.15 Summary figure of geochemical analyses conducted on Brow2011_2.

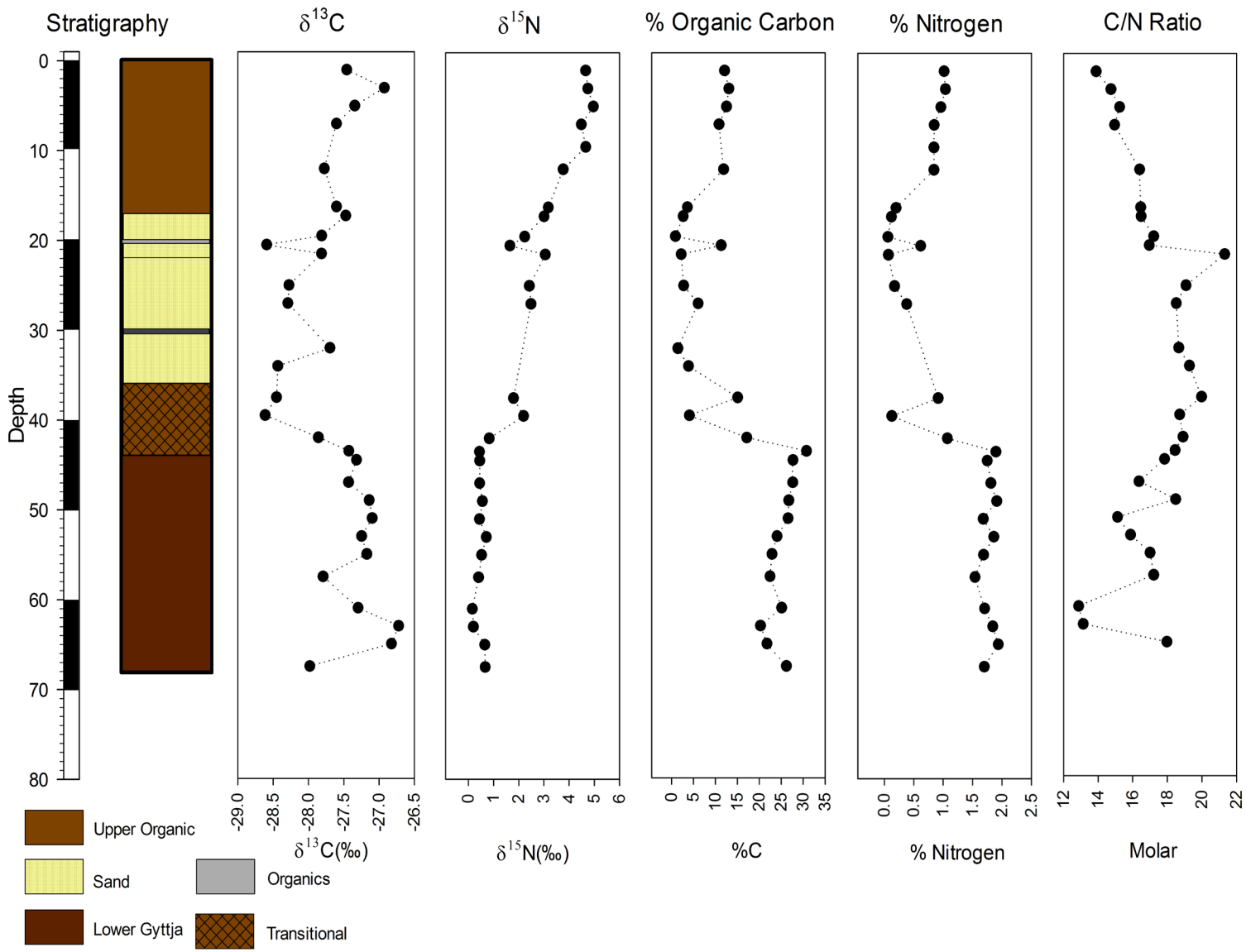

Figure 3.16 Summary figure of geochemical analyses conducted on Brow2011_3.

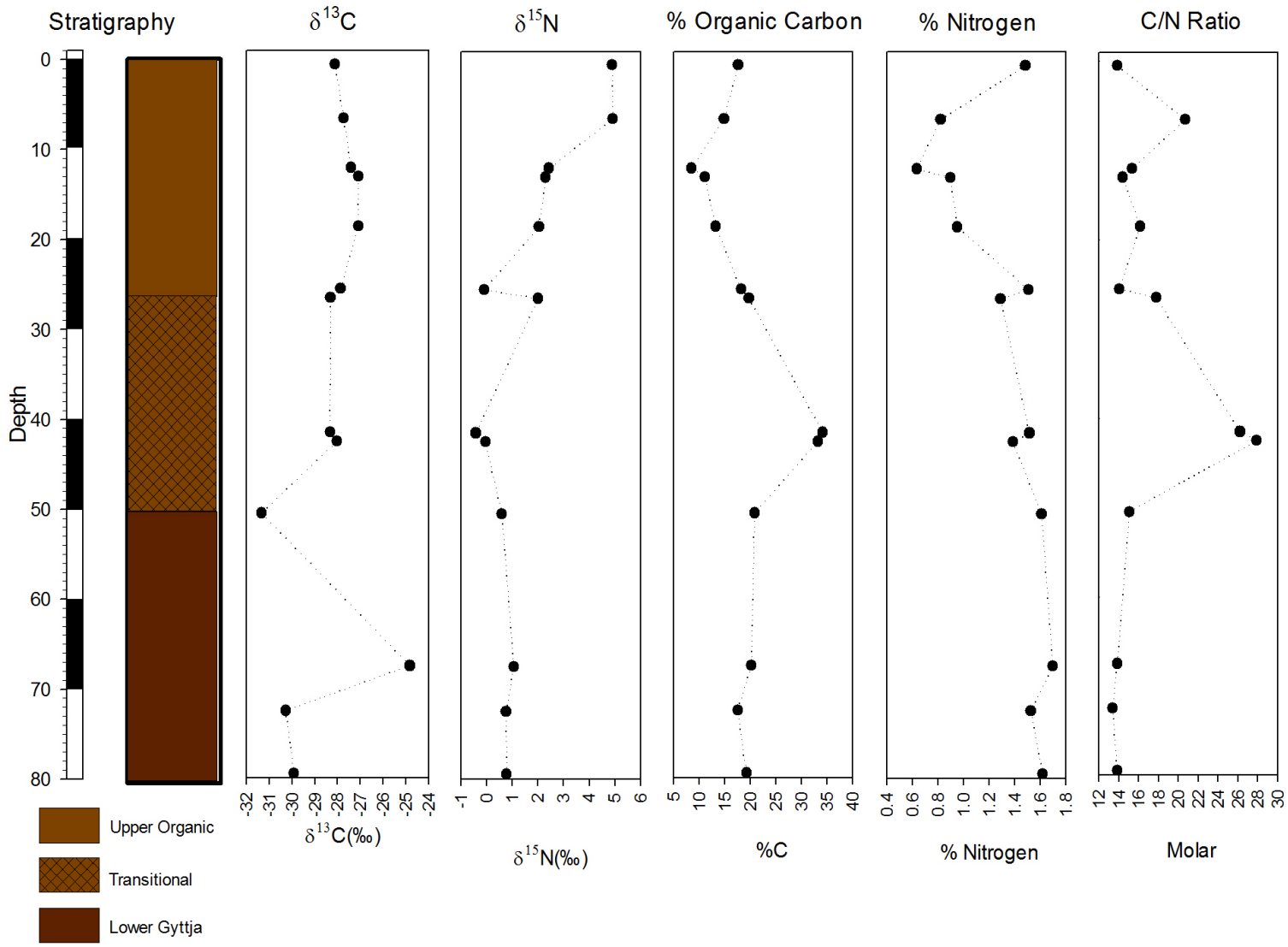

Figure 3.17 Summary figure of geochemical analyses conducted on Brow2011_4.

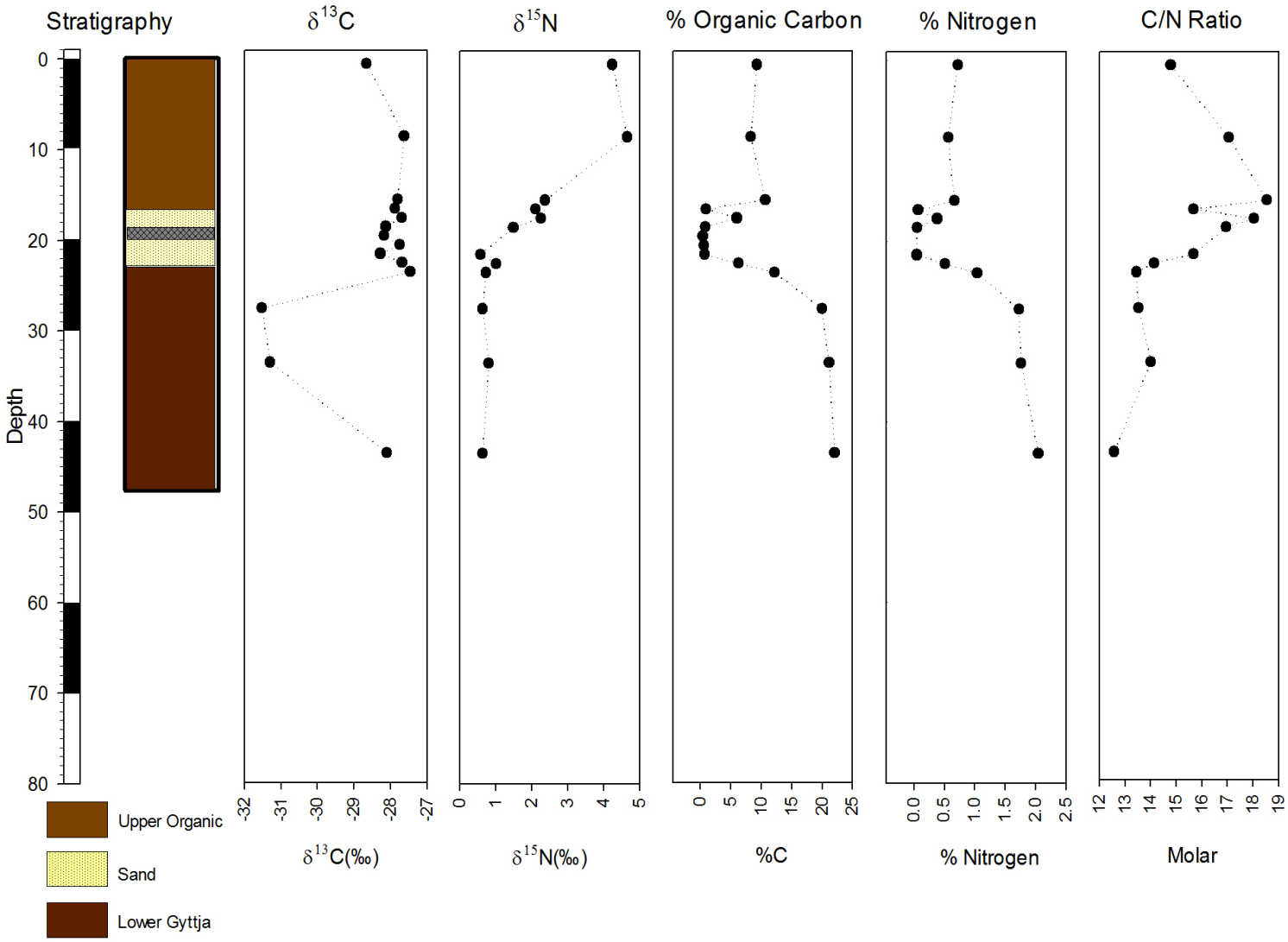

Figure 3.18 Summary figure of geochemical analyses conducted on Brow2011_5.

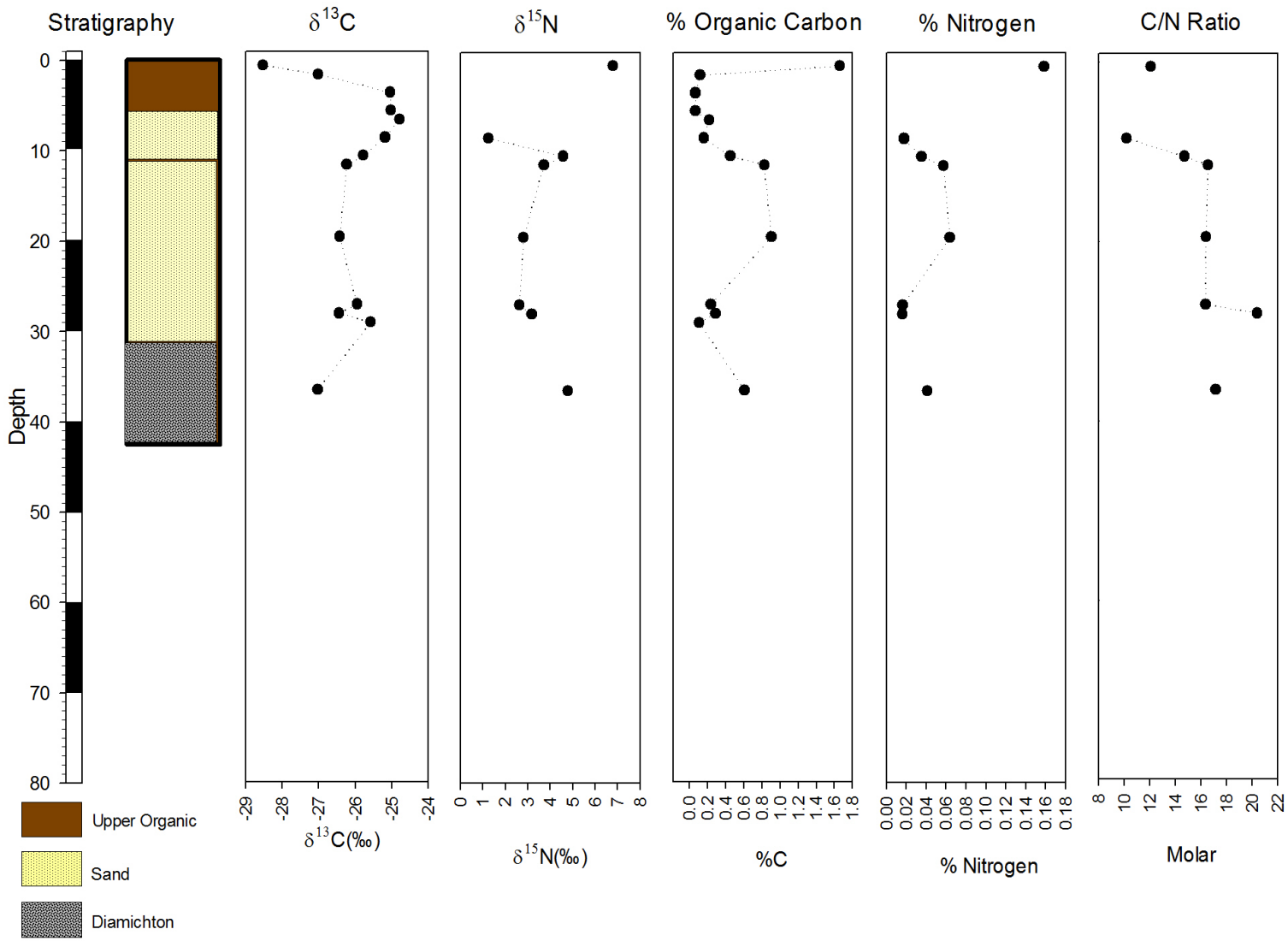

Figure 3.19 Summary figure of geochemical analyses conducted on Spiggie2011_1.

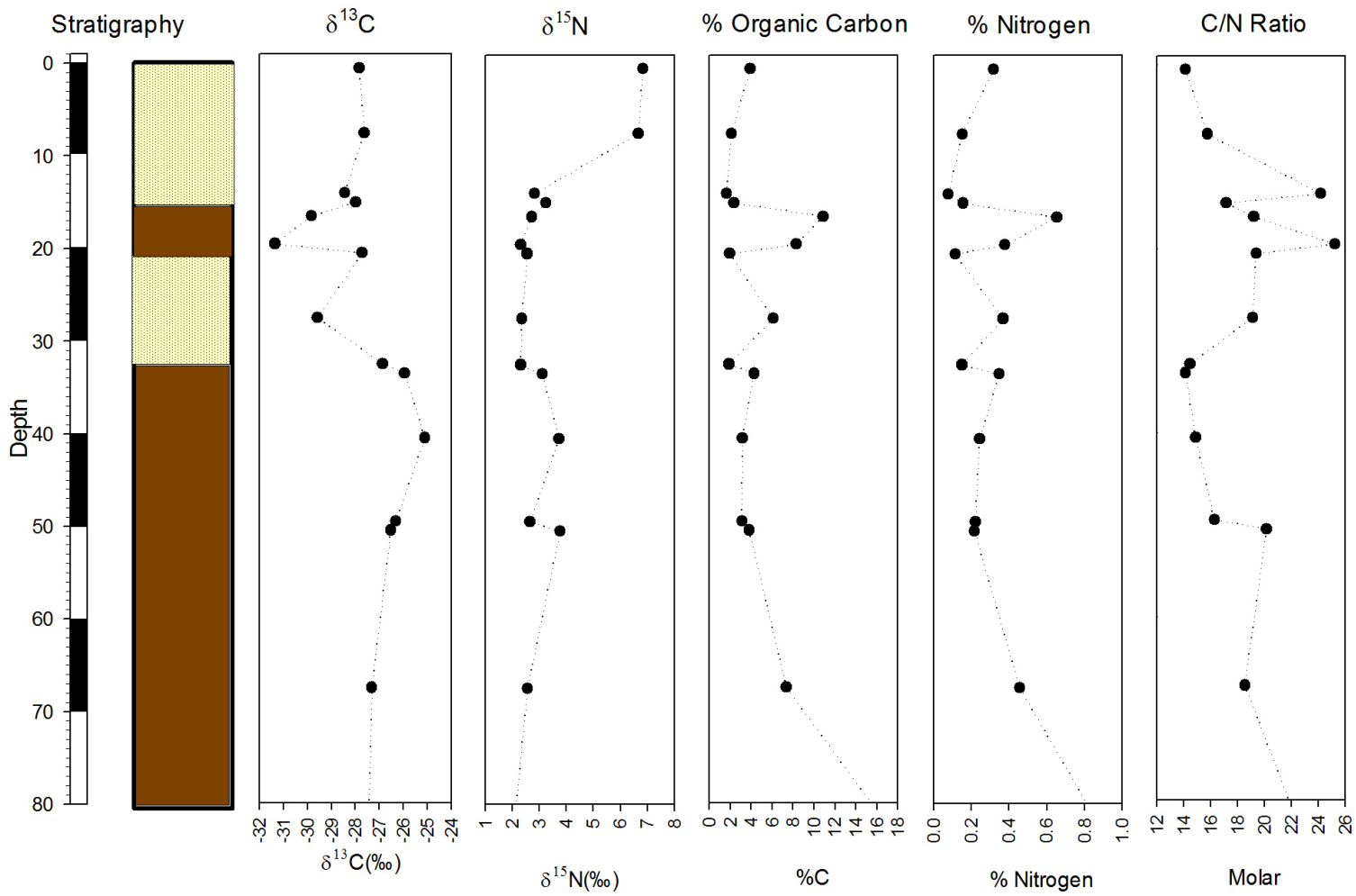

Figure 3.20 Summary figure of geochemical analyses conducted on Spiggie2011_2.

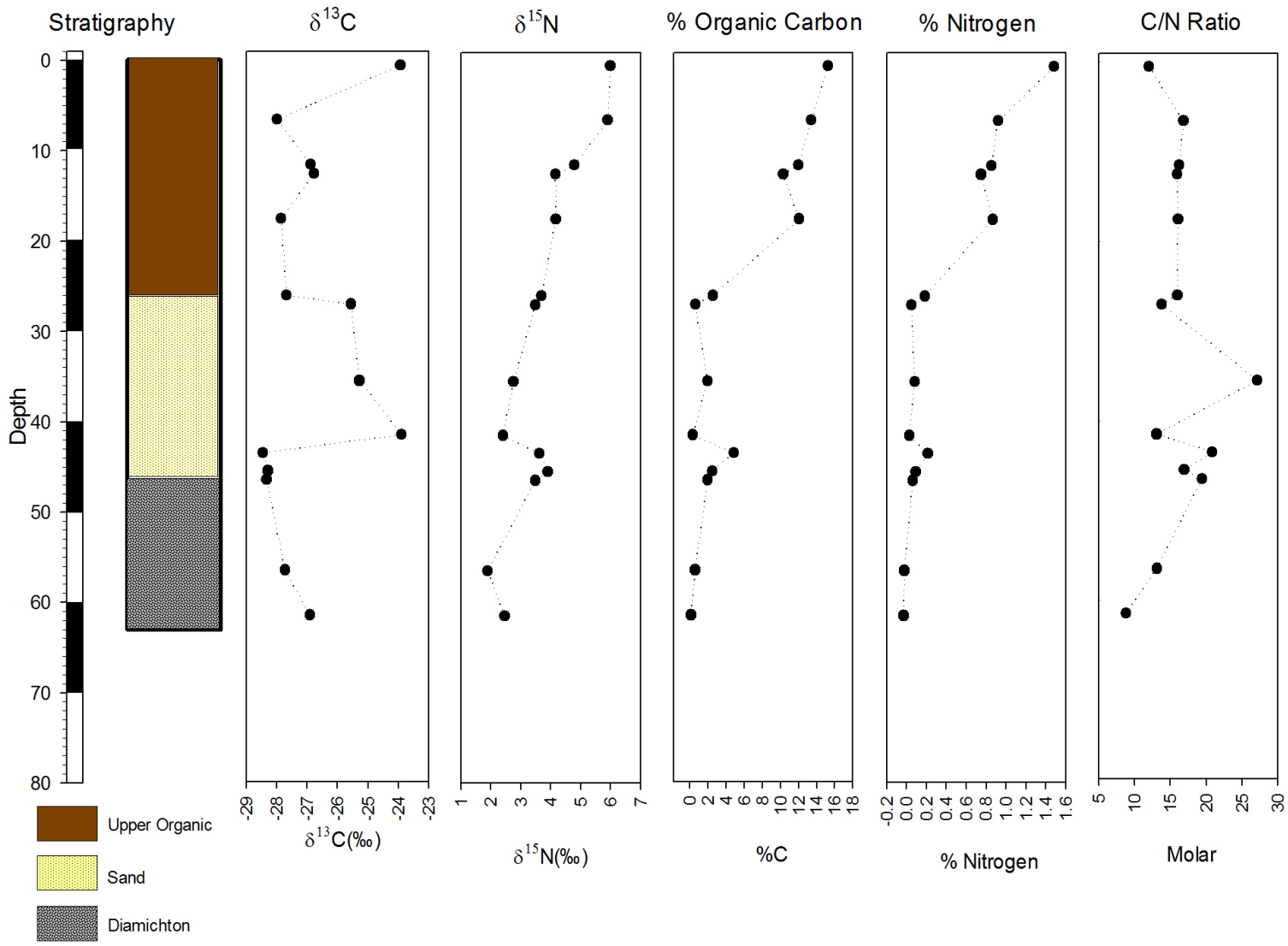

Figure 3.21 Summary figure of geochemical analyses conducted on Spiggie2011_3.

Chapter 4:

Discussion

4.1 Chronology

A definitive and reliable chronology for study area sediments was not obtained from plutonium dating of the upper 10 cm of sediment from four different cores. In all four of the sediment cores sent to Prof. Michael Ketterer at Northern Arizona University, a clear peak in Pu concentrations is not visible and can likely be attributed to bioturbation in this shallow loch (Figures 3.13). In a standard analysis of sediments, undisturbed by biological activity, there is a clear peak in Pu concentrations, indicating the 1952 onset of nuclear testing and the 1963/64 weapons test fallout maximum (Ketterer, 2004). However, in all four of the cores sampled, there were multiple spikes in Pu concentrations before activity levels were reduced to pre-bomb levels, close to zero. Due to these fluctuations only a minimum and maximum age for sediments was obtained (Table 4.1). This variability provides a large time frame in which sediments could have been deposited.

Mazur (2006) also sampled sediment cores extracted from the Loch of Brow and obtained AMS ^{14}C dates on dried macrofossils obtained from two stratigraphic horizons in her Core 9, bracketing the minerogenic layer. Mazur's Core 9 was taken from the center of the loch in close proximity to this study's equivalent core, Brow2011_3. In this analysis, Mazur sampled 4 cubic centimeters of sediment, rinsed it in distilled water with a 4.0ϕ sieve, and removed any remaining macrophytes. Dried macrophytes were then sent to Geochron for dating. Sediments at 19.5-20.5 cm depth, the upper boundary of the minerogenic layer, yielded an age of 810 ± 50 yr BP, while a sample at 51-52 cm depth, the bottom of the same unit, yielded an age of 4840± 50 yr BP. Calibrated calendar dates translate to the time period between 1186-1268 C.E. for the upper sample and 3694-3534 B.C.E. for the lower sample (Stuiver and Reimer, 1993 (version 6.0)). The AMS ^{14}C dates obtained by Mazur's analysis do not support the timing of hypothesized simultaneous deposition of the sand layer and burial of the Broo Site, as dates proposed by Mazur span an earlier 4000 year period while deposition of sand at the Broo site was confined to a much shorter and later time interval. It is possible that these sediment dates may be connected

to settlement and consequential destabilization of the landscape at nearby Scatness during the Pictish Iron Age (~200-400 CE), however further analysis is needed for conclusive remarks.

Sedimentation rates calculated from both minimum and maximum Pu peaks were used to extrapolate the age of the upper and lower boundary of the minerogenic unit in the Loch of Brow. The shallowest and deepest depths at which the 1952 onset of plutonium could potentially be seen were divided by the 60 year time interval that has passed. Calculated ages for the upper boundary of the sand unit varied from 110 to150 years BP, while ages from the lower boundary of the sand unit range from 552 to 331years BP. These dates roughly translate into the period between 1460 and 1910 CE. Sedimentation rates across the basin may appear to be variable, however if the uncertainty associated with this particular set of analyses is taken into consideration sedimentation rates across the basin all fall within the same range. Pu dates from the Loch of Spiggie also fit into the same time period.

AMS dates from the top of the minerogenic unit in Mazur's cores, on the other hand, yield a date of ~1190 CE. It appears that the Mazur dates are artificially elevated due to the uptake of "old carbon" by the plants that were dated, something that is difficult to detect independent of another more reliable chronology (MacDonald et al., 1991). Issues of the reliability of radiocarbon dating are well documented in lakes that are in a calcareous, coal-bearing, and graphite-rich bedrock, but they can also be altered in lakes with low residence times (i.e. the reservoir effect), spring fed lakes whose water supply travels through ^{14}C enriched bedrock, and in recently deglaciated areas (MacDonald et al., 1991; Riggs, 1984; Sutherland, 1980). In the case of the Lochs of Brow and Spiggie, water supply entering the lochs runs through an area of calcareous bedrock (Figure 1.2).

Other information that is important to consider are dates from artifacts at the Broo site, which yielded ages between 1680 and 1720 (Table 4.1; Bigelow, 2011). Additionally, OSL dates on the interior walls of the Broo site indicate ages between 1670-1680 CE ±30 years. While AMS^{14}C ages do not for the most part fall within the time frame of Broo's burial and Pu dates yield a time frame that may or may not synchronize with the late 17th c., the distinctive sand layer seen in the

Loch of Brow cores could still be tied to the inundation of the Broo Township. Bioturbation of sediments could have contributed to disruption of the plutonium record and the absorption of old carbon from the plants that were ultimately sampled by Mazur (2006) could have contributed to artificially old dates. A lack of synchronization between the two proxies seems to indicate that geochronology within the upper units of the Loch is flawed.

Sample	Min Sed Rate	Max Sed Rate	Approx. Age of the Upper Boundary of the Minerogenic Unit	Dating Method Used
Brow2011_2	0.25 mm/yr	1.625 mm/yr	b/n 110-552 years BP (1902-1460 CE)	$^{239+240}$Pu
Brow2011_3	0.5 mm/yr	1.2 mm/yr	b/n 119 - 552 years (1893-1460 CE)	$^{239+240}$Pu
Brow2011_5	0.25 mm/yr	1.0 mm/yr	b/n 150 – 331 years (1862-1681 CE)	$^{239+240}$Pu
Spiggie2011_3	0.4 mm/yr	1.12 mm/yr	n/a	$^{239+240}$Pu
Mazur(2006)	42 yrs/cm	n/a	810 years BP (1186- 1268 CE)	AMS ^{14}C
Mazur(2006)	93 yrs/cm	n/a	4840 years BP (3694- 3534 BCE)	AMS ^{14}C
Artifact from Broo Site: Delft Merry Man Plate	n/a	n/a	1690-1715	Artifact Dating
Artifact from Broo Site: 9 Kaolin Pipe Stems 5.5-6\64 inch	n/a	n/a	1680-1720	Artifact Dating
Broo Site 1 Enclosure Wall	n/a	n/a	1670 ± 30	OSL
Broo Site 1 Structure Interior	n/a	n/a	1680 ± 30	OSL
Broo Site 1 Structure Interior	n/a	n/a	1717 ± 30	OSL

Table 4.1
Summary of various attempts to establish chronologies on materials from the Broo Site and surrounding lochs. Dating techniques employed thus far include $^{239+240}$Pu, AMS ^{14}C, OSL, and the dating of artifacts. Analyses of ^{210}Pb concentrations within the sediment cores is in progress.

4.2 Loch of Brow

4.2.1 Limnology

The Loch of Brow is a shallow lake, with a well-mixed water column at the end of May when sampling occurred (Figure 3.2). Assuming that similar conditions exist for the remainder of the year, a logical assumption given the minimal variability in average daily temperature throughout the year and frequency of wind events regardless of the season (Roy, 1993), stable temperature, dissolved oxygen, and salinity profiles indicate a well-mixed continuous cold polymictic lake (Lewis Jr., 1983). Continuous cold polymictic lakes are characterized by seasonal ice cover and during the ice free months of the year, constant mixing that does not allow for temperature stratification (Lewis Jr., 1983). The small size of the Loch of Brow and the frequency of wind allows for the frequent turnover of water in the loch during most of the year. While Shetland does not experience a particularly bitter winter, the loch does freeze over for part of the winter season (Harold Sunderland, personal communication, 2011).

4.2.2 Sedimentary Data

Within the transect of cores across the Loch of Brow, a distinct minerogenic sand layer can be seen in four of the five sediment cores. It was hypothesized that this sand layer is directly connected to the sand blows that inundated the Broo site and this section will seek to establish the correctness of the hypothesis, and to what extent it can be determined where the sand unit originated.

Grain size increases within the sand unit towards the eastern side of the loch. Here the coarsest particles can be found within Brow2011_5, the core farthest east and closest to a beach that contains red stained sediments (likely related to the Old Red Sandstone). Additionally, the sand unit of interest also thinned towards the east.

The thinning of sand to the east and the general increase in median grain size towards Brow2011_5 (Figure 3.7) are important to bear in mind when thinking about the sourcing of sand. Since the prevailing wind direction in the area is from the southwest (Wheeler and Mays,

1997), grain size should decrease across the loch, with the largest sand grains seen in the west and the smallest in the east. Since this is not the observed trend, a few other possibilities exist. One includes the transport of sand during a storm event where the winds were blowing from the east. This would account for the variations in grain size, but does not account for an eastern source of sediment. Sand in this scenario is not the same as the Quendale dunes that buried the Broo Site, but rather sand generated from the erosion of groundcover somewhere in the eastern upland area of the loch. If over-cultivation and over-grazing occurred in the upland area (Figure 3.1), it would provide an eastern source for the sand seen in the Loch of Brow. A current parallel to this type of erosion is not seen in Shetland today, nor does a source of sand lie to the east. Beaches from the eastern portion of the study area tend to be rocky, not the medium grained sand seen along the southern and western coastal boundaries of the study area. Finally, it is possible that the sand in the loch is not from an aeolian event, but from the erosion and transport of the beach, located on the eastern side of the loch.

4.2.3 Geochemical Data

C/N Ratios

The C/N ratio of aquatic systems is governed by the mixing of both terrestrial and autochthonous organic matter (Meyers, 1997; Thornton and McManus, 1994; Ostrom and Macko, 1992). C/N values span a wide range across the two lochs, falling between 8 and 31, indicating that at some points in the sedimentary record there has been a combination of aquatic and terrestrial sources of organic matter, while at other points either aquatic or terrestrial sources dominate. Terrestrial inputs of organic matter span a wide range of C/N ratios, but it is widely accepted that values greater than 12 to17 are associated with terrigenous inputs (King et al., 2008; Graham et al., 2001; Thornton and McManus, 1994; Orem et al., 1991), while values less than 10 tend to indicate a phytoplankton origin (Thornton and McManus, 1994; Biggs et al., 1983).

C/N ratios are generally elevated within the sandy minerogenic unit offering evidence that the origin of the organic matter entering the loch was terrestrial. During the time of sand deposition the influx of organic material into the loch far exceeded the rate of production of

organic material within the water column. This may represent movement of soil organic matter into the basin. C/N ratios also decrease towards the top of many cores, as there is a shift from a more terrestrial signal to a more aquatic signal at the top, likely reflective of an increase in primary productivity or the presence of ruminant animals.

Stable Carbon Isotopes

Bulk isotopic data point to terrestrial productivity as the primary input into the Loch of Brow. Several different indicators show that the origin of organic material within each of the cores is terrestrial. $\delta^{13}C$ values ranged from -24.84‰ to -31.52‰ across the basin with an average value of -27.97 ‰. O'Leary (1988) and others including Fogel and Cifuentes (1993) state that the accepted stable carbon isotopic signature of C_3 plants (the photosynthetic pathway employed by ~75% of terrestrial plants) averages -27‰ (with a range of 12‰). Since the pasture land surrounding the lochs is comprised of C_3 plants, it seems likely that the organic inputs into the Loch of Brow are coming from the surrounding pastureland and to a lesser extent lacustrine productivity within the water column. The observed values from across the Loch of Brow fall closer to this range, far from the -12‰ to -16‰ range that is observed for plants of an aquatic origin (O'Leary, 1988).

$\delta^{13}C$ values for the five Brow cores tend to be fairly homogenous, fluctuating within 1‰ of each other (mean δ13C: Brow2011_1 -27.8‰, Brow2011_2 -28.1‰, Brow2011_3 -27.7‰, Brow2011_4 -28.1‰, Brow2011_5 -28.4‰), with a few exceptions. In Brow2011_1, there is one point of enrichment in the upper organic rich unit of the core at 7.5 cm. Only 1 other data point in the entire set of Brow cores showed a similar enrichment of ^{13}C, a subsample from Brow2011_4 at 67.5 cm depth with a value of -24.83‰. These two subsamples are not constrained within the same stratigraphic unit and are anomalous to both surrounding samples and similar stratigraphy. These could potentially reflect an influx of marine organic matter. On the other hand, these values could be reflective of a shift in $\delta^{13}C$ values that signals colder temperatures at this horizon. Lower temperatures are associated with increased rates of gas dissolution and consequently more dissolved carbon dioxide become available to aquatic plants. Greater availability of carbon

dioxide, leads to a fractionation in carbon isotope values that may be reflected with this shift (Zhang et al., 1995; Freeman and Hayes, 1992). It is possible that this is reflective of an increase in aquatic inputs. Further evidence of this relationship can be seen in the C/N ratios, where a decrease in values at the same stratigraphic horizon indicates a mix of organic matter. Lower C/N ratios, in conjunction with an enrichment in $\delta^{13}C$ could be connected to an increase in phytoplankton. There were 5 horizons with $\delta^{13}C$ values significantly depleted relative to the average, 3 of which occur in the lower gyttja unit of Brow2011_4 and 2 of which occur in the gyttja unit of Brow2011_5. Increased rates of depletion at these two sites is interesting as they represent the two points closest to shore, but on opposite ends of the lake. Additional measurements of the isotopic ratios of sediments from these horizons are needed to confirm either theory.

Stable Nitrogen Isotopes

$\delta^{15}N$ values within the Loch of Brow show an up-core enrichment of ^{15}N which seems to operate independent of the stratigraphy and is seen in all five of the Loch of Brow cores. With nitrogen signatures peaking in values at the top of the core near 5‰, it seems likely that there are additional inputs of nitrogen into the system other than from the deposition of plant matter. Elevated $\delta^{15}N$ for nitrogen in a lacustrine setting have been associated with the presence of fecal matter from humans and animals, as well as fertilizer inputs (Macko and Ostrom, 1994; Fogel and Cifuentes, 1993). With values from these additional terrestrial sources ranging from 10‰ to 22‰ for human and animal waste (Valiela et al., 2000; Herbel and Spalding, 1993), to a 3‰ to 12‰ in the case of organic soil nitrates (Tiessen et al., 1984), the Brow catchment appears to be influenced by at least one of these sources. Further analysis to determine the sourcing of the bulk organic matter using lipid biomarker analysis for coprostanol and n-sterols would allow for confirmation of this hypothesis and the exact sourcing of organic matter (Tygai et al., 2009; Tygai et al., 2008; Evershed et al., 2006; Bull et al., 2002; Simpson et al., 1999a; Bull et al., 1999; Simpson et al., 1999b).

The up-core enrichment seen in all five cores from the Loch of Brow indicate that there is an influx of enriched nitrogen entering the system, likely through 3 small inlet streams that wind their way through the upland pastures. This seems to indicate a trend in the predominance of agriculture on the landscape independent of the sand blows. If trends were to parallel stratigraphy, a correlation could be made between an increase in agriculture and destabilization of the dunes, as the isotopic record of the lake would show a gradual increase in $\delta^{15}N$ from baseline up to the bottom of the sand unit. These values would then drop significantly, concurrent with massive and rapid sedimentation of the lake. Finally, once agricultural practices resumed on the landscape, $\delta^{15}N$ values would increase to contemporary levels. This scenario may or may not be the case, as other reasons for the lack of an enriched $\delta^{15}N$ signal during the sand blows include high mobilization of sand and rapid sedimentation that dilutes the organic signal. Additionally, increased aridity and decreased temperatures could contribute to sand mobility, but not enough fecal matter was present to affect the $\delta^{15}N$ overall during this stratigraphic interval. In fact in all five of the cores extracted from the Loch of Brow, $\delta^{15}N$ began to increase starting at the base of the minerogenic unit, thus potentially indicating that agriculture played a role in the destabilization of the landscape.

4.3 Loch of Spiggie

4.3.1 Limnology

The Loch of Spiggie is deeper than the Loch of Brow and is thermally stratified at the end of May (Figure 3.2). A 1-2 degree temperature shift is seen starting at 3 meters depth, where there is a general decline in temperature that slows at about 8 meters depth, though there is a continued decline of a lesser magnitude throughout the remainder of the water column. Additionally, there is a slight decrease in the dissolved oxygen content in the water column with depth. However, even at the base of the profile dissolved oxygen values were above 9 ppm indicating that the lake is well oxygenated. The presence of oxygen at depth allows for the active presence of aerobic bacteria and other organisms that contribute to the breakdown (via respiration) of organic matter and bioturbation of the top layers of sediment (Wetzel, 1983). This disruption of the sediment is seen most clearly when looking at the graphs of plutonium activity in the upper 10 cm of the core, where there are unexpected fluctuations in Pu levels (Figures 3.13-3.17). The fluctuation seen and the lack of a consistent trend indicate that there is some degree of bioturbation or core disturbance occurring due to the presence of adequate oxygen at the base of the water column. This interpretation is corroborated by the presence of very fine rootlets in the upper unit of the stratigraphy of the Loch of Spiggie.

4.3.2 Sedimentary Data

Due to marked differences in composition, color, and grain size, the sand units contained within the Loch of Spiggie cores do not appear to be part of the same depositional event that inundated the Loch of Brow. Instead of a pulse of coarse grained material sandwiched between organic units, sand layers contained in the Loch of Spiggie are coarser, massive, and in some instances littered with shell fragments. Unlike Brow, where the minerogenic unit seems to have been deposited by strong winds, the sand unit within Spiggie is more likely the result of its former connection to the ocean and potentially flooding events which brought in large volumes of sand, from the adjacent Bay of Scousburgh. Evidence for the marine origin of deposits within the Loch

of Spiggie includes a larger median grain size than the Loch of Brow cores. High energy marine systems have a greater energy available to transport coarser grains than the energy available to aeolian deposits. The abundance of shell fragments within stratigraphic horizon also suggests a marine origin.

4.3.3 Geochemical Data

Within the Loch of Spiggie, nitrogen content was low in all samples. This is due to the inorganic nature of many of the stratigraphic units seen within the loch. In most samples %N in the Spiggie cores was less than 1%, and in many cases was less than 0.1% or was undetectable on the EA-IRMS. While there is a predominance of inorganic minerogenic layers in the Spiggie cores, it is surprising that these values are not higher as there is by all other indications quite a bit of nitrogen entering the system due to its function as the drainage basin for the surrounding agricultural highlands. However other limiting nutrients in the Loch of Spiggie such as phosphorus may prevent higher rates of productivity. Algal blooms have been reported in the past and as a result, today, it is common practice to rotate grazing areas around the northern portion of the loch as there tends to be huge influxes of organic matter from sheep and cows. The Loch of Spiggie serves as a national wildlife preservation area and duck sanctuary, so the avoidance of algal blooms is critical to the sustainability of their habitat.

Organic carbon content was significantly higher than nitrogen content in the loch, though %OC values were less than 20% for all 3 cores. However, in the Spiggie2011_1 % OC is much lower than the other two cores, with values less than 2% seen throughout the core. It is unclear why this particular section of the loch contains much less organic matter; however it can potentially be tied to the increased proportion of the sand and diamicton units within the stratigraphy relative to the other Loch of Spiggie cores. $\delta^{13}C$ values for Spiggie2011_2 and Spiggie2011_3 show a predominant terrestrial signature similar to the Loch of Brow with values ranging from -23.9‰ to -31.3‰ (Thornton and McManus, 1994). However with the slightly enriched values, mixing of both terrestrial and aquatic sources of organic matter is seen.

Closer in proximity to the ocean than the Loch of Brow, the Loch of Spiggie shows some influence of a marine environment, however the signature of organic carbon in the loch is still predominantly higher plants with the potential for influence from aquatic macrophytes. C/N molar ratios would be useful in determining the extent to which marine sources of organic matter influence the isotopic composition of the sediments. However, low nitrogen content in most subsamples and the need to run two different sets of samples to obtain satisfactory carbon and nitrogen data did not allow for a C/N molar ratio to be calculated in many instances.

4.4 Drivers of Environmental Change and Potential Origins of Minerogenic Deposits

4.4.1 Anthropogenic Activity

One of the hypothesized drivers of environmental change on Shetland is the destabilization of the landscape due to anthropogenic activity (Bigelow et al., 2005). An increase in grazing of the dune grass cover by ruminants was proposed as a potential destabilizer of the landscape. Ritchie (2000), suggests that it is possible that over-cultivation, in addition to over-grazing, had a significant impact on dune cover. In Scotland and Ireland, overgrazing of the Machair grasslands by livestock was shown to directly correlate to a destablization of soils (Cooper et al., 2005; Angus and Elliott, 1992). An increase in the rabbit population on Shetland around the time of the documented sand blows may have also contributed to destabilization (Bigelow, 2005). Burrowing animals may have a huge impact on the landscape, as they also destabilize the dune structure, though in a very different way than the sheep. Not only do they have an impact on stripping the dunes of vegetation cover, but they destabilize the dunes from the bottom up by burrowing into them. In addition to disrupting the structure of the dunes, in Australia the European rabbit has had a detrimental effect on both vegetation of rangeland and biodiversity, as it out competes many other mammals for food resources (Edwards et al., 2004).

This destabilization in addition to the occurrence of increased storminess during the Little Ice Age (Lamb, 1985), whose storms are known to have caused sand dune migration and

disruption to stable landscapes, may have created an opportunity for large scale sand movement and deposition on the landscape. In 1413, the medieval township of Forvie experienced what Lamb (1991) describes as a single severe climatic event which caused the massive inland migration of sand. Looking at a generalized model for sediment transport shows that larger grains, such as boulders and cobbles, are for the most part immobile or if they are mobile that they display minor movement close to the ground and those finer sand to silt sized grains would follow irregular trajectories dependent on fluctuations in air velocity (Sherman and Nordstrom, 1994; Anderson and Hallet, 1986).

Brow2011_5 has the thinnest sand unit yet the median grain size within this minerogenic unit is the largest of any across the basin, a medium sized sand. The Loch is fairly small, but there is the potential that the general decrease in grain size from east to west, where the sand unit pinches out and is not seen in the westernmost Brow2011_4 core, could be a function of strong winds coming from the east, during a major storm event. These easterly winds could have carried coarser grained sand shorter distances while the finer sand and silt grains were more easily transported a greater distance. This could also account for the lack of a comparable sand unit within the Loch of Spiggie.

4.4.2 Marine Inundation

Marine inundation is another potential source for the origin of the sand. Within the Loch of Spiggie, a marine origin for sand units is logical given the abundance of shell fragments within the stratigraphy. However for the Loch of Brow, it is unlikely that marine inundation is the origin of late Holocene minerogenic deposits. No sand was found in Brow2011_4, the core taken in closest proximity to the Loch of Spiggie. For marine inundation to be considered a valid hypothesis sand deposits should have been seen in the western portion of the Loch of Brow.

While ages from both plutonium dating and AMS ^{14}C dating do not definitively indicate that the sand layer from within the loch was deposited simultaneously with the sand blows, it is additionally unlikely that the influx of sediment seen here is associated with any of the tsunamis known to have reached the Shetland Islands, including the Storegga tsunami 8100 cal yr BP (7300

^{14}Cyr BP), the Garth tsunami 5500 cal yr BP (~4800 yr ^{14}Cyr BP) and the youngest Drury Voe event, about 1500 years old (Bondevik et al., 2005b). Bondevik et al. (2005b) provide AMS ^{14}C dates on plant fragments from the stratigraphic unit directly above tsunami deposits in Garth's Loch, a loch located on a northeastern peninsula of Mainland Shetland, due north of Lerwick. Fragments were determined to be 4645± 65 ^{14}C yr BP (~3518-3359 BCE calibrated calendar years; Stuiver and Reimer, 1993 (version 6.0)), indicating that even the most recent tsunami event experienced in this area of Shetland occurred well before the deposition of the minerogenic layer seen within the Loch of Brow cores.

4.4.3 Aeolian Deposition

Aeolian deposition of sand is documented as the source of many sand blows throughout Europe. Clemmensen et al. (2001) describes the destabilization of the Lodbjerg dune system, an area of Denmark that is subject to frequent intense wind events. Here, several different aeolian deposition events were dated back to the Iron Age. It was determined that variations in the Lodbjerg dune system and the episodic deposition of aeolian sand was initially a response to climate change and variations in storminess, and that land exploitation probably increasingly influenced the dynamics of the dune system (Clemmensen, 1996). In another study, of Santom Downham, a site affected by the dune fields of Breckland, East Anglia, UK, Bateman and Godby (2004) discuss several different periods of aeolian transport and potential trigger mechanisms for the sand blows. It was determined that the combination of anthropogenic activities, including an increase in land cultivation, the presence of fires on the landscape, and the influence of animals, especially the rabbit, contributed to the demise of the vegetation cover and consequently the availability of sand for transport (Bateman and Godby, 2004).

While a wide range of possibilities exist for the origin of the sand unit within the Loch of Brow, the simplest connection to the sediment that buried the Broo Site should not necessarily be discarded. Neither the geochronology established in this study nor in Mazur (2006) supports the idea that the sand unit was connected to those 17th century sand blows, however it is important to consider that these chronologies are not synchronous and neither values can be used with

confidence. Additionally, even if the minerogenic layer in the loch was not related to the sand blows that inundated the Broo Site , it is likely that the sand storms would have reached the loch at some time in the past . Median grain size for the upper unit of the Loch of Brow is well within the bounds of silt; however there is a significant proportion of sand sized particles occurring dispersed throughout this unit. Perhaps, instead of forming a distinct stratigraphic layer, particles from the sand blows were incorporated into the upper organic rich unit. Downward mixing of Pu indicates that this is real possibility. If tephra were analyzed it would likely be smeared downward as well.

Chapter 5:

Conclusions

5.1 Conclusions

The Broo Site, in South Mainland Shetland, was subjected to a series of intense sand blows during the late 17th c. It has been hypothesized that these sand blows are connected to increased storminess during the Little Ice Age and that evidence of the major depositional event can still be observed in the sedimentary record of nearby lochs. Eight sediment cores extracted from the Loch of Brow and the Loch of Spiggie, in May 2011, were utilized in an investigation of these claims through analysis of a suite of sedimentary and geochemical proxies for environmental change.

Within the Loch of Brow a distinct minerogenic sand unit was identified in 4 of 5 cores. Surrounding this unit is an upper organic rich unit with some small macrophytes (<1cm) and a lower gyttja unit containing larger macrophytes (up to 5 cm in length). Grain size analysis of these sediments revealed an increase in thickness of the minerogenic unit, as well as a decrease in grain size towards the west. Geochemical analysis of the Loch of Brow sediments indicate a dominant terrestrial source of organic matter, through a combination of elevated C/N ratios and $\delta^{13}C$ values consistent with C_3 plants. Additionally, an upcore enrichment in ^{15}N values appears to exist, for the most part, independent of the stratigraphy. $\delta^{15}N$ values of 1-2‰ were seen at the bottom of the core, with an up core enrichment seen where $\delta^{15}N$ values can increase up to 5‰.

The Loch of Spiggie differs in stratigraphy from the Loch of Brow, though it too has a massive minerogenic layer. Instead of a pulse of coarse grained material sandwiched between organic units, sand layers contained in the Loch of Spiggie are coarser, massive, and in some instances littered with shell fragments. Closer in proximity to the ocean than the Loch of Brow, the Loch of Spiggie shows some influence of a marine environment, however the signature of organic carbon in the loch is still predominantly higher plants with the potential for influence from aquatic macrophytes. Marine inundation, aeolian deposition, and anthropogenic activity on the landscape, in particular increased agricultural activity, in conjunction with increased storminess of the Little Ice Age, have been proposed as models for the genesis of sand blows.

5.2 Future Work

Further analyses that need to be completed in the area include the development of a more extensive chronology. ^{210}Pb dating and potentially OSL dates may be the key in identifying the age of the Loch of Brow sediments and consequently their place in the larger context of the massive sand blows that buried the Broo Site. Another area where there is significant room for improvement is in understanding the dynamics of the minerogenic unit within the Loch of Brow. A minerologic study of the various sands from around the area and from within the Loch of Brow cores is a logical next step, as an understanding of provenance would lead to further understanding of the sourcing of sand. Finally, use of lipid biomarkers to target higher plant leaf waxes, fatty acids, and n-alkanes would be an effective way to further isolate sourcing of organic material into the loch. Understanding the source of organic compounds could further specify the root cause of the sand blows, especially if they are in any way connected to anthropogenic shifts in land use.

References Cited:

Anderson, L., 1998, Analysis of Beach Sediments Affecting Coastal Habitation Sites in Shetland, U.K., Senior Thesis, Bates College Department of Geology, unpublished.

Anderson, R.S. and Hallet, B., 1986, Sediment transport by wind: Toward a general model, Geological Society of America Bulletin, v. 97, p. 523-535.

Angus, S. and Elliott, M.M., 1992, Erosion in Scottish machair with particular reference to the Outer Hebrides. In: Carter, R.W.G.; Curtis, T.G.F., and Sheehy-Skeffington, M.J. (eds.), Coastal Dunes: Geomorphology, Ecology and Management for Conservation, Rotterdam: Balkema, p. 93-112.

Arnold, M.S., 2009, Sedimentation in high-Arctic Lake, Linnevatnet, Svalbard: a modern process study using sediment traps, Senior Thesis, Bates College Department of Geology, unpublished.

Bateman, M.D. and Godby, S.P., 2004, Late-Holocene inland dune activity in the U.K.: a case study from Breckland, East Anglia, The Holocene, v. 14, p. 579-588.

Beltrami, H., Chapman, D., Archambault, S., and Bergeron, Y., 1995, Reconstruction of high resolution ground temperature histories combining dendrochronological and geothermal data, Earth and Planetary Science Letters, v. 136, p. 437-445.

Bigelow, G.F., 2011, personal communication.

Bigelow, G.F., Ferrante, S.M., Hall, S.T., Kimball, L.M., Proctor, R.E., and Remington, S.L., 2005, Researching catastrophic environmental changes on the northern coastlines: a geoarchaeological case study from the Shetland Islands: Arctic Anthropology, v. 42, p. 88-102.

Biggs, R.B., Sharp, J.H., Church, T.M., and Tramontano, J. M., 1983, Optical properties, suspended sediments, and chemistry associated with the turbidity maxima of the Delaware Estuary. Canadian Journal of Fisheries and Aquatic Science, v. 40, p. 172–179.

Birnie, J., Gordon, J., Bennett, K., and Hall, A., 1993, The Quaternary of Shetland Field Guide: Quaternary Research Association, 111p.

Blackadder, J.S., 2003, Shetland, Colin Baxter Island Guides, Grantow-on-Spey, Scotland.

Bondevik, S., Svendsen, J.I., Mangerud, J., 1997, Tsunami sedimentary facies deposited by the Storegga tsunami in shallow marine basins and coastal lakes, western Norway, Sedimentology, v. 44, p. 1115-1131.

Bondevik, S., Løvholt, Harbitz, C., Mangerud, J., Dawson, A., Svendsen, J.I., 2005a, The Storegga Slide tsunami-comparing field observations with numerical simulations, Marine and Petroleum Geology, v. 22, p. 195-208.

Bondevik, S., Mangerud, J., Dawson, S., Dawson, A., Lohne, O., 2003, Record-breaking Height for 8000-Year-Old Tsunami in the North Atlantic, EOS, v. 84, p. 289,293.

Bondevik, S., Mangerud, J., Dawson, S., Dawson, A., and Lohne, O., 2005b, Evidence for three North Sea tsunamis at the Shetland Islands between 8000 and 1500 years ago, Quaternary Science Reviews, v. 24, p. 1757-1775.

Brenner, M., Whitmore, T.J., Curtis, J.H., Hodell, J.H., and Schelske, C.L.,1999, Stable isotope (δ13C and δ15N) signatures of sedimented organic matter as indicators of historic lake trophic state, Journal of Paleolimnology, v. 22, p. 205–221.

Broecker, W.S., 1997, Thermohaline circulation, the Achilles heel of our climate system: will man-made CO2 upset the current balance?, Science, v. 278, p. 1582–1588.

Broecker, W.S., Kennett, J.P., Flower, B.P., Teller, J.T., Trumbore, S., 1989, Routing of meltwater from the Laurentide ice-sheet during the Younger Dryas cold episode, Nature, v. 341, p. 318–321.

Broecker, W.S., Peteet, D.M., Rind, D., 1985, Does the ocean-atmosphere system have more than one stable mode of operation?, Nature, v. 315, p. 21–26.

Broecker, W.S., Sutherland, S., and Peng, T.H., 1999, A Possible 20th-Century Slowdown of Southern Ocean Deep Water Formation, Science, v. 286, p. 1132-1135.

Bugge, T., Belderson, R.H., and Kenyon, N.H., 1988, The Storegga Slide, Philosophical Transactions of the Royal Society of London. Series A, Mathematical and Physical Sciences, v. 325, p. 357-388.

Bull, I.D., Simpson, I.A., van Bergen, P.F., and Evershed, R.P., 1999, Muck 'n' molecules: organic geochemical methods for detecting ancient manuring, Antiquity, v. 73, p. 86-96.

Bull, I.D., Lockheart, M.J., Elhmmali, M.M., Roberts, D.J., and Evershed, R.P., 2002, The origin of faeces by means of biomarker detection, Environment International, v. 27, p. 647-654.

Campbell, I., Campbell, C., Apps, M., Rutter, N., and Bush, A., 1998, Late Holocene ~1500 yr climatic periodicities and their implications, Geology, v. 26, p. 471-473.

Clemmensen, L.B., Andreasen, F., Nielse, S.T., Sten, E., 1996, The late Holocene coastal dunefield at Vejers, Denmark: characteristics, sand budget, and depositional dynamics, Geomorphology, v. 17, p. 79-98.

Clemmensen, L.B., Richardt, N.N., and Anderson, C.C., 2001, Holocene sea-level variation and spit development: data from Skagen Odde, Denmark, Holocene, v.11, p. 323-331.

Cooper, A., McCann, T., and Ballard, E., 2005, The effects of livestock grazing and recreation on Irish machair grassland vegetation, Plant Ecology, v. 181, p. 271-276.

Crowley, T.J., 2000, Causes of Climate Change Over the Past 1000 Years, Science, v. 289, p. 270-277.

Dawson, S., and Smith, D.E., 2000, The sedimentology of Middle Holocene tsunami facies in northern Sunderland, Scotland, UK, Marine Geology, v. 170, p. 69-79.

Eddy, J.A., 1976, The Maunder Minimum, Science, v. 192, p. 1189-1202.

Edwards, G.P., Saalfeld, K., and Caley, P., 2004, Introduced mammals in Australian rangelands: Future threats and the role of monitoring programmes in management strategies, Austral Ecology, v. 29, p. 40–50.

Evershed, R. P., Bull, I. D., Corr, L. T., Crossman, Z. M., van Dongen, B. E., Evans, C. J., Jim, S., Mottram, H. R., Mukherjee, A. J. and Pancost, R. D., 2006,Compound-Specific Stable Isotope Analysis in Ecological Research. In Stable Isotopes in Ecology and Environmental Science (Ecological Methods and Concepts) 2nd Edition (Eds. R. Michener and K. Lajtha), Blackwell Publishing, Oxford, UK, p. 480-540.

Fagan, B., 2000, The Little Ice Age: How climate made history 1300-1850: New York, Perseus Books Group, 246 p.

Fischer, H., Werner, M., Wagenbach, D., Schwager, M., Thorsteinnson, T., Wilhemls, F., Kipfstuhl, J., and Sommer, S., 1999, Little ice age clearly recorded in northern Greenland ice cores, Geophysical Research Letters, v. 25, n. 10, p. 1749-1752.

Flinn, D., 1967, The metamorphic rocks of the southern part of the mainland of Shetland, Geologic Journal, v. 5, p. 251-290.

Fogel, M.L. and Cifuentes, L.A., 1993, Isotopic fractionation during primary production. In: Engel, M.H. and Macko, S.A., eds, Organic geochemistry principles and applications: New York, Plenum, p. 73-94.

Freeman, K.H. and Hayes, J.M., 1992, Fractionation of Carbon Isotopes by Phytoplankton and Estimates of Ancient CO2 Levels, Global Biogeochemical Cycles, v. 6, p. 185-198.

George, D.G., and Maitland, P.S., 1984, The fresh waters of Shetland: physical and morphometric characteristics of lochs, Freshwater Biology, v. 14, p. 95-107.

Golledge, N.R., Finlayson, A., Bradwell, T., and Everest, J.D., 2008, The Last Glaciation of Shetland, North Atlantic, Geography Annual, 90 A (1), p. 37–53.

Graham M.C., Eaves M.A., Farmer J.G., Dobson J., and Fallick A.E., 2001. A study of carbon and nitrogen stable isotopes and elemental ratios as potential indicators of source and fate of organic matter in sediment of the Forth Estuary, Scotland, Estuarine Coastal Shelf Science, v. 52, p. 375- 380.

Grove, J.M., 1988, The Little Ice Age: London, Metheun and Co. Ltd., 498 p.

Grove, J.M., 2001, The Initiation of the "Little Ice Age" in Regions Round the North Atlantic, Climatic Change, v. 48, p. 53–82.

Haflidason, H., Lien, R., Sejrup, H.P., Forsberg, C.F., and Bryn, P., 2005, The dating and morphometry of the Storegga Slide, Marine and Petroleum Geology, v. 22, p. 123-136.

Herbel, M., and Spaulding, R., 1993, Vadose zone fertilizer-derived nitrate and δ15N extracts, Ground Water, v. 31, p. 376-382.

Hoppe, G., 1974, The glacial history of the Shetland Islands, Transactions of the Institute of British Geographers, Special Publication no. 7, p. 197-210.

Hurrell, J.W., 1995, Decadal Trends in the North Atlantic Oscillation: Regional Temperatures and Precipitation, Science, v. 269, p. 676-679.

Johnston, J.L., 1999, A Naturalist's Shetland: London, T & AD Poyser Ltd., 506 p.

Kaufman, D.S., Schneider, D.P., McKay, N.P., Ammann, C.M., Bardley, R.S., Briffa, K.R., Miller, G.H., Otto-Bliesner, B.L., Overpeck, J.T., Vinther, B.M., and Arctic Lakes 2k Project Members, 2009, Recent Warming Reverses Long-Term Arctic Cooling, Science, v. 325, p. 1236-1239.

Ketterer, M.E., Hafer, K.M., Jones, V.J., and Appleby, P.G., 2004, Rapid dating of recent sediments in Loch Ness: inductively coupled plasma mass spectrometric measurements of global fallout plutonium, Science of the Total Environment, v. 322, p. 221-229.

King, J., Hubeny J.B., Gibson C., Laliberte E., Ford K., Cantwell M. et al., 2008, Anthropogenic eutrophication of Narragansett Bay: evidence from dated sediment cores, in: Science for Ecosystem-Based Management: Narragansett Bay in the 21st Century, eds. Desbonnet, A. and Costa-Pierce, B.A., New York: Springer, 211–232.

Lamb, H.H., 1977, Climate: Present, Past and Future. Vol. 2: Climatic History and the Future: London, Methuen, 837 p.

Lamb, H.H., 1985, The Little Ice Age Period and Storms Within IT, The Climatic Scene, M.J. Tooley and G.M. Sheail, eds., p. 104-131, London: George Allen and Unwin.

Lamb, H.H, 1991, Historic storms of the North Sea, British Isles, and northwestern Europe: Cambridge, Cambridge University Press, 204 p.

Lamb, H.H., and Woodroffe,A.,1970, Atmospheric circulation during the last ice age, Quaternary Research, v. 1, p. 29-58.

Lambeck, K., 1993, Glacial Rebound of the British Isles- I. Preliminary model results, Geophysical Journal International, v. 115, p. 941-959.

Lewis, W.M. Jr., 1983, A Revised Classification of Lakes Based on Mixing, Canadian Journal of Fisheries and Aquatic Science, v. 40, p. 1779-1787.

Little, M. G., Schneider, R. R. , Kroon, D., Price B, Summerhayes CP, Segl M., 1997: Trade wind forcing of upwelling, seasonality, and Heinrich events as a response to sub-Milankovitch climate variability, Paleoceanography, v. 12, p. 568-576.

MacDonald, G.M., Beukens, R.P., and Kieser, W.E., 1991, Radiocarbon Dating of Limnic Sediments: A Comparative Analysis and Discussion, Ecology, v. 72, p. 1150-1155.

Macko, S.A. and Ostrom, N.E., 1994, Pollution studies using stable isotopes. In Lajtha, K. and Michener, R.H. (eds) Stable Isotopes in Ecology: London, Blackwell Scientific Publications, p. 45-62.

Mann, M., Zhang, Z., Hughes, M., Bradley, R., Miller, S., Rutherford, S., and Ni, F., 2008, Proxy-based reconstructions of hemispheric and global surface temperature variations over the past two millennia, PNAS, v. 105, n. 36, p. 13252- 13257.

Mazur, S.E., 2006, Sedimentological records of storms and climate in the Quendale Region of the Shetland Islands, Scotland: senior thesis, Bates College Department of Geology, unpublished.

McGovern, T.H., 1990, The Archaeology of the Norse North Atlantic, Annual Review of Anthropology, v. 19, p. 331-351.

Meyers, P., 1997, Organic geochemical proxies of paleooceanographic, paleolimnologic, and paleoclimatic processes, Organic Geochemistry, v. 27, p. 213-250.

Miller, G.H., Geirsdottir, A., Zhong, Y., Larsen, D.J., Otto-Bliesner, B.L., Holland, M.M., Bailey, D.A., Refsnider, K.A., Lehman, S.J., Southon, J.R., Anderson, C., Bjornsson, H., and Thordarson, T., 2012, Abrupt onset of the Little Ice Age triggered by volcanism and sustained by sea-ice/ocean feedbacks, Geophysical Research Letters, v. 39, L02708.

Mykura, B., Flinn, D., and May, F., 1976, British Regional Geology- Orkney and Shetland: London, Natural Environmental Research Council Institute of Geological Sciences, 149 p.

Nesje, A. and Dahl, S., 2003, The 'Little Ice Age'-only temperature?, The Holocene, v. 13, p. 139-145.

O'Leary, M.H., 1988, Carbon isotopes in photosynthesis, BioScience, v. 38, p. 328-336.

Orem, W. H., Burnett, W. C., Landing, W. M., Lyons, W. B. and Showers, W., 1991, Jellyfish Lake, Palau: Early diagenesis of organic matter in sediments of an anoxic marine lake, Limnology and Oceanography, v. 36, p. 526–554.

Ostrom, N.E., and Macko, S.A., 1992, Sources, cycling, and distribution of water column particulate and sedimentary organic matter in northern Newfoundland fjords and bays, in: Organic matter: productivity, accumulation and preservation in Recent and Ancient sediments, Whelan, J.K. and Farrington, J.W., eds., New York, Columbia University Press, p. 55-81.

Peach, B.N., and Horne, J., 1879, The glaciation of the Shetland Isles, Quarterly Journal of the Royal Society of London, v. 35, p. 778-811.

Peltier, W.R., Shennan, R., Drummond, R., and Horton, B., 2002, On the postglacial isostatic adjustment of the British Isles and the viscoelastic structure of the Earth, Geophysical Journal Internationa, v. 148, p. 443-475.

Reichert, B.K., Bengtsson, L., and Oerlemans, J., 2001, Midlatitude forcing mechanisms for glacier mass balance investigated using general circulation models, Journal of Climate, v. 14, p. 3767–84.

Riggs, S.R., 1984, Paleoceanographic Model of Neogene Phosphorite Deposition, U.S. Atlantic Continental Margin, Science, v. 223, p. 123-131.

Ritchie, W., 2000, The Sands of Forvie (Scotland): A Case Study in the Geomorphology and Conservational Management, Journal of Coastal Conservation, v. 6, p. 207-218.

Rodbell, D., 2009, personal communication to Prof. M. Retelle, email.

Rossby, T., 1996: The North Atlantic Current and Surrounding Waters: At the Crossroads, Review of Geophysics, 34, 463-481

Schindel, D., Schmidt, G., Miller, R., and Mann, M., 2003, Volcanic and Solar Forcing of Climate Change during the Preindustrial Era, Journal of Climate, v. 16, p. 4094-4107.

Schone, B., Fiebig, J., Pfeiffer, M., Gleb, R., Hickson, J., Johnson, A., Dreyer, W., and Oschmann, W., 2005, Climate records from a bivalved Methuselah (Arctica islandica, Mollusca; Iceland), Paleogeography, Paleoclimatology, Paleoecology, v. 228, p. 130-148.

Shennan, I., 1989, Holocene crustal movements and sea-level changes in Great Britain, Journal of Quaternary Science, v. 4, p. 77-89.

Sherman, D.J. and Nordstrom, K.F., 1994, Hazards of Wind-Blown Sand and Coastal Sand Drifts: A Review, Journal of Coastal Research, special issue no. 12, p. 263-275.

Simpson, I.A., van Bergen, P.F., Perret, V., Elhmmali, M.M., Roberts, D.J., and Evershed, R.P., 1999a, Lipid biomarkers of manuring practice in relict anthropogenic soils, The Holocene, v. 9, p. 223-229.

Simpson, I.A., Bol, R., Bull, I.D., Evershed, R.P., Petzke, K.J., and Dockrill, S.J., 1999b, Interpreting early land management through compound specific stable isotope analyses of archaeological soil, Rapid Communications in Mass Spectrometry, v. 13, p. 1315-1319.

Stuiver, M., Reimer, P.J., and Reimer, R.W., 2009, CALIB 6.1.1. (program and documentation), http://calib.qub.ac.uk/calib.

Sutherland, D.G., 1980, Problems of radiocarbon dating in newly deglaciated terrain: examples from the Scottish Late- glacial, in: Lowe, J.J., Gray, J.M., and Robinson, J.E., eds., Studies in the Lateglacial of north-west Europe: Oxford, England, Pergamon, p. 139-149.

Thornton, S. F. and McManus, J., 1994, Application of organic carbon and nitrogen stable isotope and C/N ratios as source indicators of organic matter provenance in estuarine systems: evidence from the Tay Estuary, Scotland, Estuarine Coastal Shelf Science, v. 38, p. 219–233.

Tiessen, H., Karamanos, R.E., Stewart, J.W.B., and Stelles, F., 1984, Natural nitrogen-15 abundance as an indicator of soil organic matter transformations in native and cultivated soils, Soil Science Society of America Journal, v. 48, p, 312-315.

Tyagi, P., Edwards, D.R., and Coyne, M.S., 2008, Use of sterol and bile acid biomarkers to identify domesticated animal sources of fecal pollution, Water, Air, and Soil Pollution, v. 187, p. 263-274.

Tyagi, P., Edwards, D.R., and Coyne, M.S., 2009, Fecal sterol and bile acid biomarkers: runoff concentrations in animal waste-amended pastures, Water, Air, and Soil Pollution, v. 198, p. 45-54.

Valiela, I., Geist, M., McClelland, J., Tomasky, G., 2000, Nitrogen Loading from Watersheds to Estuaries: Verification of the Waquoit Bay Nitrogen Loading Model, Biogeochemistry, v. 49, p. 277-293.

Wetzel, R.G. 1983. Limnology. 2nd ed. Saunders College Publishing, Toronto. 767 p.

Wheeler, D., and Mayes, J., 1997, Regional Climates of the British Isles: London, Routledge, 343 p.

Wool, D.C., 2011, Nitrogen and carbon isotopes in lake sediments from the Little Androscoggin Watershed, Maine, USA; a proxy for marine derived nutrients?: senior thesis, Bates College Department of Geology, unpublished.

Zhang, J., Quay, P.D., and Wilbur, D.O., 1995, Carbon isotope fractionation during gas-water exchange and dissolution of CO¬2, Geochimica et Cosmochimica Acta, v. 59, p. 107-114.

Zhong, Y., Miller, G.H., Otto-Bliesner, B.L., Holland, M.M., Bailey, D.A., Schneider, D.P. Geirsdottir,A., 2011, Centennial-scale climate change from decadally-paced explosive volcanism: a coupled sea ice-ocean mechanism, Climate Dynamics.

Appendix A: Water Quality Data

STA	Sample Date	Rep	Fo	Fa	Fs	r/r-1	Fo-Fa	Chlasam (ug/l	*Dil	Chla (sam*dil)
Loch of Tingwall	6-Jun	A	41.5	23.4	1	1.98	18.1	35.838	1	35.838
		B	33	19.4	1	1.98	13.6	26.928	1	26.928
Spiggie Inlet	29-May	A	29.2	18.1	1	1.98	11.1	21.978	1	21.978
		B	69.3	44.0	1	1.98	25.3	50.094	1	50.094
Loch of Spiggie	28-May	A	16.7	10.7	1	1.98	6	11.88	1	11.88
		B	68.1	37.9	1	1.98	30.2	59.796	1	59.796
Spiggie Outlet	29-May	A	66.7	37.2	1	1.98	29.5	58.41	1	58.41
		B	59.4	33.8	1	1.98	25.6	50.688	1	50.688
Loch of Brow	30-May	A	10.8	6.5	1	1.98	4.34	8.5932	1	8.5932
		B	10.3	6.3	1	1.98	3.99	7.9002	1	7.9002
Loch of Clumlie	4-Jun	A	11	6.7	1	1.98	4.32	8.5536	1	8.5536
		B	56.2	31.9	1	1.98	24.3	48.114	1	48.114

STA	*.010L (extr)	Vol filtered (L)	*1/Vol filtered	r	r*Fa	"r*Fa"-Fo	Phasam (ug/L)
Loch of Tingwall	0.35838	1	0.36	2.02	47.268	5.768	11.42064
	0.26928	1	0.27	2.02	39.188	6.188	12.25224
Spiggie Inlet	0.21978	0.5	0.44	2.02	36.562	7.362	14.57676
	0.50094	0.5	1.00	2.02	88.88	19.58	38.7684
Loch of Spiggie	0.1188	0.5	0.24	2.02	21.614	4.914	9.72972
	0.59796	0.5	1.20	2.02	76.558	8.458	16.74684
Spiggie Outlet	0.5841	0.5	1.17	2.02	75.144	8.444	16.71912
	0.50688	0.5	1.01	2.02	68.276	8.876	17.57448
Loch of Brow	0.085932	0.5	0.17	2.02	13.0492	2.2492	4.453416
	0.079002	0.5	0.16	2.02	12.7462	2.4462	4.843476
Loch of Clumlie	0.085536	1	0.09	2.02	13.4936	2.4936	4.937328
	0.48114	1	0.48	2.02	64.438	8.238	16.31124

	Method=StreamCations-JL(v5)												
	SampleName=Clumlie inlet 1												
Sample	Elem	WL	Units	Avg	Stddev	RSD	Rep1	Rep2	Rep3	Intensity 1	Intensity 2	Intensity 3	Intensity a
10 ppm std	Zn2025	202.548	ppm	C .0000	0	0	C .0000	C .0000	C .0000	C 5039.	C 5139.	C 5192.	#DIV/0!
10 ppm std	Zn2062	206.200	ppm	C .0000	0	0	C .0000	C .0000	C .0000	C 4074.	C 4167.	C 4201.	#DIV/0!
10 ppm std	Zn2138	213.856	ppm	C .0000	0	0	C .0000	C .0000	C .0000	C 14180.	C 14390.	C 14440.	#DIV/0!
10 ppm std	Pb2203	220.353	ppm	9.241	0.096	1.038	9.132	9.283	9.309	1569	1594	1599	1587.333333
10 ppm std	Cd2265	226.502	ppm	9.14	0.1039	1.136	9.024	9.173	9.223	22310	22680	22810	22600
10 ppm std	Co2378	237.862	ppm	9.549	0.0312	0.3272	9.555	9.515	9.576	9565	9526	9584	9558.333333
10 ppm std	Fe2599	259.940	ppm	9.396	0.0233	0.2481	9.418	9.372	9.399	32850	32690	32800	32780
10 ppm std	Mn2605	260.569	ppm	9.596	0.0296	0.3088	9.613	9.562	9.613	100100	99590	100100	99930
10 ppm std	Cr2843	284.325	ppm	9.528	0.033	0.3466	9.559	9.493	9.531	21720	21590	21660	21656.66667
10 ppm std	Mg2852	285.213	ppm	9.731833	0.0299	0.3115	9.641	9.586	9.595	65140	64750	64830	64906.66667
10 ppm std	V_3093	309.311	ppm	9.516	0.0267	0.2811	9.541	9.487	9.52	89550	89070	89360	89326.66667
10 ppm std	Cu3273	327.396	ppm	9.385	0.0545	0.581	9.448	9.359	9.349	28230	27970	27950	28050
10 ppm std	Ni3414	341.476	ppm	9.412	0.0307	0.3262	9.44	9.417	9.379	6750	6746	6727	6741
10 ppm std	Al3944	394.401	ppm	9.662	0.062	0.6414	9.733	9.632	9.621	7891	7822	7846	7853
10 ppm std	Ca3968	396.847	ppm	8.514	0.0474	0.5566	8.491	8.483	8.569	1721000	1720000	1737000	1726000
10 ppm std	Sr4215	421.552	ppm	9.219	0.1289	1.398	9.365	9.12	9.173	1928000	1878000	1889000	1898333.333
10 ppm std	Ca4226	422.673	ppm	10.00112	0.0446	0.5002	8.959	8.916	8.87	26900	26790	26690	26793.33333
10 ppm std	Na5889	588.995	ppm	9.902	0.0547	0.5527	9.965	9.87	9.87	76240	75810	75990	76013.33333
10 ppm std	Na5895	589.592	ppm	9.969	0.0637	0.6394	10.04	9.941	9.924	42630	42320	42330	42426.66667
10 ppm std	K_7664	766.490	ppm	9.393	0.0402	0.4279	9.435	9.355	9.388	14010	13980	14070	14020
10 ppm std	K_7698	769.896	ppm	9.252	0.018	0.1943	9.266	9.232	9.259	7559	7580	7632	7590.333333
Brow Inlet 1	Zn2025	202.548	ppm	0.0044	0.0006	13.88	0.0037	0.0047	0.0047	23.71	24.1	24.47	24.09333333
Brow Inlet 1	Zn2062	206.200	ppm	0.0045	0.0003	7.099	0.0042	0.0044	0.0049	23.48	23.67	23.85	23.66666667
Brow Inlet 1	Zn2138	213.856	ppm	0.0044	0.0003	7.032	0.0046	0.0046	0.0041	39.67	39.81	38.9	39.46
Brow Inlet 1	Pb2203	220.353	ppm	0.0018	0.0019	104.7	0.0002	0.0039	0.0012	36.88	37.29	37.22	37.13
Brow Inlet 1	Cd2265	226.502	ppm	0	0.0002	2625	-0.0002	0.0002	0	43.93	44.82	44.39	44.38
Brow Inlet 1	Co2378	237.862	ppm	0.0021	0.0007	30.77	0.0024	0.0014	0.0026	104.6	102.8	103.9	103.7666667
Brow Inlet 1	Fe2599	259.940	ppm	0.3267	0.0054	1.638	0.3207	0.3287	0.3308	1278	1302	1309	1296.333333
Brow Inlet 1	Mn2605	260.569	ppm	0.1221	0.0009	0.7129	0.1211	0.1226	0.1226	1411	1425	1424	1420

	Method=StreamCations-JL(v5)												
	SampleName=Clumlie inlet 1												
Sample	Elem	WL	Units	Avg	Stddev	RSD	Rep1	Rep2	Rep3	Intensity 1	Intensity 2	Intensity 3	Intensity avg
Brow Inlet 1	Cr2843	284.325	ppm	-0.001	0.0014	131.8	-0.0026	-0.0005	0	151.4	153.1	153.1	152.5333333
Brow Inlet 1	Mg2852	285.213	ppm	4.54917	0.0307	0.6852	4.449	4.497	4.506	30120	30440	30500	30353.33333
Brow Inlet 1	V_3093	309.311	ppm	0.0079	0.0003	4	0.0082	0.0076	0.0077	604.5	603.4	597.8	601.9
Brow Inlet 1	Cu3273	327.396	ppm	0.0007	0.0003	36.37	0.0008	0.0004	0.0008	522.8	517.4	517.8	519.3333333
Brow Inlet 1	Ni3414	341.476	ppm	0.0081	0.0041	50.88	0.0083	0.0039	0.0122	606.1	596.6	596.2	599.6333333
Brow Inlet 1	Al3944	394.401	ppm	0.0678	0.0091	13.46	0.0729	0.0573	0.0732	1073	1061	1056	1063.333333
Brow Inlet 1	Sr4215	421.552	ppm	0.0329	0.0003	1.06	0.0325	0.0331	0.0332	8490	8572	8591	8551
Brow Inlet 1	Ca4226	422.673	ppm	8.546308	0.05	0.6595	7.518	7.594	7.612	22770	22960	23000	22910
Brow Inlet 1	Na5889	588.995	ppm	27.28	0.2323	0.8517	27.03	27.33	27.49	190500	192300	193200	192000
Brow Inlet 1	Na5895	589.592	ppm	27.15	0.1913	0.7045	26.94	27.2	27.32	106000	106900	107300	106733.3333
Brow Inlet 1	K_7664	766.490	ppm	0.2366	0.0085	3.593	0.2391	0.2271	0.2435	4995	4935	4902	4944
Brow Inlet 1	K_7698	769.896	ppm	0.2247	0.0303	13.51	0.1963	0.2566	0.2211	3156	3143	3097	3132
Brow Inlet 2	Zn2025	202.548	ppm	0.0114	0.0004	3.629	0.0117	0.0114	0.0109	29.55	29.65	29.79	29.66333333
Brow Inlet 2	Zn2062	206.200	ppm	0.0112	0.0004	3.338	0.0112	0.0116	0.0109	28.7	28.73	28.36	28.59666667
Brow Inlet 2	Zn2138	213.856	ppm	0.0116	0.0001	0.9411	0.0115	0.0116	0.0117	55.52	55.5	56.11	55.71
Brow Inlet 2	Pb2203	220.353	ppm	0.0033	0.0001	4.147	0.0031	0.0034	0.0034	38.33	38.67	38.2	38.4
Brow Inlet 2	Cd2265	226.502	ppm	0	0.0001	805.3	-0.0001	0.0001	0	45.54	45.95	45.89	45.79333333
Brow Inlet 2	Co2378	237.862	ppm	-0.0013	0.0033	257.5	-0.0019	0.0022	-0.0042	100.7	105.8	102.3	102.9333333
Brow Inlet 2	Fe2599	259.940	ppm	0.1339	0.0012	0.8642	0.1332	0.1353	0.1334	622.6	634.2	627.1	627.9666667
Brow Inlet 2	Mn2605	260.569	ppm	0.0884	0.0006	0.6338	0.0879	0.089	0.0885	1064	1078	1074	1072
Brow Inlet 2	Cr2843	284.325	ppm	0.0003	0.0012	369.4	0.0016	-0.0008	0.0002	156	154.2	157.1	155.7666667
Brow Inlet 2	Mg2852	285.213	ppm	6.052573	0.0183	0.3064	5.958	5.975	5.995	40250	40380	40500	40376.66667
Brow Inlet 2	V_3093	309.311	ppm	0.0114	0.0003	2.516	0.0111	0.0115	0.0116	638.4	650.5	643.4	644.1
Brow Inlet 2	Cu3273	327.396	ppm	0.0018	0.0003	16.11	0.0015	0.0018	0.0021	525.2	532	533.6	530.2666667
Brow Inlet 2	Ni3414	341.476	ppm	0.0078	0.0028	35.26	0.0072	0.0108	0.0054	596.3	608.4	601.1	601.9333333
Brow Inlet 2	Al3944	394.401	ppm	0.0397	0.0038	9.591	0.036	0.0436	0.0395	1049	1073	1071	1064.333333
Brow Inlet 2	Sr4215	421.552	ppm	0.0599	0.0001	0.1374	0.0599	0.06	0.0598	14070	14120	14100	14096.66667
Brow Inlet 2	Ca4226	422.673	ppm	11.75314	0.0456	0.4296	10.65	10.64	10.56	31540	31550	31320	31470
Brow Inlet 2	Na5889	588.995	ppm	41.98	0.0402	0.0958	42.01	41.93	41.99	290600	290400	290800	290600

	Method=StreamCations-JL(v5)												
	SampleName=Clumlie inlet 1												
Sample	Elem	WL	Units	Avg	Stddev	RSD	Rep1	Rep2	Rep3	Intensity 1	Intensity 2	Intensity 3	Intensity avg
Brow Inlet 2	Na5895	589.592	ppm	41.78	0.0415	0.0993	41.81	41.74	41.8	161700	161500	161700	161633.3333
Brow Inlet 2	K_7664	766.490	ppm	0.7786	0.0086	1.111	0.785	0.7688	0.7821	5452	5521	5532	5501.666667
Brow Inlet 2	K_7698	769.896	ppm	0.7888	0.0313	3.966	0.8145	0.7978	0.754	3394	3440	3421	3418.333333
Brow Outlet	Zn2025	202.548	ppm	0.0025	0.0003	13.44	0.0024	0.0022	0.0028	23.49	23.77	23.87	23.71
Brow Outlet	Zn2062	206.200	ppm	0.0034	0.001	30.02	0.0031	0.0025	0.0045	23.84	23.48	24.36	23.89333333
Brow Outlet	Zn2138	213.856	ppm	0.0025	0.0001	2.772	0.0025	0.0024	0.0025	36.18	36.5	36.73	36.47
Brow Outlet	Pb2203	220.353	ppm	0.0026	0.001	37.71	0.0015	0.0035	0.0027	38.23	38.43	38.5	38.38666667
Brow Outlet	Cd2265	226.502	ppm	0	0.0001	3368	-0.0001	0.0001	0	45.37	46.1	45.69	45.72
Brow Outlet	Co2378	237.862	ppm	-0.001	0.0015	149.1	-0.0028	-0.0003	0	102.6	104.7	102.8	103.3666667
Brow Outlet	Fe2599	259.940	ppm	0.0715	0.0002	0.3322	0.0712	0.0715	0.0717	409.9	411.6	406.5	409.3333333
Brow Outlet	Mn2605	260.569	ppm	0.0723	0.0006	0.7673	0.0718	0.0721	0.0729	902.2	902.2	909	904.4666667
Brow Outlet	Cr2843	284.325	ppm	0.0009	0.001	103	0.002	0.0006	0.0002	166.5	162.1	154	160.8666667
Brow Outlet	Mg2852	285.213	ppm	5.78459	0.0176	0.3079	5.69	5.711	5.725	38470	38600	38700	38590
Brow Outlet	V_3093	309.311	ppm	0.0108	0.0004	3.952	0.0106	0.0113	0.0105	637.6	635.3	630.9	634.6
Brow Outlet	Cu3273	327.396	ppm	0.0034	0.0014	41.27	0.0022	0.005	0.0031	537.4	539.6	527.3	534.7666667
Brow Outlet	Ni3414	341.476	ppm	0.008	0.0058	73.04	0.0112	0.0013	0.0115	617.2	603.4	598.2	606.2666667
Brow Outlet	Al3944	394.401	ppm	0.0241	0.008	33.18	0.0281	0.0149	0.0292	1072	1056	1048	1058.666667
Brow Outlet	Sr4215	421.552	ppm	0.0662	0.0003	0.5025	0.066	0.0661	0.0666	15370	15380	15460	15403.33333
Brow Outlet	Ca4226	422.673	ppm	12.64476	0.0682	0.5951	11.4	11.44	11.54	33710	33800	34040	33850
Brow Outlet	Na5889	588.995	ppm	36.84	0.1925	0.5224	36.65	36.84	37.04	255100	256100	257300	256166.6667
Brow Outlet	Na5895	589.592	ppm	36.67	0.2201	0.6004	36.45	36.66	36.89	141700	142400	143200	142433.3333
Brow Outlet	K_7664	766.490	ppm	1.722	0.0162	0.9399	1.703	1.732	1.731	6455	6432	6379	6422
Brow Outlet	K_7698	769.896	ppm	1.68	0.0378	2.247	1.649	1.669	1.722	3874	3858	3834	3855.333333
Clumlie Inlet 1	Zn2025	202.548	ppm	0.0072	0.0002	3.057	0.0074	0.0073	0.007	27.87	27.66	27.34	27.62333333
Clumlie Inlet 1	Zn2062	206.200	ppm	0.0074	0.0005	6.285	0.0078	0.0069	0.0075	27.14	26.47	26.69	26.76666667
Clumlie Inlet 1	Zn2138	213.856	ppm	0.0076	0.0002	2.723	0.0079	0.0075	0.0076	48.19	47.56	47.75	47.83333333
Clumlie Inlet 1	Pb2203	220.353	ppm	0.0015	0.0022	142.7	-0.001	0.003	0.0025	38.79	38.98	39.07	38.94666667
Clumlie Inlet 1	Cd2265	226.502	ppm	0	0.0001	131.2	0	-0.0001	0	46.28	46.26	46.05	46.19666667

	Method=StreamCations-JL(v5)												
	SampleName=Clumlie inlet 1												
Sample	Elem	WL	Units	Avg	Stddev	RSD	Rep1	Rep2	Rep3	Intensity 1	Intensity 2	Intensity 3	Intensity avg
Clumlie Inlet 1	Co2378	237.862	ppm	0.0005	0.0022	431.8	-0.0013	0.0029	-0.0001	105.6	108.4	104.5	106.1666667
Clumlie Inlet 1	Fe2599	259.940	ppm	0.095	0.0008	0.7982	0.0946	0.0958	0.0944	493.2	498.6	492.8	494.8666667
Clumlie Inlet 1	Mn2605	260.569	ppm	0.1933	0.0006	0.3086	0.1937	0.1937	0.1926	2168	2170	2157	2165
Clumlie Inlet 1	Cr2843	284.325	ppm	-0.0005	0.0003	62.14	-0.0009	-0.0002	-0.0005	153.8	154	153.8	153.8666667
Clumlie Inlet 1	Mg2852	285.213	ppm	7.765961	0.0186	0.2422	7.658	7.677	7.696	51670	51800	51930	51800
Clumlie Inlet 1	V_3093	309.311	ppm	0.0163	0.0007	4.262	0.0163	0.0156	0.017	717.5	711.9	716.6	715.3333333
Clumlie Inlet 1	Cu3273	327.396	ppm	0.0026	0.0026	99.99	-0.0001	0.0028	0.005	532.8	536.8	541.1	536.9
Clumlie Inlet 1	Ni3414	341.476	ppm	0.0018	0.0047	265.4	0.0061	-0.0033	0.0025	619.3	613.9	612.6	615.2666667
Clumlie Inlet 1	Al3944	394.401	ppm	0.0525	0.0061	11.54	0.0515	0.0471	0.0591	1099	1099	1088	1095.333333
Clumlie Inlet 1	Sr4215	421.552	ppm	0.0664	0.0004	0.5803	0.066	0.0664	0.0668	15410	15490	15540	15480
Clumlie Inlet 1	Ca4226	422.673	ppm	12.53737	0.0322	0.2836	11.32	11.33	11.38	33500	33540	33650	33563.33333
Clumlie Inlet 1	Na5889	588.995	ppm	54.87	0.283	0.5157	54.77	55.19	54.65	376400	379000	375600	377000
Clumlie Inlet 1	Na5895	589.592	ppm	55.38	0.2432	0.4391	55.21	55.26	55.66	212500	212600	214100	213066.6667
Clumlie Inlet 1	K_7664	766.490	ppm	1.006	0.0085	0.8401	1.016	0.9995	1.004	5856	5854	5807	5839
Clumlie Inlet 1	K_7698	769.896	ppm	0.9794	0.0195	1.992	0.996	0.9579	0.9843	3613	3602	3581	3598.666667
Clumlie Inlet 2	Zn2025	202.548	ppm	0.0083	0.0006	7.494	0.0086	0.0086	0.0076	27.15	27.36	26.77	27.09333333
Clumlie Inlet 2	Zn2062	206.200	ppm	0.0081	0.0003	3.726	0.0079	0.0079	0.0085	25.99	25.39	26.14	25.84
Clumlie Inlet 2	Zn2138	213.856	ppm	0.0086	0.0003	2.944	0.0083	0.0086	0.0088	47.92	48.13	48.43	48.16
Clumlie Inlet 2	Pb2203	220.353	ppm	0.0015	0.001	68.97	0.0027	0.0007	0.0011	37.35	37.03	37.14	37.17333333
Clumlie Inlet 2	Cd2265	226.502	ppm	0	0	100.9	0	0	0	44.61	44.21	44.06	44.29333333
Clumlie Inlet 2	Co2378	237.862	ppm	-0.0001	0.0008	715.2	-0.001	0.0002	0.0004	104.5	106.6	105.6	105.5666667
Clumlie Inlet 2	Fe2599	259.940	ppm	0.2683	0.0033	1.243	0.2647	0.2713	0.2689	1084	1108	1098	1096.666667
Clumlie Inlet 2	Mn2605	260.569	ppm	0.0853	0.0004	0.4777	0.0855	0.0856	0.0848	1043	1043	1036	1040.666667
Clumlie Inlet 2	Cr2843	284.325	ppm	0.0016	0.0005	32.82	0.0014	0.0022	0.0012	156.8	158.9	162.2	159.3
Clumlie Inlet 2	Mg2852	285.213	ppm	5.868585	0.0301	0.5189	5.766	5.825	5.786	38970	39370	39110	39150
Clumlie Inlet 2	V_3093	309.311	ppm	0.0107	0.0002	1.789	0.0109	0.0106	0.0106	649.1	645	643.2	645.7666667
Clumlie Inlet 2	Cu3273	327.396	ppm	0.0011	0.0004	39.56	0.0015	0.0009	0.0008	527.8	530	525.2	527.6666667
Clumlie Inlet 2	Ni3414	341.476	ppm	0.0063	0.0059	93.78	0.0111	0.008	-0.0003	610	609.3	602.7	607.3333333
Clumlie Inlet 2	Al3944	394.401	ppm	0.12	0.0134	11.13	0.1147	0.1101	0.1352	1105	1105	1109	1106.333333

	Method=StreamCations-JL(v5)												
	SampleName=Clumlie inlet 1												
Sample	Elem	WL	Units	Avg	Stddev	RSD	Rep1	Rep2	Rep3	Intensity 1	Intensity 2	Intensity 3	Intensity avg
Clumlie Inlet 2	Sr4215	421.552	ppm	0.0464	0.0002	0.4945	0.0462	0.0466	0.0464	11300	11400	11340	11346.66667
Clumlie Inlet 2	Ca4226	422.673	ppm	6.284792	0.0174	0.3213	5.405	5.439	5.417	16830	16920	16870	16873.33333
Clumlie Inlet 2	Na5889	588.995	ppm	44.72	0.2945	0.6586	44.48	45.05	44.63	307600	311000	308600	309066.6667
Clumlie Inlet 2	Na5895	589.592	ppm	44.78	0.2116	0.4725	44.59	45.01	44.73	172200	174100	172800	173033.3333
Clumlie Inlet 2	K_7664	766.490	ppm	1.033	0.0141	1.369	1.018	1.036	1.046	5797	5827	5804	5809.333333
Clumlie Inlet 2	K_7698	769.896	ppm	0.9946	0.0112	1.129	1.006	0.9939	0.9838	3564	3567	3551	3560.666667
Clumlie Outlet	Zn2025	202.548	ppm	0.0037	0.0004	11.48	0.0042	0.0034	0.0035	24.7	24.37	24.65	24.57333333
Clumlie Outlet	Zn2062	206.200	ppm	0.0034	0.0007	20.19	0.0026	0.0036	0.0039	23.65	24.03	24.15	23.94333333
Clumlie Outlet	Zn2138	213.856	ppm	0.0036	0.0002	5.246	0.0037	0.0034	0.0037	38.64	38.45	38.77	38.62
Clumlie Outlet	Pb2203	220.353	ppm	0.003	0.0029	97.78	0.0057	-0.0001	0.0032	38.56	38.11	38.4	38.35666667
Clumlie Outlet	Cd2265	226.502	ppm	0.0001	0.0001	148.2	0.0001	0.0001	0	46.02	45.73	45.09	45.61333333
Clumlie Outlet	Co2378	237.862	ppm	0.0009	0.0006	67.32	0.0007	0.0004	0.0016	105.6	106.6	107.5	106.5666667
Clumlie Outlet	Fe2599	259.940	ppm	0.113	0.0012	1.035	0.112	0.1126	0.1143	555.5	555.2	561.4	557.3666667
Clumlie Outlet	Mn2605	260.569	ppm	0.0302	0	0.1483	0.0302	0.0302	0.0302	469.3	468.4	470.6	469.4333333
Clumlie Outlet	Cr2843	284.325	ppm	0.0016	0.0017	110.6	-0.0001	0.0015	0.0034	156.7	161.2	164.8	160.9
Clumlie Outlet	Mg2852	285.213	ppm	6.750527	0.0596	0.8932	6.611	6.663	6.73	44650	44990	45450	45030
Clumlie Outlet	V_3093	309.311	ppm	0.0139	0.0001	0.4719	0.0139	0.0139	0.0138	671.8	675.8	675.2	674.2666667
Clumlie Outlet	Cu3273	327.396	ppm	0.0004	0.0006	169.7	-0.0003	0.0006	0.0008	528.2	530.5	534.6	531.1
Clumlie Outlet	Ni3414	341.476	ppm	0.0016	0.001	59.84	0.0013	0.0009	0.0027	612.5	612.6	608.5	611.2
Clumlie Outlet	Al3944	394.401	ppm	0.0353	0.0123	34.93	0.0235	0.0481	0.0344	1061	1071	1069	1067
Clumlie Outlet	Sr4215	421.552	ppm	0.0529	0.0004	0.7052	0.0525	0.0529	0.0532	12620	12680	12760	12686.66667
Clumlie Outlet	Ca4226	422.673	ppm	8.803554	0.0441	0.5644	7.756	7.838	7.824	23470	23690	23630	23596.66667
Clumlie Outlet	Na5889	588.995	ppm	51.11	0.3682	0.7204	50.86	50.93	51.53	350300	350900	354700	351966.6667
Clumlie Outlet	Na5895	589.592	ppm	52.21	0.311	0.5958	51.88	52.23	52.5	199900	201300	202300	201166.6667
Clumlie Outlet	K_7664	766.490	ppm	1.748	0.0172	0.9865	1.73	1.751	1.764	6526	6528	6558	6537.333333
Clumlie Outlet	K_7698	769.896	ppm	1.724	0.0148	0.8559	1.738	1.709	1.725	3941	3926	3938	3935
Spiggie 1	Zn2025	202.548	ppm	0.0336	0.0004	1.105	0.0331	0.0338	0.0337	46.29	46.21	46.05	46.18333333
Spiggie 1	Zn2062	206.200	ppm	0.0329	0.0006	1.972	0.0333	0.0321	0.0332	42.31	41.46	41.83	41.86666667

	Method=StreamCations-JL(v5)												
	SampleName=Clumlie inlet 1												
Sample	Elem	WL	Units	Avg	Stddev	RSD	Rep1	Rep2	Rep3	Intensity 1	Intensity 2	Intensity 3	Intensity avg
Spiggie 1	Zn2138	213.856	ppm	0.0343	0.0002	0.4647	0.0343	0.0345	0.0341	103.8	104.3	103.4	103.8333333
Spiggie 1	Pb2203	220.353	ppm	0.0014	0.003	212.9	-0.0018	0.0018	0.0043	39.17	39.16	39.01	39.11333333
Spiggie 1	Cd2265	226.502	ppm	0.0001	0.0001	125.5	0	0.0002	0.0001	46.68	47.41	46.53	46.87333333
Spiggie 1	Co2378	237.862	ppm	0.0009	0.0015	175.3	-0.0008	0.0014	0.002	102.9	104.2	105.4	104.1666667
Spiggie 1	Fe2599	259.940	ppm	0.0052	0.0004	7.547	0.0048	0.0056	0.0054	178.4	178.9	179.8	179.0333333
Spiggie 1	Mn2605	260.569	ppm	0.0013	0.0002	14.66	0.0014	0.0015	0.0011	165.6	168	166.7	166.7666667
Spiggie 1	Cr2843	284.325	ppm	0.0007	0.0006	76.39	0.0001	0.0011	0.001	155.6	158	156.9	156.8333333
Spiggie 1	Mg2852	285.213	ppm	8.374422	0.0657	0.7938	8.313	8.326	8.206	56070	56150	55350	55856.66667
Spiggie 1	V_3093	309.311	ppm	0.0184	0.0002	1.28	0.0181	0.0184	0.0186	723.6	726.7	729.1	726.4666667
Spiggie 1	Cu3273	327.396	ppm	0.0074	0.0021	28.75	0.0059	0.0099	0.0066	543.6	549.2	545.8	546.2
Spiggie 1	Ni3414	341.476	ppm	0.0086	0.0036	41.89	0.0112	0.0045	0.01	610.2	607	611.1	609.4333333
Spiggie 1	Al3944	394.401	ppm	0.0121	0.008	66.26	0.0159	0.0175	0.0029	1077	1069	1067	1071
Spiggie 1	Sr4215	421.552	ppm	0.1033	0.0008	0.7996	0.1035	0.104	0.1024	23080	23170	22860	23036.66667
Spiggie 1	Ca4226	422.673	ppm	15.21472	0.0727	0.523	13.88	13.97	13.83	40660	40930	40540	40710
Spiggie 1	Na5889	588.995	ppm	59.39	0.471	0.793	58.85	59.67	59.66	403700	409100	409200	407333.3333
Spiggie 1	Na5895	589.592	ppm	60.42	0.4626	0.7656	60.53	60.82	59.91	232400	233500	230100	232000
Spiggie 1	K_7664	766.490	ppm	3.646	0.0247	0.6781	3.662	3.658	3.618	8380	8363	8346	8363
Spiggie 1	K_7698	769.896	ppm	3.598	0.033	0.9185	3.634	3.569	3.59	4847	4807	4840	4831.333333
Spiggie 2	Zn2025	202.548	ppm	0.0051	0.0004	7.005	0.0053	0.0047	0.0054	27.65	27.3	27.89	27.61333333
Spiggie 2	Zn2062	206.200	ppm	0.0052	0.0002	3.429	0.0054	0.0051	0.005	26.87	27.15	27.04	27.02
Spiggie 2	Zn2138	213.856	ppm	0.0051	0.0002	3.422	0.005	0.0053	0.005	44.21	44.69	44.43	44.44333333
Spiggie 2	Pb2203	220.353	ppm	0.0009	0.0011	126.4	0.0021	0	0.0005	41.07	41.17	40.98	41.07333333
Spiggie 2	Cd2265	226.502	ppm	0.0001	0.0003	322.4	-0.0002	0.0005	0.0001	48.21	49.19	48.72	48.70666667
Spiggie 2	Co2378	237.862	ppm	0.0003	0.001	346.7	-0.0001	0.0014	-0.0004	106.5	107.1	107.7	107.1
Spiggie 2	Fe2599	259.940	ppm	0.007	0.0002	2.242	0.0072	0.007	0.0069	187.3	188.8	188.5	188.2
Spiggie 2	Mn2605	260.569	ppm	0.0007	0.0001	17.66	0.0006	0.0008	0.0007	162.6	162.6	162.9	162.7
Spiggie 2	Cr2843	284.325	ppm	0.0001	0.0002	204.2	0.0001	-0.0001	0.0003	155.5	148.2	152.5	152.0666667
Spiggie 2	Mg2852	285.213	ppm	11.32523	0.079	0.7051	11.22	11.29	11.13	75590	76040	74960	75530
Spiggie 2	V_3093	309.311	ppm	0.0253	0.0005	2.083	0.0251	0.0248	0.0258	803	810.8	811.1	808.3

	Method=StreamCations-JL(v5)												
	SampleName=Clumlie inlet 1												
Sample	Elem	WL	Units	Avg	Stddev	RSD	Rep1	Rep2	Rep3	Intensity 1	Intensity 2	Intensity 3	Intensity avg
Spiggie 2	Cu3273	327.396	ppm	0.0044	0.0013	28.81	0.0036	0.0059	0.0038	547.9	548.8	545.4	547.3666667
Spiggie 2	Ni3414	341.476	ppm	0.004	0.0068	170.5	0.0111	-0.0024	0.0033	616.8	611.4	611.2	613.1333333
Spiggie 2	Al3944	394.401	ppm	0.0095	0.0081	85.37	0.0102	0.0011	0.0173	1100	1098	1099	1099
Spiggie 2	Sr4215	421.552	ppm	0.1356	0.0011	0.8104	0.1359	0.1365	0.1344	29750	29890	29430	29690
Spiggie 2	Ca4226	422.673	ppm	19.12211	0.1172	0.6659	17.55	17.73	17.51	51000	51530	50890	51140
Spiggie 2	Na5889	588.995	ppm	80.22	0.4809	0.5995	80.12	80.74	79.8	546300	550300	544100	546900
Spiggie 2	Na5895	589.592	ppm	81.06	0.4903	0.6049	81	81.58	80.6	309400	311500	307900	309600
Spiggie 2	K_7664	766.490	ppm	3.455	0.008	0.2313	3.459	3.459	3.445	8220	8230	8202	8217.333333
Spiggie 2	K_7698	769.896	ppm	3.405	0.0418	1.229	3.364	3.447	3.404	4728	4781	4754	4754.333333
Spiggie Inlet	Zn2025	202.548	ppm	0.0045	0.0003	7.376	0.0049	0.0044	0.0043	27.01	26.83	26.71	26.85
Spiggie Inlet	Zn2062	206.200	ppm	0.0041	0.001	23.58	0.005	0.0041	0.0031	26.66	26.5	26.19	26.45
Spiggie Inlet	Zn2138	213.856	ppm	0.0047	0	0.7934	0.0047	0.0047	0.0047	43.32	43.39	43.13	43.28
Spiggie Inlet	Pb2203	220.353	ppm	0.0028	0.0025	88.27	0.0004	0.0053	0.0027	40.43	41.58	40.87	40.96
Spiggie Inlet	Cd2265	226.502	ppm	0	0.0001	971.1	0.0001	0	-0.0001	48.65	48.8	48.09	48.51333333
Spiggie Inlet	Co2378	237.862	ppm	0	0.0018	6279	-0.0014	-0.0005	0.002	103.9	105.1	108.5	105.8333333
Spiggie Inlet	Fe2599	259.940	ppm	0.0748	0.0003	0.4618	0.0751	0.0745	0.0749	426.6	425.2	426.2	426
Spiggie Inlet	Mn2605	260.569	ppm	0.3145	0.0012	0.368	0.3132	0.3149	0.3154	3414	3430	3439	3427.666667
Spiggie Inlet	Cr2843	284.325	ppm	-0.0006	0.001	170.1	-0.0017	0	0	158.8	156.1	157.3	157.4
Spiggie Inlet	Mg2852	285.213	ppm	8.796894	0.0499	0.5735	8.659	8.686	8.756	58400	58570	59050	58673.33333
Spiggie Inlet	V_3093	309.311	ppm	0.0185	0.0002	0.9697	0.0183	0.0187	0.0185	728.4	736	731.8	732.0666667
Spiggie Inlet	Cu3273	327.396	ppm	0.0029	0.0013	46.04	0.0019	0.0023	0.0044	543.6	541.1	555.6	546.7666667
Spiggie Inlet	Ni3414	341.476	ppm	0.0053	0.0057	108.2	0.011	0.0052	-0.0004	623.7	617.3	618	619.6666667
Spiggie Inlet	Al3944	394.401	ppm	0.0357	0.0183	51.28	0.0179	0.0545	0.0347	1114	1126	1129	1123
Spiggie Inlet	Sr4215	421.552	ppm	0.1209	0.0006	0.5308	0.1202	0.1209	0.1215	26530	26670	26810	26670
Spiggie Inlet	Ca4226	422.673	ppm	19.87512	0.0603	0.3293	18.25	18.37	18.31	53000	53310	53140	53150
Spiggie Inlet	Na5889	588.995	ppm	48.53	0.2054	0.4233	48.77	48.44	48.39	336000	334200	333800	334666.6667
Spiggie Inlet	Na5895	589.592	ppm	49.05	0.1902	0.3877	48.84	49.14	49.18	188500	189600	189800	189300
Spiggie Inlet	K_7664	766.490	ppm	1.212	0.0159	1.309	1.205	1.2	1.23	6040	6016	6078	6044.666667
Spiggie Inlet	K_7698	769.896	ppm	1.195	0.0204	1.708	1.216	1.194	1.176	3697	3686	3701	3694.666667

	Method=StreamCations-JL(v5)												
	SampleName=Clumlie inlet 1												
Sample	Elem	WL	Units	Avg	Stddev	RSD	Rep1	Rep2	Rep3	Intensity 1	Intensity 2	Intensity 3	Intensity avg
Spiggie Outlet	Zn2025	202.548	ppm	0.0033	0.0003	7.896	0.0035	0.0034	0.003	26.47	26.76	26.88	26.70333333
Spiggie Outlet	Zn2062	206.200	ppm	0.0035	0.0005	14.01	0.0033	0.0031	0.004	25.95	26.04	26.67	26.22
Spiggie Outlet	Zn2138	213.856	ppm	0.0037	0.0001	2.881	0.0035	0.0037	0.0038	41.27	41.72	42.03	41.67333333
Spiggie Outlet	Pb2203	220.353	ppm	0.0009	0.0024	278	-0.0018	0.0031	0.0013	40.47	41.39	41.35	41.07
Spiggie Outlet	Cd2265	226.502	ppm	0.0001	0.0001	164.6	0	0	0.0002	48.73	49.11	49.14	48.99333333
Spiggie Outlet	Co2378	237.862	ppm	-0.0001	0.001	1850	0.0001	0.0009	-0.0011	105.7	107.5	103	105.4
Spiggie Outlet	Fe2599	259.940	ppm	0.0155	0.0009	5.892	0.0161	0.0144	0.0158	219.5	217.9	218.3	218.5666667
Spiggie Outlet	Mn2605	260.569	ppm	0.0137	0.0002	1.386	0.0137	0.0139	0.0135	298.8	302.6	295.4	298.9333333
Spiggie Outlet	Cr2843	284.325	ppm	0.0003	0.0005	173.4	-0.0001	0.0001	0.0008	155.1	155.7	156.9	155.9
Spiggie Outlet	Mg2852	285.213	ppm	11.46172	0.0444	0.3916	11.3	11.35	11.39	76150	76430	76740	76440
Spiggie Outlet	V_3093	309.311	ppm	0.0254	0.0002	0.758	0.0252	0.0254	0.0256	806.4	811	809	808.8
Spiggie Outlet	Cu3273	327.396	ppm	0.0023	0.0022	97.16	0.0013	0.0007	0.0048	542.7	543.8	548.8	545.1
Spiggie Outlet	Ni3414	341.476	ppm	0.0067	0.0012	17.93	0.0063	0.0057	0.008	618.9	622.8	614.1	618.6
Spiggie Outlet	Al3944	394.401	ppm	0.0134	0.0089	65.98	0.0198	0.0033	0.0172	1104	1109	1098	1103.666667
Spiggie Outlet	Sr4215	421.552	ppm	0.1362	0.001	0.7278	0.1352	0.1361	0.1372	29620	29810	30020	29816.66667
Spiggie Outlet	Ca4226	422.673	ppm	19.01722	0.1621	0.9265	17.32	17.53	17.64	50370	50980	51230	50860
Spiggie Outlet	Na5889	588.995	ppm	81.56	0.3169	0.3885	81.42	81.34	81.92	555200	554300	558500	556000
Spiggie Outlet	Na5895	589.592	ppm	82.71	0.5158	0.6236	82.19	82.72	83.22	313800	315900	317600	315766.6667
Spiggie Outlet	K_7664	766.490	ppm	3.524	0.0344	0.9748	3.507	3.502	3.564	8296	8338	8309	8314.333333
Spiggie Outlet	K_7698	769.896	ppm	3.463	0.0619	1.788	3.404	3.457	3.527	4772	4827	4811	4803.333333
Tingwall	Zn2025	202.548	ppm	0.0037	0.0004	11.75	0.0041	0.0033	0.0036	25.98	25.86	26.05	25.96333333
Tingwall	Zn2062	206.200	ppm	0.0039	0.0007	18.92	0.0045	0.0042	0.0031	26.73	26.45	26.28	26.48666667
Tingwall	Zn2138	213.856	ppm	0.0041	0.0001	3.608	0.0043	0.0041	0.004	42.39	42.23	41.91	42.17666667
Tingwall	Pb2203	220.353	ppm	-0.0005	0.0039	722.4	0.0039	-0.0036	-0.0019	40.92	40.45	40.82	40.73
Tingwall	Cd2265	226.502	ppm	0	0.0001	1140	0.0001	0	-0.0001	48.71	48.75	48.93	48.79666667
Tingwall	Co2378	237.862	ppm	0.0014	0.0015	105.9	0.0032	0.0009	0.0002	106.6	105.7	105.4	105.9
Tingwall	Fe2599	259.940	ppm	0.0075	0.0002	3.208	0.0075	0.0077	0.0072	189.6	192.8	189.6	190.6666667
Tingwall	Mn2605	260.569	ppm	0.0008	0.0003	37.81	0.0006	0.0007	0.0011	160.7	162.6	165.1	162.8

	Method=StreamCations-JL(v5)												
	SampleName=Clumlie inlet 1												
Sample	Elem	WL	Units	Avg	Stddev	RSD	Rep1	Rep2	Rep3	Intensity 1	Intensity 2	Intensity 3	Intensity avg
Tingwall	Cr2843	284.325	ppm	-0.0002	0.0024	1152	-0.0009	-0.0021	0.0024	157.8	160.3	166.3	161.4666667
Tingwall	Mg2852	285.213	ppm	4.54817	0.0248	0.554	4.497	4.453	4.495	30450	30150	30440	30346.66667
Tingwall	V_3093	309.311	ppm	0.0078	0.0002	2.837	0.0077	0.008	0.0076	619.5	626.1	620.8	622.1333333
Tingwall	Cu3273	327.396	ppm	0.004	0.0014	33.9	0.0038	0.0055	0.0028	541.7	553.3	541.1	545.3666667
Tingwall	Ni3414	341.476	ppm	0.0056	0.0071	127.4	0.0049	-0.0012	0.0131	618.2	619.9	621.4	619.8333333
Tingwall	Al3944	394.401	ppm	0.0764	0.0071	9.314	0.0843	0.0747	0.0704	1186	1191	1184	1187
Tingwall	Sr4215	421.552	ppm	0.1722	0.0013	0.7588	0.173	0.1707	0.1729	37400	36940	37370	37236.66667
Tingwall	Ca4226	422.673	ppm	29.03607	0.1225	0.454	27.07	26.85	27.05	77820	77210	77780	77603.33333
Tingwall	Na5889	588.995	ppm	30.43	0.2044	0.6717	30.52	30.19	30.56	214200	212100	214500	213600
Tingwall	Na5895	589.592	ppm	30.36	0.1836	0.6046	30.48	30.15	30.45	119400	118200	119200	118933.3333
Tingwall	K_7664	766.490	ppm	1.918	0.0143	0.7464	1.91	1.91	1.935	6722	6771	6751	6748
Tingwall	K_7698	769.896	ppm	1.929	0.0157	0.8126	1.947	1.917	1.924	4056	4081	4062	4066.333333

Hydrolab Data

Loch of Brow								
5/31/2011								
WP 122								
sunny close to 50° light to moderate winds under 15 mph								
cored early in the morning around 8:30								
Depth	Temp	SpC	pH	DO	notes			
0	12.69	0.396	n/a	10.74				
0.2	12.68	0.397	n/a	10.65				
0.4	12.67	0.397	n/a	10.62			Secchi Depth: 1.5 m	
0.6	12.67	0.397	n/a	10.64				visable on l
0.8	12.68	0.397	n/a	10.6				
1	12.67	0.397	n/a	10.59				
1.2	12.68	0.395	n/a	10.01				
1.4	12.67	0.396	n/a	n/a	in mud			

Loch of Spiggie#1								
5/28/2011								
WP 1								
45-50° with alternating rain and sun								
high winds probably 30 mph that caused boat to drift significantly								
	Temp(°C)	SpC(µS/mol)	pH	DO(mg/L)				
0.0	11.25	0.621	n/a	11.55				
0.5	11.25	0.622	n/a	11.37			Secchi Depth: 1.0 r	
1.0	11.25	0.622	n/a	11.31				
1.5	11.25	0.622	n/a	11.27				
2.0	11.25	0.622	n/a	11.27				
2.5	11.25	0.622	n/a	11.26				
3.0	11.25	0.622	n/a	11.25				
3.5	11.25	0.622	n/a	11.19				
4.0	11.25	0.622	n/a	11.16				
4.5	11.25	0.623	n/a	11.15				
5.0	11.25	0.622	n/a	11.21				
5.5	11.25	0.623	n/a	11.29				
6.0	11.26	0.623	n/a	11.15				
6.5	11.25	0.623	n/a	11.74				
7.0	11.23	0.624	n/a	7.34				

Loch of Spiggie #2								
5/31/2011								
WP 126								
55° sunny with light wind gusts less than 5 mph								
Depth(m)	Temp(°C)	SpC(µS/mol)	pH	DO(mg/L)				
0.0	12.71	0.626	n/a	11.54				
0.5	12.74	0.628	n/a	11.42				
1.0	12.73	0.628	n/a	11.36				
1.5	12.72	0.628	n/a	11.32				
2.0	12.73	0.629	n/a	11.45			Secchi Depth: 1.3 r	
2.5	12.71	0.629	n/a	11.35				
3.0	12.7	0.629	n/a	11.22				
3.5	12.6	0.629	n/a	11.28				
4.0	12.27	0.629	n/a	11.09				
4.5	12.05	0.629	n/a	10.95				
5.0	11.79	0.63	n/a	10.86				
5.5	11.75	0.63	n/a	10.71				
6.0	11.55	0.63	n/a	10.92				
6.5	11.47	0.63	n/a	10.87				
7.0	11.45	0.63	n/a	10.74				
7.5	11.4	0.63	n/a	10.84				
8.0	11.34	0.631	n/a	10.77				
8.5	11.33	0.631	n/a	10.65				
9.0	11.3	0.631	n/a	10.61				
9.5	11.29	0.631	n/a	10.7				
10.0	11.26	0.631	n/a	10.7				
10.5	11.24	0.632	n/a	10.52				
10.9	11.21	0.631	n/a	9.62				

Loch of Tingwall								
6/6/2011								
Bev, Mike, and Julie								
data received from Bev								
WP 136								
Depth(m)	Temp(°C)	SpC(µS/mo	pH	DO(mg/L)				
0	12.94	0.336	n/a	11.20				
1	12.94	0.335	n/a	11.23				
2	2.94	0.335	n/a	11.18				
3	12.93	0.335	n/a	11.17				
4	12.86	0.335	n/a	11.17			Secchi Depth: 5.0 m	
5	12.54	0.335	n/a	11.14				
6	12.46	0.335	n/a	11.01				
7	12.22	0.335	n/a	10.90				
8	12.16	0.335	n/a	10.69				
9	12.07	0.335	n/a	10.67				
10	12.05	0.335	n/a	10.58				
11	12.03	0.335	n/a	10.44				
12	11.96	0.335	n/a	10.34				
13	11.96	0.336	n/a	10.34				
14	11.95	0.336	n/a	10.38				
15	11.974	0.336	n/a	10.30				
16	11.94	0.335	n/a	10.30				
16.2	11.93	0.336	n/a	10.05				
16.5	11.93	0.338	n/a	8.45				

Loch of Clumlie								
6/4/2011								
Bev, Mike, and Julie								
data received from Bev								
Center of S. Basin								
Depth(m)	Temp(°C)	SpC(µS/mo	pH	DO(mg/L)				
0	13.74	0.381	n/a	10.3				
0.5	13.72	0.38	n/a	9.98		Secchi Disk visable on bottom		
1	13.72	0.38	n/a	9.98				
N. Basin								
Depth(m)	Temp(°C)	SpC(µS/mo	pH	DO(mg/L)				
0	13.04	0.378	n/a	10.3				
0.5	13.76	0.378	n/a	9.98		Secchi Disk visable on bottom		
0.8	13.72	0.378	n/a	9.98				
0.9	13.7	0.378	n/a					

Appendix B:

Sedimentary Data

Core	Crucible #	Depth	Crucible Wt(g)	Crucible + Sample(g)	Wet Sample(g)	Crucible + Dry Sample(g)	Dry Sample(g)	%H2O	Dry Bulk Density	Run 1 Mean	Run 1 Median
Brow2011_1	1	.5-1.5	21.5802	22.5737	0.9935	21.8276	0.2474	75.098138	0.2474	n/a	n/a
Brow2011_1	2	7-8	18.5744	19.5709	0.9965	18.8728	0.2984	70.055193	0.2984	47.31	36.45
Brow2011_1	3	13.5-14.5	19.2226	20.2592	1.0366	19.5148	0.2922	71.811692	0.2922	45.48	34.82
Brow2011_1	4	14.5-15.5	21.0781	22.7499	1.6718	21.9486	0.8705	47.930374	0.8705	68.29	37.29
Brow2011_1	5	18-19	17.5551	18.8345	1.2794	18.1426	0.5875	54.080038	0.5875	56.15	50.49
Brow2011_1	6	22-23	19.9369	21.2607	1.3238	20.4653	0.5284	60.084605	0.5284	52.01	45.4
Brow2011_1	7	23-24	21.5265	22.8721	1.3456	21.9953	0.4688	65.160523	0.4688	50.34	40.27
Brow2011_1	8	24.5-25.5	20.6259	22.3214	1.6955	21.6667	1.0408	38.613978	1.0408	69.49	65.35
Brow2011_1	9	25.5-26.5	21.2279	22.5811	1.3532	21.8394	0.6115	54.810819	0.6115	n/a	n/a
Brow2011_1	10	27.5-28.5	15.2232	16.5957	1.3725	15.8058	0.5826	57.551913	0.5826	65.03	60.47
Brow2011_1	11	28.5-29.5	17.8259	19.41265	1.58675	18.5161	0.6902	56.502285	0.6902	78.25	72.26
Brow2011_1	12	29.5-30.5	19.1055	20.4369	1.3314	19.8279	0.7224	45.741325	0.7224	70.14	66.49
Brow2011_1	13	30.5-31.5	17.9771	19.4145	1.4374	18.7362	0.7591	47.18937	0.7591	65.7	63.28
Brow2011_1	14	32-33	19.2017	20.6156	1.4139	19.9867	0.785	44.479808	0.785	n/a	n/a
Brow2011_1	15	34.5-35.5	20.259	21.6074	1.3484	20.9276	0.6686	50.415307	0.6686	66.54	63.42
Brow2011_1	16	35.5-36.5	15.5771	16.899	1.3219	16.2678	0.6907	47.749452	0.6907	74.24	66
Brow2011_1	17	43-44	17.8396	18.9667	1.1271	17.9981	0.1585	85.937361	0.1585	34.78	16.84
Brow2011_1	18	48-49	18.7839	19.9472	1.1633	18.9206	0.1367	88.248947	0.1367	27.67	14.97
Brow2011_2	19	0-1	16.631	17.8203	1.1893	16.9953	0.3643	69.368536	0.3643	40.99	29.04
Brow2011_2	20	1-2	18.2559	19.8431	1.5872	18.7435	0.4876	69.279234	0.4876	49.43	36.75
Brow2011_2	21	2.5-3.5	18.2368	19.5657	1.3289	18.7296	0.4928	62.916698	0.4928	48.25	33.4
Brow2011_2	22	15-16	18.741	20.0319	1.2909	19.2293	0.4883	62.173677	0.4883	n/a	n/a
Brow2011_2	23	30-31	19.8657	21.3479	1.4822	20.5765	0.7108	52.044259	0.7108	93.9	75.08
Brow2011_2	24	40-41	18.6738	19.8081	1.1343	18.895	0.2212	80.498986	0.2212	55.94	26.98
Brow2011_2	25	41-42	17.7838	18.8139	1.0301	17.9509	0.1671	83.778274	0.1671	41.07	21.68
Brow2011_2	26	50-51	20.8309	21.8657	1.0348	20.9259	0.095	90.819482	0.095	35.1	15.99
Brow2011_2	27	66-67	15.9257	17.1485	1.2228	16.0455	0.1198	90.202813	0.1198	41.86	18.38
Brow2011_3	8546.0000	1	20.6981	22.1704	1.4723	21.0379	0.3398	76.920465	0.3398	35.76	21.11
Brow2011_3	8729	3									
Brow2011_3	8730	5									
Brow2011_3	8731	7									
Brow2011_3	8547.0000	9.5	17.4222	18.681	1.2588	17.7667	0.3445	72.632666	0.3445	39.39	26.67
Brow2011_3	8732	12									

Core	Run 2 Mean	Run 2 Median	Run 3 Mean	Run 3 Median	Average Mean Uncorrected	Average Median Uncorrected	Obscuration %	Fraunhofer Run 1 Mean	Run 1 Median	Run 2 Mean
Brow2011_1	35.15	21.17	34.65	20.72	34.9	20.945	9	36.1626	21.43	35.7431
Brow2011_1	46.66	35.84	52.36	36.84	48.77666667	36.37666667	10	52.2733	37.0875	51.1092
Brow2011_1	46.83	35.03	48.36	35.07	46.89	34.97333333	8	47.491	35.3281	47.5003
Brow2011_1	67.9	66.81	66.52	65.2	67.57	56.43333333	10	67.4522	66.7394	67.1753
Brow2011_1	55.14	49.18	54.4	49.32	55.23	49.66333333	10	55.7131	50.2907	58.5566
Brow2011_1	56.65	46.37	52.62	45.87	53.76	45.88	8	52.6412	45.8693	52.6711
Brow2011_1	50.02	40.01	50.46	39.82	50.27333333	40.03333333	5	51.1267	40.4468	50.6775
Brow2011_1	70.75	65.95	70.24	65.17	70.16	65.49	6	70.3593	65.8166	70.414
Brow2011_1	n/a	n/a	n/a	n/a			14	61.4812	54.8785	61.7082
Brow2011_1	64.14	59.6	63.45	58.43	64.20666667	59.5	8	64.9129	59.613	64.4865
Brow2011_1	76.05	71.37	73.38	71.69	75.89333333	71.77333333	5	75.0692	70.0952	75.1896
Brow2011_1	70.07	65.92	69.67	66.08	69.96	66.16333333	13	69.6356	66.1646	69.6886
Brow2011_1	66.01	63.44	65.91	63.01	65.87333333	63.24333333	10	66.6002	63.8055	66.5273
Brow2011_1	59.59	55.13	59.49	54.77	59.54	54.95	7	60.5268	55.5528	60.4092
Brow2011_1	66.79	63.7	65.15	62.73	66.16	63.28333333	6	67.3099	63.9297	66.3972
Brow2011_1	69.86	64.95	69.1	64.56	71.06666667	65.17	8	78.9591	66.5023	76.7136
Brow2011_1	31.91	16.63	32.66	16.6	33.11666667	16.69	5	34.481	16.8068	34.1572
Brow2011_1	30.18	15.33	27.82	14.96	28.55666667	15.08666667	6	28.9422	15.2312	28.9161
Brow2011_2	41.01	29.27	38.93	27.62	40.31	28.64333333	10	40.879	28.967	40.5048
Brow2011_2	57.03	38.41	56.74	38.18	54.4	37.78	13	55.4116	38.1782	54.8594
Brow2011_2	51.87	33.69	50.34	33.61	50.15333333	33.56666667	8	47.2192	32.8756	47.4127
Brow2011_2	61.12	48.21	57	46.49	59.06	47.35	11	57.7458	47.2828	57.8155
Brow2011_2	90.16	74.27	75.94	70.04	86.66666667	73.13	7	83.9718	73.0161	89.6245
Brow2011_2	54.33	26.93	57.89	25.5	56.05333333	26.47	6	54.6644	26.995	56.2143
Brow2011_2	43.76	22.19	47.04	22.25	43.95666667	22.04	4	44.4122	22.4628	44.0667
Brow2011_2	26	14.36	26.24	14.37	29.11333333	14.90666667	4	30.2044	15.0103	31.7098
Brow2011_2	39.3	18.3	40.16	18.23	40.44	18.30333333	7	40.8908	18.4043	38.535
Brow2011_3	37.53	21.64	35.44	20.39	36.24333333	21.04666667	10	37.4297	21.5567	37.4626
Brow2011_3								21.3570	16.4174	21.7684
Brow2011_3								25.7968	20.6974	25.8501
Brow2011_3								24.7880	20.1159	24.6375
Brow2011_3	37.41	25.62	38.46	26.04	38.42	26.11	10	38.7268	26.4147	38.2691
Brow2011_3								21.4189	25.3894	29.2594

Core	Run 2 Median	Run 3 Mean	Run 3 Median	Average Mean	Fraunhofer Mean	Average Median	Fraunhofer Median
Brow2011_1	21.3074	35.8166	21.2741	35.907433	0.2240158	21.337167	0.082102
Brow2011_1	36.707	51.9024	36.8353	51.761633	0.5946794	36.8766	0.193583
Brow2011_1	35.242	47.8371	35.4114	47.609467	0.1971911	35.327167	0.084704
Brow2011_1	66.5119	66.8924	66.1433	67.1733	0.2799054	66.464867	0.30082
Brow2011_1	50.7556	55.4611	50.0537	56.576933	1.7190655	50.366667	0.357063
Brow2011_1	45.7125	52.3703	45.6244	52.560867	0.1657113	45.7354	0.124046
Brow2011_1	40.1094	50.4655	40.0017	50.756567	0.3376167	40.185967	0.232218
Brow2011_1	65.4342	70.3662	65.4532	70.379833	0.0297897	65.568	0.215503
Brow2011_1	54.9131	61.5508	54.8203	61.580067	0.1162955	54.870633	0.046897
Brow2011_1	59.3154	63.9878	58.8656	64.4624	0.4630206	59.264667	0.376274
Brow2011_1	70.1475	75.7487	70.4225	75.335833	0.3625854	70.221733	0.175825
Brow2011_1	66.2592	69.423	65.9124	69.5824	0.140565	66.112067	0.179269
Brow2011_1	63.686	66.3192	63.3793	66.482233	0.1458201	63.6236	0.219845
Brow2011_1	55.3358	60.0584	55.2119	60.331467	0.2436832	55.366833	0.172556
Brow2011_1	63.2589	66.5767	63.391	66.761267	0.4835328	63.526533	0.355345
Brow2011_1	65.9823	76.3477	65.6069	77.340133	1.4139521	66.0305	0.449642
Brow2011_1	16.8394	33.6465	16.6764	34.0949	0.4207238	16.7742	0.086251
Brow2011_1	15.1906	28.6188	15.0628	28.8257	0.1796553	15.161533	0.087882
Brow2011_2	28.7257	40.2957	28.4863	40.559833	0.2955186	28.726333	0.240351
Brow2011_2	37.886	53.7829	37.5969	54.684633	0.8282955	37.887033	0.290651
Brow2011_2	32.9342	46.8559	32.4857	47.1626	0.2826822	32.765167	0.243792
Brow2011_2	47.2469	57.1547	46.8099	57.572	0.3630689	47.1132	0.263278
Brow2011_2	73.9496	81.0465	71.8877	84.880933	4.3606666	72.951133	1.032484
Brow2011_2	26.8927	54.1989	26.6433	55.025867	1.0552028	26.843667	0.180904
Brow2011_2	22.0634	43.6081	21.9047	44.029	0.4033735	22.143633	0.287571
Brow2011_2	15.1717	31.0292	14.9945	30.981133	0.7538502	15.058833	0.098064
Brow2011_2	18.1042	39.1566	18.1695	39.527467	1.2209033	18.226	0.157826
Brow2011_3	21.4085	37.5123	21.2518	37.4682	0.0415838	21.405667	0.15247
Brow2011_3	16.5719	21.3627	16.3861	21.496033	0.2358937	16.458467	0.099475
Brow2011_3	20.7468	25.8634	20.7809	25.836767	0.0352452	20.7417	0.041983
Brow2011_3	19.9957	24.7484	20.0638	24.724633	0.0780141	20.058467	0.060277
Brow2011_3	26.0454	38.2487	25.8335	38.414867	0.2703347	26.097867	0.294131
Brow2011_3	25.1856	29.2617	25.1723	26.646667	4.5273789	25.2491	0.121685

Core	Crucible #	Depth	Crucible Wt(g)	Crucible + Sample(g)	Wet Sample(g)	Crucible + Dry Sample(g)	Dry Sample(g)	%H2O	Dry Bulk Density	Run 1 Mean	Run 1 Median
Brow2011_3	8548.0000	16.25	17.4297	18.8008	1.3711	17.9522	0.5225	61.891912	0.5225	75.31	34.42
Brow2011_3	8549.0000	17.25	19.7608	21.612	1.8512	20.6522	0.8914	51.84745	0.8914	78.12	71.74
Brow2011_3	8550.0000	19.5	20.1956	21.8815	1.6859	21.114	0.9184	45.524646	0.9184	73.93	69.65
Brow2011_3	8551.0000	20.5	20.0337	21.7837	1.75	21.086	1.0523	39.868571	1.0523	82.63	74.4
Brow2011_3	8552	21.5	21.7384	23.073	1.3346	22.1679	0.4295	67.818073	0.4295	69.39	50.49
Brow2011_3	8553	22.5	18.4032	20.0796	1.6764	19.4142	1.011	39.692198	1.011	72.77	62.68
Brow2011_3	8733	25		s							
Brow2011_3	8734	27									
Brow2011_3	8554.0000	29.5	19.9528	21.0567	1.1039	20.3784	0.4256	61.445783	0.4256	54.08	45.37
Brow2011_3	8735	32									
Brow2011_3	8736	34									
Brow2011_3	8555.0000	35.5	18.1084	19.5015	1.3931	18.7389	0.6305	54.741225	0.6305	66.75	53.01
Brow2011_3	8556.0000	36.5	19.6126	21.1241	1.5115	20.2416	0.629	58.38571	0.629	72.38	58.16
Brow2011_3	8737	37.5									
Brow2011_3	8557.0000	39.5	18.6589	19.9479	1.289	19.1281	0.4692	63.59969	0.4692	73.95	56.2
Brow2011_3	8738	42									
Brow2011_3	8558.0000	43.5	17.5166	18.4058	0.8892	17.605	0.0884	90.05848	0.0884	39.67	17.43
Brow2011_3	8559.0000	44.5	19.9292	20.9886	1.0594	20.0216	0.0924	91.278082	0.0924	n/a	n/a
Brow2011_3	8739	47									
Brow2011_3	8740	49									
Brow2011_3	8741	51									
Brow2011_3	8742	53									
Brow2011_3	8743	55									
Brow2011_3	8560.0000	57.5	21.8621	22.7622	0.9001	21.9644	0.1023	88.634596	0.1023	30.73	14.21
Brow2011_3	8744	61									
Brow2011_3	8745	63									
Brow2011_3	8746	65									
Brow2011_3	8561.0000	67.5	19.1722	20.3568	1.1846	19.2978	0.1256	89.397265	0.1256	63.66	35.79
Brow2011_4	44	0-1	18.4943	19.5706	1.0763	18.6564	0.1621	84.939143	0.1621	n/a	n/a
Brow2011_4	45	6-7	19.2589	20.3154	1.0565	19.5009	0.242	77.094179	0.242	39.45	27.95
Brow2011_4	46	11.5-12.5	18.8947	20.0109	1.1162	19.1842	0.2895	74.063788	0.2895	43.87	35.82
Brow2011_4	47	12.5-13.5	18.892	20.0592	1.1672	19.1198	0.2278	80.483208	0.2278	39.13	28.4
Brow2011_4	48	18-19	18.6742	19.8494	1.1752	18.8923	0.2181	81.441457	0.2181	34.84	21.36
Brow2011_4	49	25-26	17.5892	18.7635	1.1743	17.8532	0.264	77.518522	0.2640	53.5400	34.0800

Core	Run 2 Mean	Run 2 Median	Run 3 Mean	Run 3 Median	Average Mean Uncorrected	Average Median Uncorrected	Obscuration %	Fraunhofer Run 1 Mean	Run 1 Median	Run 2 Mean
Brow2011_3	73.24	62.74	73.7	64.3	74.08333333	53.82	6	75.6509	64.7133	74.0732
Brow2011_3	79.71	71.75	75.67	70.39	77.83333333	71.29333333	13	79.8967	71.8345	79.0249
Brow2011_3	73.97	69.57	74.67	70.14	74.19	69.78666667	12	74.8521	70.0142	74.6143
Brow2011_3	84.35	77.59	84.44	74.5	83.80666667	75.49666667	10	83.1574	75.9024	83.3381
Brow2011_3	70.63	50.56	67.68	48.14	69.23333333	49.73	10	70.5641	51.3115	69.8433
Brow2011_3	72.26	62.41	76.22	64.23	73.75	63.10666667	9	72.8026	63.0814	72.2708
Brow2011_3								52.0884	46.4450	51.4365
Brow2011_3								40.4445	37.5784	40.3343
Brow2011_3	54.62	45.64	55.06	45.78	54.58666667	45.59666667	10	55.1208	45.7965	54.6668
Brow2011_3								56.0751	51.3548	56.3644
Brow2011_3								55.2732	49.5443	54.8464
Brow2011_3	69.08	53.31	72.5	54.48	69.44333333	53.6	12	70.8544	54.6773	70.8641
Brow2011_3	73.18	58.12	70.87	56.53	72.14333333	57.60333333	11	74.9819	58.9922	75.7455
Brow2011_3								111.4290	67.1365	74.5745
Brow2011_3	75.13	56.69	70.98	53.14	73.35333333	55.34333333	11	71.9628	54.9388	73.1554
Brow2011_3								54.8368	33.9387	52.6546
Brow2011_3	43.04	18.43	42.64	17.71	41.78333333	17.85666667	8	40.2745	17.61	40.2855
Brow2011_3	21.87	13.85	24.25	14.45	23.06	14.15	7	26.4503	14.8513	25.9376
Brow2011_3								47.0782	36.8355	43.6871
Brow2011_3								57.7682	41.1007	45.9752
Brow2011_3								70.8255	45.8841	50.5139
Brow2011_3								60.0017	45.0983	56.0859
Brow2011_3								84.4051	55.4781	66.0309
Brow2011_3	34.45	14.7	34.56	14.35	33.24666667	14.42	6	32.4098	14.2887	34.3542
Brow2011_3								73.2782	62.5346	93.4029
Brow2011_3								78.6597	69.0588	102.3520
Brow2011_3								274.1780	86.3739	294.2070
Brow2011_3	52.13	31.41	64.01	34.37	59.93333333	33.85666667	7	65.517	36.104	64.4318
Brow2011_4	21.61	10.02	20.62	9.996	21.115	10.008	8	22.3926	10.2066	21.1312
Brow2011_4	38.75	28.31	40.13	28.11	39.44333333	28.12333333	7	39.9201	28.1522	40.2603
Brow2011_4	43.4	35.6	43.76	35.94	43.67666667	35.78666667	7	43.2375	35.715	43.7923
Brow2011_4	41.62	28.97	39.55	28.9	40.1	28.75666667	6	41.4248	29.4725	41.1472
Brow2011_4	31.7	20.98	38.73	22.47	35.09	21.60333333	4	36.4732	22.0903	37.0425
Brow2011_4	53.1200	34.0800	48.1200	32.7300	51.5933	33.6300	8.0000	50.8567	33.3141	50.9006

Core	Run 2 Median	Run 3 Mean	Run 3 Median	Average Mean	Fraunhofer Mean	Average Median	Fraunhofer Median
Brow2011_3	63.7211	75.4238	64.1107	75.0493	0.8529197	64.1817	0.499896
Brow2011_3	71.1011	78.7752	70.7078	79.232267	0.5888049	71.214467	0.571841
Brow2011_3	69.8903	74.7436	69.7774	74.736667	0.1190515	69.893967	0.118443
Brow2011_3	75.8182	82.6838	75.1212	83.059767	0.3378999	75.613933	0.428791
Brow2011_3	50.5475	69.5584	50.1266	69.9886	0.5183553	50.661867	0.600672
Brow2011_3	65.5038	72.7639	62.8992	72.612433	0.2964952	63.828133	1.454027
Brow2011_3	45.8452	51.2456	45.7368	51.590167	0.4419141	46.009	0.381457
Brow2011_3	37.5494	39.8060	37.0433	40.194933	0.3413032	37.390367	0.300918
Brow2011_3	45.3884	54.9722	45.6087	54.919933	0.2314689	45.597867	0.204266
Brow2011_3	51.4081	55.2852	50.7944	55.908233	0.5586157	51.185767	0.33998
Brow2011_3	49.3358	54.3726	48.9891	54.830733	0.4505044	49.289733	0.280452
Brow2011_3	54.4892	70.7522	54.1767	70.823567	0.0619953	54.447733	0.252863
Brow2011_3	58.9627	75.0106	58.7608	75.246	0.4328176	58.905233	0.12595
Brow2011_3	63.1679	75.4749	63.0134	87.159467	21.022853	64.439267	2.33715
Brow2011_3	55.0949	71.2431	54.2722	72.120433	0.9658463	54.768633	0.436951
Brow2011_3	30.3520	43.4696	27.6453	50.320333	6.032405	30.645333	3.156937
Brow2011_3	17.6145	42.735	17.9866	41.098333	1.4174056	17.737033	0.216143
Brow2011_3	14.7404	25.9746	14.7642	26.120833	0.2859256	14.7853	0.058383
Brow2011_3	33.5387	45.3827	35.1691	45.382667	1.69555	35.1811	1.648433
Brow2011_3	36.2258	43.2181	33.8139	48.987167	7.7285387	37.0468	3.712128
Brow2011_3	38.0772	48.3034	35.5760	56.5476	12.414322	39.845767	5.376812
Brow2011_3	39.8482	54.6493	37.3406	56.9123	2.7702435	40.762367	3.95882
Brow2011_3	46.6891	60.6334	42.7601	70.356467	12.462196	48.3091	6.511926
Brow2011_3	14.427	32.6719	14.266	33.1453	1.0551083	14.327233	0.087143
Brow2011_3	81.2886	79.7299	68.9153	82.137	10.276015	70.912833	9.535236
Brow2011_3	91.4780	87.0125	77.2154	89.3414	12.016618	79.250733	11.34734
Brow2011_3	79.2926	315.0300	76.4246	294.47167	20.427286	80.697033	5.121178
Brow2011_3	35.5314	64.886	35.2157	64.944933	0.5449951	35.617033	0.450299
Brow2011_4	10.1096	22.0079	10.1675	21.8439	0.646494	10.161233	0.048803
Brow2011_4	28.1585	39.8695	28.024	40.016633	0.2125328	28.111567	0.0759
Brow2011_4	35.7426	43.3661	35.5057	43.4653	0.2903984	35.654433	0.129544
Brow2011_4	29.2749	40.3411	29.0045	40.971033	0.5629187	29.250633	0.234942
Brow2011_4	22.1541	36.7989	22.1186	36.771533	0.2856349	22.121	0.031968
Brow2011_4	33.1206	51.5113	33.088	51.089533	0.3659196	33.174233	0.12222

Core	Crucible #	Depth	Crucible Wt(g)	Crucible + Sample(g)	Wet Sample(g)	Crucible + Dry Sample(g)	Dry Sample(g)	%H2O	Dry Bulk Density	Run 1 Mean	Run 1 Median
Brow2011_4	50	26-27	17.6034	18.7219	1.1185	17.8253	0.2219	80.16093	0.2219	54.6200	40.7300
Brow2011_4	51	36-37	20.709	22.0698	1.3608	20.8103	0.1013	92.55585	0.1013	176.7300	75.8100
Brow2011_4	52	41-42	17.8684	18.9684	1.1	17.9567	0.0883	91.972727	0.0883	48.4700	25.3700
Brow2011_4	53	42-43	17.2434	18.7337	1.4903	17.3821	0.1387	90.693149	0.1387	86.2900	44.3100
Brow2011_4	54	50-51	19.8095	21.1852	1.3757	19.9493	0.1398	89.837901	0.1398	21.4000	10.5200
Brow2011_4	55	66-67	20.7817	21.9946	1.2129	20.9563	0.1746	85.604749	0.1746	20.3600	10.6200
Brow2011_4	56	67-68	18.8683	19.8998	1.0315	19.0043	0.136	86.815317	0.1360	20.0200	10.5900
Brow2011_4	57	72-73	19.2054	20.2443	1.0389	19.353	0.1476	85.792665	0.1476	18.5600	10.5000
Brow2011_4	58	79-80	18.461	19.457	0.996	18.5875	0.1265	87.299197	0.1265	13.2900	6.5350
Brow2011_5	59	0-1	17.7812	19.1795	1.3983	18.3677	0.5865	58.056211	0.5865	52.8900	46.7300
Brow2011_5	60	8-9	21.352	22.6238	1.2718	21.7352	0.3832	69.869476	0.3832	48.7000	37.3800
Brow2011_5	61	15-16	18.5767	19.6386	1.0619	18.9093	0.3326	68.678783	0.3326	53.9400	36.8600
Brow2011_5	62	16-17	19.1959	20.7591	1.5632	20.0773	0.8814	43.61566	0.8814	95.3100	91.6200
Brow2011_5	63	17-18	17.246	18.6861	1.4401	17.7822	0.5362	62.766475	0.5362	78.8400	54.2900
Brow2011_5	64	18-19	18.339	19.7125	1.3735	19.0542	0.7152	47.928649	0.7152	104.1000	98.0900
Brow2011_5	65	19-20	20.8092	22.3567	1.5475	21.7028	0.8936	42.25525	0.8936	121.2000	104.6000
Brow2011_5	66	20-21	20.7672	22.5708	1.8036	21.9428	1.1756	34.81925	1.1756	141.1000	134.3000
Brow2011_5	67	21-22	19.5466	21.1129	1.5663	20.5078	0.9612	38.632446	0.9612	155.0000	146.4000
Brow2011_5	68	22-23	19.5517	21.0868	1.5351	20.1045	0.5528	63.989317	0.5528	98.2000	62.4800
Brow2011_5	69	23-24	18.4877	19.5267	1.039	18.6114	0.1237	88.094321	0.1237	31.8500	10.2600
Brow2011_5	70	27-28	20.0683	21.2094	1.1411	20.1796	0.1113	90.246254	0.1113	14.9200	9.6680
Brow2011_5	71	33-34	17.9031	18.9248	1.0217	18.01	0.1069	89.537046	0.1069	17.1200	11.2400
Brow2011_5	72	43-44	17.9386	19.0522	1.1136	18.0619	0.1233	88.927802	0.1233	15.7600	9.9740
Brow2011_5	73	47-48	17.714	18.7632	1.0492	17.8301	0.1161	88.934426	0.1161	22.4900	17.6400
Spiggie2011_1	74	0-1	20.1538	21.4578	1.304	21.0457	0.8919	31.602761	0.8919	205.4000	171.7000
Spiggie2011_1	75	1-2	19.5469	21.0309	1.484	20.7185	1.1716	21.051213	1.1716	216.0000	168.4000
Spiggie2011_1	76	3-4	18.9188	20.5456	1.6268	20.2306	1.3118	19.363167	1.3118	n/a	n/a
Spiggie2011_1	77	5-6	20.7666	22.1173	1.3507	21.9054	1.1388	15.688162	1.1388	271.6000	274.2000
Spiggie2011_1	78	6-7	17.4982	19.0299	1.5317	18.7815	1.2833	16.217275	1.2833	328.3000	217.5000
Spiggie2011_1	79	8-9	18.1412	19.3328	1.1916	19.1093	0.9681	18.756294	0.9681	227.9000	159.3000
Spiggie2011_1	80	10-11	19.5832	21.1392	1.556	20.8956	1.3124	15.655527	1.3124	386.4000	298.6000
Spiggie2011_1	81	11-12	17.5394	18.8407	1.3013	18.5092	0.9698	25.474525	0.9698	139.3000	82.1400
Spiggie2011_1	82	19-20	17.6354	19.4422	1.8068	18.8585	1.2231	32.305734	1.2231	117.9000	57.0600

Core	Run 2 Mean	Run 2 Median	Run 3 Mean	Run 3 Median	Average Mean Uncorrected	Average Median Uncorrected	Obscuration %	Fraunhofer Run 1 Mean	Run 1 Median	Run 2 Mean
Brow2011_4	53.6000	39.9600	52.0100	38.7400	53.4100	39.8100	5.0000	58.8937	42.0501	60.7454
Brow2011_4	88.9500	43.0300	83.9100	40.9800	116.5300	53.2733	4.0000	91.8575	42.7109	89.5329
Brow2011_4	55.4400	27.8800	53.8400	27.7500	52.5833	27.0000	4.0000	58.9137	29.5358	58.1084
Brow2011_4	152.2000	60.8200	103.8000	45.3600	114.0967	50.1633	5.0000	112.94	50.4591	113.465
Brow2011_4	20.5800	10.3200	21.0700	10.4200	21.0167	10.4200	5.0000	22.388	10.5004	20.3732
Brow2011_4	18.3200	10.4500	17.5600	10.2200	18.7467	10.4300	6.0000	20.8456	10.6924	20.6718
Brow2011_4	20.9000	10.7200	20.0800	10.5200	20.3333	10.6100	5.0000	21.1777	10.7822	20.5142
Brow2011_4	16.6600	10.1000	16.1300	10.1300	17.1167	10.2433	7.0000	16.388	10.2316	16.4326
Brow2011_4	13.3600	6.6280	13.0300	6.5580	13.2267	6.5737	5.0000	13.5319	6.67004	13.5404
Brow2011_5	53.3200	47.1300	54.1800	48.0300	53.4633	47.2967	7.0000	54.1738	48.0132	54.1372
Brow2011_5	47.2700	36.5100	47.4700	36.6800	47.8133	36.8567	10.0000	47.1537	36.8742	46.7701
Brow2011_5	52.8300	36.1300	58.6000	40.4900	55.1233	37.8267	5.0000	59.9294	38.9315	60.5044
Brow2011_5	101.7000	89.7100	112.4000	91.6000	103.1367	90.9767	3.0000	104.58	92.5469	103.414
Brow2011_5	80.9700	53.1300	92.3000	55.7000	84.0367	54.3733	5.0000	77.4082	52.1015	79.3897
Brow2011_5	111.6000	105.1000	106.4000	98.0900	107.3667	100.4267	3.0000	113.73	101.8	115.123
Brow2011_5	116.7000	103.2000	120.3000	103.9000	119.4000	103.9000	6.0000	122.826	106.157	118.525
Brow2011_5	148.2000	130.8000	141.2000	135.9000	143.5000	133.6667	3.0000	143.349	132.943	143.018
Brow2011_5	160.6000	157.9000	156.7000	150.3000	157.4333	151.5333	4.0000	158.393	153.119	157.037
Brow2011_5	110.9000	84.6400	104.5000	74.3000	104.5333	73.8067	4.0000	110.369	79.1369	112.09
Brow2011_5	14.4600	8.7050	19.1300	8.9600	21.8133	9.3083	2.0000	15.3178	8.9426	15.0354
Brow2011_5	15.1900	9.8310	14.4900	9.4450	14.8667	9.6480	2.0000	14.6863	9.37033	14.6209
Brow2011_5	18.0200	11.5300	16.9500	11.0600	17.3633	11.2767	2.0000	17.3338	11.2563	16.6608
Brow2011_5	14.9700	9.6540	16.5900	9.9890	15.7733	9.8723	2.0000	16.1473	10.0533	15.9693
Brow2011_5	21.1300	16.4200	19.6100	13.5000	21.0767	15.8533	3.0000	27.2372	19.8355	21.9813
Spiggie2011_1	234.7000	165.9000	175.8000	158.7000	205.3000	165.4333	8.0000	213.869	161.072	156.134
Spiggie2011_1	237.2000	191.3000	n/a	n/a	226.6000	179.8500	3.0000	227.455	189.427	230.09
Spiggie2011_1	377.5000	342.4000	262.8000	265.3000	320.1500	303.8500	3.0000	270.073	266.135	285.007
Spiggie2011_1	305.9000	295.9000	249.9000	265.8000	275.8000	278.6333	5.0000	302.117	299.89	298.114
Spiggie2011_1	308.8000	224.4000	176.9000	118.0000	271.3333	186.6333	3.0000	285.539	212.464	228.1
Spiggie2011_1	169.5000	109.5000	265.0000	139.0000	220.8000	135.9333	7.0000	172.238	109.258	201.956
Spiggie2011_1	287.6000	236.7000	316.4000	311.9000	330.1333	282.4000	4.0000	348.679	269.808	365.174
Spiggie2011_1	133.4000	83.5400	120.8000	68.4900	131.1667	78.0567	7.0000	156.662	92.9329	148.895
Spiggie2011_1	117.3000	57.3500	162.1000	75.5200	132.4333	63.3100	15.0000	102.034	30.5207	128.422

Core	Run 2 Median	Run 3 Mean	Run 3 Median	Average Mean	Fraunhofer Mean	Average Median	Fraunhofer Median
Brow2011_4	42.3786	58.6978	41.5647	59.445633	1.1298846	41.9978	0.409463
Brow2011_4	42.1044	92.3544	42.6391	91.248267	1.5061838	42.4848	0.331386
Brow2011_4	28.8565	56.3152	28.3766	57.7791	1.3301802	28.922967	0.582451
Brow2011_4	51.1541	112.797	50.5468	113.06733	0.3517333	50.72	0.37849
Brow2011_4	10.3099	20.8548	10.3845	21.205333	1.0521454	10.398267	0.095993
Brow2011_4	10.6479	20.5635	10.6464	20.693633	0.1423117	10.662233	0.026136
Brow2011_4	10.649	20.6695	10.6294	20.787133	0.3470393	10.686867	0.083141
Brow2011_4	10.229	16.1037	10.1486	16.3081	0.1784147	10.203067	0.047187
Brow2011_4	6.68022	13.3785	6.63604	13.4836	0.0911184	6.6621	0.023135
Brow2011_5	47.9023	53.8074	47.5249	54.039467	0.2018071	47.813467	0.255984
Brow2011_5	36.5453	46.8409	36.3091	46.921567	0.2041264	36.5762	0.283814
Brow2011_5	39.067	61.8204	38.7003	60.7514	0.9693952	38.8996	0.18542
Brow2011_5	91.0338	102.489	91.4114	103.49433	1.0478122	91.664033	0.78755
Brow2011_5	52.4968	75.652	51.1029	77.4833	1.8699814	51.9004	0.71838
Brow2011_5	101.957	113.979	100.236	114.27733	0.7428757	101.331	0.951541
Brow2011_5	104.483	120.315	105.066	120.55533	2.1605486	105.23533	0.84975
Brow2011_5	131.224	144.449	132.547	143.60533	0.7491464	132.238	0.900195
Brow2011_5	152.498	158.42	150.856	157.95	0.7907964	152.15767	1.169257
Brow2011_5	81.4869	112.587	80.4182	111.682	1.1639283	80.347333	1.176602
Brow2011_5	8.84947	15.1778	8.84352	15.177	0.1412017	8.87853	0.055566
Brow2011_5	9.42265	14.27	9.18462	14.525733	0.2238726	9.3258667	0.125089
Brow2011_5	10.8555	16.992	10.9326	16.995533	0.3365139	11.0148	0.212668
Brow2011_5	9.96126	16.1187	9.98537	16.078433	0.0955879	9.9999767	0.047727
Brow2011_5	17.0033	19.9389	15.7448	23.052467	3.765215	17.527867	2.095193
Spiggie2011_1	138.437	158.199	137.639	176.06733	32.753482	145.716	13.30467
Spiggie2011_1	184.584	215.54	175.129	224.36167	7.7525582	183.04667	7.271915
Spiggie2011_1	277.431	272.735	264.604	275.93833	7.9656825	269.39	7.005658
Spiggie2011_1	298.296	296.45	295.119	298.89367	2.9128392	297.76833	2.428875
Spiggie2011_1	178.827	262.605	196.111	258.748	28.913094	195.80067	16.82065
Spiggie2011_1	116.688	201.382	117.262	191.85867	16.994419	114.40267	4.464646
Spiggie2011_1	285.315	329.707	254.189	347.85333	17.74791	269.77067	15.56303
Spiggie2011_1	88.5994	150.953	90.9401	152.17	4.0239768	90.824133	2.169076
Spiggie2011_1	63.4055	138.12	65.1436	122.85867	18.675194	53.023267	19.50716

Core	Crucible #	Depth	Crucible Wt(g)	Crucible + Sample(g)	Wet Sample(g)	Crucible + Dry Sample(g)	Dry Sample(g)	%H2O	Dry Bulk Density	Run 1 Mean	Run 1 Median
Spiggie2011_1	83	26.5-27.5	21.195	22.8028	1.6078	22.4839	1.2889	19.834557	1.2889	210.4000	162.5000
Spiggie2011_1	84	27.5-28.5	18.2562	19.8903	1.6341	19.526	1.2698	22.293617	1.2698	215.3000	168.0000
Spiggie2011_1	85	28.5-29.5	19.893	21.2911	1.3981	21.0421	1.1491	17.809885	1.1491	197.2000	144.1000
Spiggie2011_1	86	29.5-30.5	20.723	22.001	1.278	21.806	1.083	15.258216	1.0830	n/a	n/a
Spiggie2011_1	87	30.5-31.5	17.8216	19.0775	1.2559	18.7399	0.9183	26.881121	0.9183	159.4000	86.9100
Spiggie2011_1	88	31.5-32.5	18.1843	20.3765	2.1922	19.9129	1.7286	21.147706	1.7286	177.5000	47.7600
Spiggie2011_1	89	36-37	19.3226	20.7299	1.4073	20.3042	0.9816	30.249414	0.9816	136.5000	80.3800
Spiggie2011_1	90	41-42	21.3022	22.5027	1.2005	22.3387	1.0365	13.660975	1.0365	86.0100	43.9500
Spiggie2011_2	91	0-1	18.6412	19.7349	1.0937	18.9991	0.3579	67.276218	0.3579	n/a	n/a
Spiggie2011_2	92	7-8	16.1102	17.7859	1.6757	16.9958	0.8856	47.150445	0.8856	n/a	n/a
Spiggie2011_2	93	13.5-14.5	17.9934	19.6091	1.6157	19.0003	1.0069	37.680262	1.0069	138.0000	134.1000
Spiggie2011_2	94	14.5-15.5	18.6914	20.0931	1.4017	19.3858	0.6944	50.460156	0.6944	132.8000	121.0000
Spiggie2011_2	95	16-17	18.1414	19.1612	1.0198	18.3843	0.2429	76.181604	0.2429	34.6100	14.2500
Spiggie2011_2	96	19-20	18.7104	19.661	0.9506	18.9044	0.194	79.591837	0.1940	38.0700	11.9900
Spiggie2011_2	97	20-21	19.1773	20.8035	1.6262	20.1174	0.9401	42.190382	0.9401	126.1000	118.0000
Spiggie2011_2	98	27-28	19.8485	20.9043	1.0558	20.1883	0.3398	67.815874	0.3398	22.0900	14.2500
Spiggie2011_2	99	32-33	17.8032	18.9925	1.1893	18.2406	0.4374	63.222063	0.4374	29.6700	14.4100
Spiggie2011_2	100	33-34	19.0176	20.3406	1.323	19.5666	0.549	58.503401	0.5490	n/a	n/a
Spiggie2011_2	101	40-41	19.5704	20.8396	1.2692	20.126	0.5556	56.224393	0.5556	n/a	n/a
Spiggie2011_2	102	49-50	20.6414	21.9612	1.3198	21.343	0.7016	46.84043	0.7016	101.7000	80.4200
Spiggie2011_2	103	50-51	19.0418	20.4184	1.3766	19.8656	0.8238	40.156908	0.8238	n/a	n/a
Spiggie2011_2	104	67-68	18.6034	19.8956	1.2922	19.0865	0.4831	62.614146	0.4831	43.0800	22.5500
Spiggie2011_2	105	80-81	20.8126	21.9846	1.172	21.1565	0.3439	70.656997	0.3439	65.2200	32.9800
Spiggie2011_3	106	.5-1.5	18.5876	19.5367	0.9491	18.7538	0.1662	82.488673	0.1662	15.0100	11.9400
Spiggie2011_3	107	6-7	18.3598	19.5457	1.1859	18.6423	0.2825	76.17843	0.2825	n/a	n/a
Spiggie2011_3	108	11-12	18.3275	19.4127	1.0852	18.5552	0.2277	79.017693	0.2277	20.1200	12.8400
Spiggie2011_3	109	12-13	18.712	19.8948	1.1828	18.9728	0.2608	77.950626	0.2608	25.7900	17.8200
Spiggie2011_3	110	17-18	18.4622	19.4611	0.9989	18.6565	0.1943	80.548603	0.1943	17.9600	9.5310
Spiggie2011_3	111	25.5-26.5	18.7766	19.959	1.1824	19.239	0.4624	60.893099	0.4624	n/a	n/a
Spiggie2011_3	112	26.5-27.5	20.5034	22.0881	1.5847	21.6022	1.0988	30.661955	1.0988	n/a	n/a
Spiggie2011_3	113	35-36	18.2643	19.9785	1.7142	19.4172	1.1529	32.744137	1.1529	n/a	n/a
Spiggie2011_3	114	40-41	18.6969	20.5569	1.86	20.022	1.3251	28.758065	1.3251	219.0000	229.0000
Spiggie2011_3	115	41-42	18.1307	19.8661	1.7354	19.1814	1.0507	39.454881	1.0507	n/a	n/a

Core	Run 2 Mean	Run 2 Median	Run 3 Mean	Run 3 Median	Average Mean Uncorrected	Average Median Uncorrected	Obscuration %	Fraunhofer Run 1 Mean	Run 1 Median	Run 2 Mean
Spiggie2011_1	210.0000	169.1000	n/a	n/a	210.2000	165.8000	3.0000	248.625	183.677	248.777
Spiggie2011_1	n/a	n/a	228.3000	185.3000	221.8000	176.6500	5.0000	301.441	215.309	255.806
Spiggie2011_1	171.4000	144.2000	218.8000	191.6000	208.0000	159.9667	9.0000	238.07	200.701	223.467
Spiggie2011_1	213.0000	203.4000	210.6000	201.7000	211.8000	135.0333	8.0000	290.687	281.419	280.292
Spiggie2011_1	168.2000	81.6500	160.5000	70.4700	162.7000	79.6767	10.0000	149.174	87.4395	162.763
Spiggie2011_1	109.7000	43.8100	144.9000	43.3800	144.0333	44.9833	13.0000	170.112	46.8211	149.8
Spiggie2011_1	130.9000	83.0000	n/a	n/a	89.1333	54.4600	7.0000	147.286	97.513	156.69
Spiggie2011_1	157.9000	53.4800	n/a	n/a	81.3033	32.4767	13.0000	139.865	49.3586	166.904
Spiggie2011_2	80.2500	40.3700	86.7500	41.8500	83.5000	41.1100	14.0000	91.2606	47.4448	89.7523
Spiggie2011_2	116.0000	82.2400	123.1400	80.1700	119.5700	81.2050	17.0000	109.997	81.1199	110.302
Spiggie2011_2	138.7000	129.9000	134.5000	125.3000	137.0667	129.7667	14.0000	137.714	131.975	134.516
Spiggie2011_2	126.0000	116.0000	131.9000	121.2000	130.2333	119.4000	7.0000	129.367	120.073	126.506
Spiggie2011_2	48.5000	19.1000	n/a	n/a	41.5550	16.6750	6.0000	34.0406	14.1875	36.0855
Spiggie2011_2	30.8200	11.5100	25.5600	10.5700	31.4833	11.3567	5.0000	37.307	12.1283	33.1625
Spiggie2011_2	117.1000	103.7000	116.7000	105.6000	119.9667	109.1000	15.0000	134.79	124.498	126.703
Spiggie2011_2	21.8400	14.3100	21.1500	14.0900	21.6933	14.2167	14.0000	21.5342	14.1805	21.5973
Spiggie2011_2	n/a	n/a	n/a	n/a	29.6700	14.4100	14.0000	30.5837	14.6574	30.382
Spiggie2011_2	49.5000	27.9800	45.2600	26.7700	47.3800	27.3750	17.0000	53.5507	34.3596	48.4528
Spiggie2011_2	n/a	n/a	n/a	n/a	n/a	n/a	21.0000	58.2236	25.94	57.9608
Spiggie2011_2	n/a	n/a	90.2900	77.2900	95.9950	78.8550	15.0000	92.9682	76.8552	96.7607
Spiggie2011_2	n/a	n/a	n/a	n/a	n/a	n/a	21.0000	85.3955	65.9291	84.5995
Spiggie2011_2	54.7100	24.1000	42.0000	22.0700	46.5967	22.9067	8.0000	42.3792	22.3796	42.7552
Spiggie2011_2	72.8500	33.5700	68.1900	30.2100	68.7533	32.2533	17.0000	67.8604	34.2482	66.0106
Spiggie2011_3	14.3700	11.5500	n/a	n/a	14.6900	11.7450	1.0000	14.4625	11.6649	14.4553
Spiggie2011_3	n/a	n/a	n/a	n/a	n/a	n/a		17.4391	10.6382	17.1587
Spiggie2011_3	n/a	n/a	17.2900	12.1300	18.7050	12.4850	7.0000	22.1068	13.2475	18.5183
Spiggie2011_3	23.3800	16.6300	n/a	n/a	24.5850	17.2250	9.0000	27.617	18.6646	25.9265
Spiggie2011_3	17.3700	9.3200	16.8500	9.1580	17.3933	9.3363	8.0000	16.7363	8.92301	16.6564
Spiggie2011_3	89.0900	54.8000	98.2000	60.2300	93.6450	57.5150	6.0000	99.7612	60.144	94.1373
Spiggie2011_3	125.9000	99.6600	176.1000	119.7000	151.0000	109.6800	10.0000	167.675	116.034	162.309
Spiggie2011_3	146.9000	116.6000	152.1000	124.0000	149.5000	120.3000	3.0000	152.966	125.12	147.19
Spiggie2011_3	223.0000	194.0000	158.0000	136.0000	200.0000	186.3333	2.0000	218.822	210.146	210.859
Spiggie2011_3	114.5000	60.5900	130.3000	60.3700	122.4000	60.4800	12.0000	125.747	60.3226	135.918

Core	Run 2 Median	Run 3 Mean	Run 3 Median	Average Mean	Fraunhofer Mean	Average Median	Fraunhofer Median
Spiggie2011_1	184	249.401	179.668	248.93433	0.4112291	182.44833	2.413249
Spiggie2011_1	198.279	263.783	195.832	273.67667	24.373178	203.14	10.60945
Spiggie2011_1	181.524	220.482	181.115	227.33967	9.4118328	187.78	11.19178
Spiggie2011_1	248.6	264.783	230.689	278.58733	13.035863	253.56933	25.72749
Spiggie2011_1	77.7006	166.492	85.37	159.47633	9.1148184	83.503367	5.130768
Spiggie2011_1	45.3994	146.906	43.2311	155.606	12.645625	45.150533	1.807893
Spiggie2011_1	99.5896	156.865	99.442	153.61367	5.4806186	98.8482	1.15867
Spiggie2011_1	51.5053	156.917	50.8406	154.562	13.672469	50.568167	1.098975
Spiggie2011_2	44.9682	87.4372	42.3972	89.483367	1.9258351	44.936733	2.523947
Spiggie2011_2	80.1741	110.82	79.9167	110.373	0.4160685	80.403567	0.633572
Spiggie2011_2	129.145	134.35	128.132	135.52667	1.8961037	129.75067	1.991805
Spiggie2011_2	118.376	125.258	116.672	127.04367	2.1066049	118.37367	1.700501
Spiggie2011_2	14.3646	34.6067	14.2429	34.910933	1.0558515	14.265	0.090595
Spiggie2011_2	11.601	23.0653	10.2762	31.178267	7.3252571	11.335167	0.954237
Spiggie2011_2	114.435	123.409	109.356	128.30067	5.8562953	116.09633	7.706495
Spiggie2011_2	14.2163	21.6203	14.1931	21.583933	0.0445792	14.196633	0.01816
Spiggie2011_2	14.6225	30.0419	14.5532	30.335867	0.2738303	14.611033	0.053038
Spiggie2011_2	29.7978	45.3599	27.4537	49.121133	4.1360976	30.537033	3.511796
Spiggie2011_2	25.9668	54.5326	25.3905	56.905667	2.0593324	25.765767	0.325267
Spiggie2011_2	77.4613	90.003	74.4269	93.243967	3.3872796	76.2478	1.605801
Spiggie2011_2	65.2616	86.265	65.8323	85.42	0.8330203	65.674333	0.3607
Spiggie2011_2	22.2897	43.0901	22.1741	42.7415	0.355648	22.281133	0.103017
Spiggie2011_2	32.9842	64.7063	31.9628	66.192433	1.5848925	33.065067	1.144844
Spiggie2011_3	11.6656	14.3864	11.6088	14.434733	0.0420124	11.646433	0.032593
Spiggie2011_3	10.5439	16.9189	10.4568	17.172233	0.2603639	10.5463	0.090724
Spiggie2011_3	12.5282	17.6997	12.2577	19.4416	2.3441405	12.6778	0.511577
Spiggie2011_3	17.5006	24.3809	16.6568	25.9748	1.6185906	17.607333	1.008146
Spiggie2011_3	8.93153	16.4982	8.84896	16.6303	0.1211768	8.9011667	0.045413
Spiggie2011_3	58.423	92.8734	57.0016	95.590633	3.6666852	58.522867	1.573579
Spiggie2011_3	116.216	156.407	112.914	162.13033	5.6361243	115.05467	1.856104
Spiggie2011_3	118.307	147.292	119.026	149.14933	3.3057237	120.81767	3.743233
Spiggie2011_3	193.505	198.317	184.973	209.33267	10.337361	196.208	12.80233
Spiggie2011_3	63.7735	128.708	60.5267	130.12433	5.2313297	61.540933	1.936151

Core	Crucible #	Depth	Crucible Wt(g)	Crucible + Sample(g)	Wet Sample(g)	Crucible + Dry Sample(g)	Dry Sample(g)	%H2O	Dry Bulk Density	Run 1 Mean	Run 1 Median
Spiggie2011_3	116	43-44	18.6515	20.1411	1.4896	19.4502	0.7987	46.381579	0.7987	132.3000	62.9100
Spiggie2011_3	117	45-46	17.8229	19.2995	1.4766	18.5955	0.7726	47.677096	0.7726	96.6200	38.7900
Spiggie2011_3	118	46-47	21.276	22.6127	1.3367	22.1531	0.8771	34.383182	0.8771	231.6000	63.9600
Spiggie2011_3	119	56-57	22.4733	23.8696	1.3963	23.5197	1.0464	25.059085	1.0464	23.0200	16.9800
Spiggie2011_3	120	61-62	20.7304	23.3632	2.6328	22.0006	1.2702	51.754786	1.2702	103.6000	22.4900

Core	Run 2 Mean	Run 2 Median	Run 3 Mean	Run 3 Median	Average Mean Uncorrected	Average Median Uncorrected	Obscuration %	Fraunhofer Run 1 Mean	Run 1 Median	Run 2 Mean
Spiggie2011_3	n/a	n/a	120.8000	65.6500	126.5500	64.2800	9.0000	154.279	69.2972	150.859
Spiggie2011_3	94.4700	39.4800	93.4300	41.3700	94.8400	39.8800	10.0000	115.986	39.9558	119.471
Spiggie2011_3	574.6000	184.2000	112.0000	38.5100	306.0667	95.5567	16.0000	104.298	35.9816	90.8986
Spiggie2011_3	22.8100	16.7700	23.1500	16.9400	22.9933	16.8967	17.0000	22.8983	16.9126	22.9124
Spiggie2011_3	71.1000	19.0500	160.8000	25.9600	111.8333	22.5000	27.0000	116.054	20.6806	136.714

Core	Run 2 Median	Run 3 Mean	Run 3 Median	Average Mean	Fraunhofer Mean	Average Median	Fraunhofer Median
Spiggie2011_3	66.6419	146.572	63.0115	150.57	3.8616192	66.316867	3.15543
Spiggie2011_3	41.0268	101.366	39.4574	112.27433	9.6062536	40.146667	0.801921
Spiggie2011_3	6.3649	93.4226	36.9877	96.2064	7.1202624	26.444733	17.39692
Spiggie2011_3	16.8864	22.8362	16.8315	22.8823	0.0405415	16.876833	0.041388
Spiggie2011_3	23.4275	121.469	21.5102	124.74567	10.71267	21.872767	1.408885

BCID	Core #	Depth	Initial Sample Weight	Dilution Factor	Sample Volume	Abs @ 810.0	Abs @ 815.0
8519	Brow2011_1	1	0.0053	30	28	0.1017	0.1012
8520	Brow2011_1	7.5	0.0053	30	44	0.0791	0.0793
8522	Brow2011_1	15	0.0048	30	34	0.0639	0.0631
8523	Brow2011_1	18.5	0.0052	30	39	0.0694	0.0692
8524	Brow2011_1	22.5	0.0059	30	33	0.047	0.0474
8525	Brow2011_1	23.5	0.0046	30	40	0.0406	0.0304
8526	Brow2011_1	25	0.0069	30	39	0.0272	0.0273
8527	Brow2011_1	26	0.0045	30	35	0.0267	0.0267
8528	Brow2011_1	28	0.0068	30	43	0.0355	0.0354
8530	Brow2011_1	30	0.0053	30	29	0.0355	0.0347
8531	Brow2011_1	31	0.0047	30	30	0.0285	0.0287
8532	Brow2011_1	32.5	0.0057	30	28	0.0775	0.0775
8533	Brow2011_1	35	0.0054	30	31	0.0451	0.0461
8534	Brow2011_1	36	0.0052	30	27	0.1313	0.1326
8535	Brow2011_1	43.5	0.0059	30	28	0.0856	0.0867
8536	Brow2011_1	48.5	0.0053	30	11	0.1521	0.1531
8546	Brow2011_3	1	0.0058	30	31	0.0845	0.0859
8547	Brow2011_3	9.5	0.0042	30	29	0.123	0.124
8548	Brow2011_3	16	0.0065	30	30	0.0478	0.0478
8549	Brow2011_3	17	0.0068	30	33	0.0194	0.019
8550	Brow2011_3	19.5	0.0052	30	22	0.0625	0.0623
8551	Brow2011_3	20.5	0.0066	30	39	0.0617	0.0615
8552	Brow2011_3	21.5	0.0071	30	27	0.0867	0.0867
8554	Brow2011_3	29.5	0.0061	30	25	0.0795	0.0807
8555	Brow2011_3	35.5	0.0063	30	29	0.0477	0.0476
8556	Brow2011_3	36.5	0.0053	30	32.5	0.0849	0.0848
8557	Brow2011_3	39.5	0.0052	30	30	0.4581	0.4574
8558	Brow2011_3	43.5	0.0059	30	41	0.3617	0.3613
8559	Brow2011_3	44.5	0.0048	30	30	0.9965	0.9955
8560	Brow2011_3	57.5	0.0049	30	26	0.4838	0.4833
8561	Brow2011_3	67.5	0.0068	30	47	0.5265	0.5261
8729	Brow2011_3	3	0.0054	30	22	0.413	0.4134
8730	Brow2011_3	5	0.0068	30	25	0.3448	0.3449

BCID	Abs @ 820.0	Average Absorbance	Corrected to Cuvettes	Corrected to Proc	PPM Silica	Date Run	%Silica
8519	0.0995	0.1008	0.1008	0.087616667	0.28781504	1/19/2012	4.561597
8520	0.0784	0.078933333	0.073933333	0.06075	0.19131121	1/19/2012	4.764732
8522	0.0621	0.063033333	0.063033333	0.04985	0.15215891	1/19/2012	3.233377
8523	0.0697	0.069433333	0.064433333	0.05125	0.15718764	1/19/2012	3.536722
8524	0.0471	0.047166667	0.047166667	0.033983333	0.09516657	1/19/2012	1.596863
8525	0.03	0.033666667	0.028666667	0.015483333	0.02871542	1/19/2012	0.749098
8526	0.0272	0.027233333	0.027233333	0.01405	0.02356695	1/19/2012	0.399614
8527	0.0264	0.0266	0.0216	0.008416667	0.00333228	1/19/2012	0.077753
8528	0.0351	0.035333333	0.035333333	0.02215	0.05266178	1/19/2012	0.999025
8530	0.0348	0.035	0.03	0.016816667	0.03350469	1/19/2012	0.549983
8531	0.0283	0.0285	0.0285	0.015316667	0.02811676	1/19/2012	0.538406
8532	0.0767	0.077233333	0.072233333	0.05905	0.18520489	1/19/2012	2.729335
8533	0.0454	0.045533333	0.045533333	0.03235	0.08929971	1/19/2012	1.537939
8534	0.1313	0.131733333	0.126733333	0.11355	0.38096638	1/19/2012	5.934284
8535	0.0857	0.086	0.086	0.072816667	0.23465412	1/19/2012	3.340838
8536	0.1512	0.152133333	0.147133333	0.13395	0.45424224	1/19/2012	2.828301
8546	0.0847	0.085033333	0.085033333	0.07185	0.2311819	1/19/2012	3.706882
8547	0.123	0.123333333	0.118333333	0.10515	0.35079397	1/19/2012	7.266446
8548	0.0471	0.047566667	0.047566667	0.034383333	0.09660335	1/19/2012	1.337585
8549	0.0186	0.019	0.014	0.000816667	-0.02396657	1/19/2012	0
8550	0.0616	0.062133333	0.062133333	0.04895	0.14892615	1/19/2012	1.890217
8551	0.0599	0.061033333	0.056033333	0.04285	0.12701523	1/19/2012	2.251634
8552	0.0857	0.086366667	0.086366667	0.073183333	0.23597117	1/19/2012	2.692065
8554	0.0786	0.0796	0.0746	0.061416667	0.19370584	1/19/2012	2.381629
8555	0.0471	0.047466667	0.047466667	0.034283333	0.09624416	1/19/2012	1.329086
8556	0.0839	0.084533333	0.079533333	0.06635	0.21142615	1/19/2012	3.889443
8557	0.4527	0.456066667	0.456066667	0.442883333	1.56391657	1/19/2012	27.06779
8558	0.3575	0.360166667	0.355166667	0.341983333	1.20148841	1/19/2012	25.04798
8559	0.9857	0.992566667	0.992566667	0.979383333	3.4909999	1/19/2012	65.45625
8560	0.4786	0.4819	0.4769	0.463716667	1.63874895	1/19/2012	26.08621
8561	0.5213	0.524633333	0.524633333	0.51145	1.81020489	1/19/2012	37.53513
8729	0.4102	0.4122	0.4122	0.404333333	1.42544674	1/22/2012	0.712723
8730	0.3418	0.343833333	0.338833333	0.330966667	1.16191705	1/22/2012	0.51261

BCID	Core #	Depth	Initial Sample Weight	Dilution Factor	Sample Volume	Abs @ 810.0	Abs @ 815.0
8731	Brow2011_3	7	0.0056	30	24	0.1947	0.1993
8732	Brow2011_3	12	0.0049	30	23.5	0.1721	0.1719
8733	Brow2011_3	25	0.0064	30	24.5	0.057	0.0561
8734	Brow2011_3	27	0.0059	30	27	0.2553	0.2552
8735	Brow2011_3	32	0.0057	30	25	0.0673	0.067
8736	Brow2011_3	34	0.0065	30	34	0.0808	0.0811
8737	Brow2011_3	37.5	0.0066	30	25.5	0.0802	0.0804
8738	Brow2011_3	42	0.0048	30	25	0.3462	0.3466
8739	Brow2011_3	47	0.0062	30	26	0.3595	0.36
8740	Brow2011_3	49	0.0063	30	28	0.8507	0.8511
8741	Brow2011_3	51	0.0061	30	31	0.7314	0.7322
8742	Brow2011_3	53	0.006	30	32	0.398	0.3979
8743	Brow2011_3	55	0.0063	30	39	0.5489	0.5489
8744	Brow2011_3	61	0.0052	30	31.5	0.3418	0.3416
8745	Brow2011_3	63	0.005	30	34	0.3173	0.3157
8746	Brow2011_3	65	0.005	30	24	0.5345	0.5324

BCID	Abs @ 820.0	Average Absorbance	Corrected to Cuvettes	Corrected to Proc	PPM Silica	Date Run	%Silica
8731	0.1929	0.195633333	0.195633333	0.187766667	0.64754923	1/22/2012	0.335338
8732	0.17	0.171333333	0.166333333	0.158466667	0.54230498	1/22/2012	0.315422
8733	0.0548	0.055966667	0.055966667	0.0481	0.14587299	1/22/2012	0.067238
8734	0.2528	0.254433333	0.249433333	0.241566667	0.84079636	1/22/2012	0.456025
8735	0.0661	0.0668	0.0668	0.058933333	0.18478582	1/22/2012	0.097256
8736	0.0802	0.0807	0.0757	0.067833333	0.21675421	1/22/2012	0.130053
8737	0.0798	0.080133333	0.080133333	0.072266667	0.23267854	1/22/2012	0.107526
8738	0.344	0.3456	0.3406	0.332733333	1.16826284	1/22/2012	0.730164
8739	0.3575	0.359	0.359	0.351133333	1.23435479	1/22/2012	0.617177
8740	0.8461	0.8493	0.8443	0.836433333	2.97753008	1/22/2012	1.559659
8741	0.7259	0.729833333	0.729833333	0.721966667	2.56637107	1/22/2012	1.51458
8742	0.394	0.396633333	0.391633333	0.383766667	1.35157222	1/22/2012	0.83347
8743	0.5441	0.5473	0.5473	0.539433333	1.91071973	1/22/2012	1.334471
8744	0.3388	0.340733333	0.335733333	0.327866667	1.15078199	1/22/2012	0.80776
8745	0.313	0.315333333	0.315333333	0.307466667	1.07750613	1/22/2012	0.840455
8746	0.5275	0.531466667	0.526466667	0.5186	1.83588736	1/22/2012	1.064815

Appendix C:

Geochronology

Depth(cm)	Core	Mass(g)	Date Collected	Geologist	Type of Sed	Tare	Gross	Net	Bq/kg	Bq/kg sd
0-.5	Brow2011_2	0.304	5/30/2011	Lindelof	lake	15.274	15.578	0.304	0.50	0.12
.5-1.0	Brow2011_2	0.415	5/30/2011	Lindelof	lake	15.243	15.658	0.415	0.78	0.45
1.0-1.5	Brow2011_2	0.206	5/30/2011	Lindelof	lake	15.259	15.465	0.206	1.37	0.09
1.5-2.0	Brow2011_2	0.233	5/30/2011	Lindelof	lake	15.152	15.385	0.233	1.11	0.11
2.0-2.5	Brow2011_2	0.267	5/30/2011	Lindelof	lake	15.331	15.598	0.267	0.81	0.31
2.5-3.0	Brow2011_2	0.284	5/30/2011	Lindelof	lake	15.282	15.566	0.284	0.84	0.04
3.0-3.5	Brow2011_2	0.216	5/30/2011	Lindelof	lake	15.257	15.473	0.216	0.87	0.12
3.5-4.0	Brow2011_2	0.139	5/30/2011	Lindelof	lake	15.224	15.363	0.139	0.82	0.21
4.0-4.5	Brow2011_2	0.241	5/30/2011	Lindelof	lake	15.364	15.605	0.241	0.40	0.23
4.5-5.0	Brow2011_2	0.223	5/30/2011	Lindelof	lake	15.371	15.594	0.223	0.72	0.05
5.0-5.5	Brow2011_2	0.283	5/30/2011	Lindelof	lake	15.335	15.618	0.283	0.97	0.08
5.5-6.0	Brow2011_2	0.18	5/30/2011	Lindelof	lake	15.249	15.429	0.18	1.02	0.11
6.0-6.5	Brow2011_2	0.142	5/30/2011	Lindelof	lake	15.308	15.45	0.142	1.17	0.15
6.5-7.0	Brow2011_2	0.22	5/30/2011	Lindelof	lake	15.259	15.479	0.22	1.33	0.32
7.0-7.5	Brow2011_2	0.253	5/30/2011	Lindelof	lake	15.317	15.57	0.253	1.36	0.21
7.5-8.0	Brow2011_2	0.162	5/30/2011	Lindelof	lake	15.245	15.407	0.162	1.40	0.36
8.0-8.5	Brow2011_2	0.233	5/30/2011	Lindelof	lake	15.325	15.558	0.233	1.16	0.05
8.5-9.0	Brow2011_2	0.178	5/30/2011	Lindelof	lake	15.21	15.388	0.178	0.79	0.54
9.0-9.5	Brow2011_2	0.203	5/30/2011	Lindelof	lake	15.336	15.539	0.203	0.53	0.27
9.5-10.0	Brow2011_2	0.23	5/30/2011	Lindelof	lake	15.341	15.571	0.23	0.00	
0-.5	Spiggie2011_3	0.103	5/31/2011	Lindelof	lake	15.383	15.486	0.103	2.51	0.27
.5-1.0	Spiggie2011_3	0.082	5/31/2011	Lindelof	lake	15.324	15.406	0.082	2.76	0.50
1.0-1.5	Spiggie2011_3	0.062	5/31/2011	Lindelof	lake	15.371	15.433	0.062	3.17	0.33
1.5-2.0	Spiggie2011_3	0.05	5/31/2011	Lindelof	lake	15.342	15.392	0.05	3.11	0.95
2.0-2.5	Spiggie2011_3	0.074	5/31/2011	Lindelof	lake	15.447	15.521	0.074	2.85	0.99
2.5-3.0	Spiggie2011_3	0.114	5/31/2011	Lindelof	lake	15.29	15.404	0.114	0.91	0.11
3.0-3.5	Spiggie2011_3	0.113	5/31/2011	Lindelof	lake	15.335	15.448	0.113	2.78	0.16
3.5-4.0	Spiggie2011_3	0.074	5/31/2011	Lindelof	lake	15.262	15.336	0.074	1.25	0.02
4.0-4.5	Spiggie2011_3	0.115	5/31/2011	Lindelof	lake	15.338	15.453	0.115	0.85	0.33
4.5-5.0	Spiggie2011_3	0.13	5/31/2011	Lindelof	lake	15.229	15.359	0.13	0.79	0.07
5.0-5.5	Spiggie2011_3	0.204	5/31/2011	Lindelof	lake	15.382	15.586	0.204	1.26	0.06
5.5-6.0	Spiggie2011_3	0.136	5/31/2011	Lindelof	lake	15.302	15.438	0.136	0.68	0.36
6.0-6.5	Spiggie2011_3	0.171	5/31/2011	Lindelof	lake	15.237	15.408	0.171	0.54	0.21
6.5-7.0	Spiggie2011_3	0.239	5/31/2011	Lindelof	lake	15.377	15.616	0.239	0.00	
7.0-7.5	Spiggie2011_3	0.176	5/31/2011	Lindelof	lake	15.288	15.464	0.176	0.00	
7.5-8.0	Spiggie2011_3	0.265	5/31/2011	Lindelof	lake	15.295	15.56	0.265	0.00	

Depth(cm)	Core	Mass(g)	Date Collected	Geologist	Type of Sed	Tare	Gross	Net	Bq/kg	Bq/kg sd
8.0-8.5	Spiggie2011_3	0.213	5/31/2011	Lindelof	lake	15.274	15.487	0.213	0.00	
8.5-9.0	Spiggie2011_3	0.14	5/31/2011	Lindelof	lake	15.315	15.455	0.14	0.00	
9.0-9.5	Spiggie2011_3	0.146	5/31/2011	Lindelof	lake	15.413	15.559	0.146	0.00	
9.5-10.0	Spiggie2011_3	0.136	5/31/2011	Lindelof	lake	15.226	15.362	0.136	0.00	
0-.5	Brow2011_3	0.116	5/31/2011	Lindelof	lake	15.273	15.389	0.116	1.62	0.77
.5-1.0	Brow2011_3	0.122	5/31/2011	Lindelof	lake	15.348	15.47	0.122	1.70	0.33
1.0-1.5	Brow2011_3	0.165	5/31/2011	Lindelof	lake	15.34	15.505	0.165	1.82	0.31
1.5-2.0	Brow2011_3	0.144	5/31/2011	Lindelof	lake	15.282	15.426	0.144	2.43	0.11
2.0-2.5	Brow2011_3	0.145	5/31/2011	Lindelof	lake	15.323	15.468	0.145	1.85	0.25
2.5-3.0	Brow2011_3	0.152	5/31/2011	Lindelof	lake	15.256	15.408	0.152	1.29	0.20
3.0-3.5	Brow2011_3	0.16	5/31/2011	Lindelof	lake	15.212	15.372	0.16	2.18	0.24
3.5-4.0	Brow2011_3	0.097	5/31/2011	Lindelof	lake	15.295	15.392	0.097	1.78	0.55
4.0-4.5	Brow2011_3	0.091	5/31/2011	Lindelof	lake	15.356	15.447	0.091	0.79	0.42
4.5-5.0	Brow2011_3	0.131	5/31/2011	Lindelof	lake	15.323	15.454	0.131	1.41	0.16
5.0-5.5	Brow2011_3	0.092	5/31/2011	Lindelof	lake	15.29	15.382	0.092	0.92	0.92
5.5-6.0	Brow2011_3	0.135	5/31/2011	Lindelof	lake	15.263	15.398	0.135	0.98	0.03
6.0-6.5	Brow2011_3	0.127	5/31/2011	Lindelof	lake	15.223	15.35	0.127	0.37	0.07
6.5-7.0	Brow2011_3	0.134	5/31/2011	Lindelof	lake	15.211	15.345	0.134	0.63	0.31
7.0-7.5	Brow2011_3	0.147	5/31/2011	Lindelof	lake	15.246	15.393	0.147	0	
7.5-8.0	Brow2011_3	0.169	5/31/2011	Lindelof	lake	15.343	15.512	0.169	0	
8.0-8.5	Brow2011_3	0.183	5/31/2011	Lindelof	lake	15.384	15.567	0.183	0	
8.5-9.0	Brow2011_3	0.188	5/31/2011	Lindelof	lake	15.209	15.397	0.188	0	
9.0-9.5	Brow2011_3	0.238	5/31/2011	Lindelof	lake	15.264	15.502	0.238	0	
9.5-10.0	Brow2011_3	0.155	5/31/2011	Lindelof	lake	15.197	15.352	0.155	0	
0-.5	Brow2011_5	0.202	5/31/2011	Lindelof	lake	15.197	15.399	0.202	1.04	0.13
.5-1.0	Brow2011_5	0.186	5/31/2011	Lindelof	lake	15.227	15.413	0.186	0.87	0.01
1.0-1.5	Brow2011_5	0.253	5/31/2011	Lindelof	lake	15.277	15.53	0.253	1.04	0.09
1.5-2.0	Brow2011_5	0.26	5/31/2011	Lindelof	lake	15.347	15.607	0.26	0.95	0.16
2.0-2.5	Brow2011_5	0.316	5/31/2011	Lindelof	lake	15.223	15.539	0.316	0.78	0.04
2.5-3.0	Brow2011_5	0.296	5/31/2011	Lindelof	lake	15.258	15.554	0.296	1.16	0.12
3.0-3.5	Brow2011_5	0.215	5/31/2011	Lindelof	lake	15.356	15.571	0.215	0.84	0.00
3.5-4.0	Brow2011_5	0.325	5/31/2011	Lindelof	lake	15.214	15.539	0.325	0.75	0.20
4.0-4.5	Brow2011_5	0.223	5/31/2011	Lindelof	lake	15.209	15.432	0.223	1.04	0.29
4.5-5.0	Brow2011_5	0.188	5/31/2011	Lindelof	lake	15.372	15.56	0.188	0.81	0.01
5.0-5.5	Brow2011_5	0.299	5/31/2011	Lindelof	lake	15.329	15.628	0.299	0.36	0.12
5.5-6.0	Brow2011_5	0.179	5/31/2011	Lindelof	lake	15.295	15.474	0.179	0.00	

Depth(cm)	Core	Mass(g)	Date Collected	Geologist	Type of Sed	Tare	Gross	Net	Bq/kg	Bq/kg sd
6.0-6.5	Brow2011_5	0.219	5/31/2011	Lindelof	lake	15.402	15.621	0.219	0.00	
6.5-7.0	Brow2011_5	0.181	5/31/2011	Lindelof	lake	15.348	15.529	0.181	0.00	
7.0-7.5	Brow2011_5	0.173	5/31/2011	Lindelof	lake	15.322	15.495	0.173	0.00	
7.5-8.0	Brow2011_5	0.138	5/31/2011	Lindelof	lake	15.32	15.458	0.138	0.00	
8.0-8.5	Brow2011_5	0.149	5/31/2011	Lindelof	lake	15.379	15.528	0.149	0.00	
8.5-9.0	Brow2011_5	0.151	5/31/2011	Lindelof	lake	15.294	15.445	0.151	0.00	
9.0-9.5	Brow2011_5	0.198	5/31/2011	Lindelof	lake	15.209	15.407	0.198	0.00	
9.5-10.0	Brow2011_5	0.109	5/31/2011	Lindelof	lake	15.262	15.371	0.109	0.00	

Appendix D:

Geochemical Data

		Sample	Mass		umoles			umoles		C/N	
Analysis	Sample ID	Type	(mg)	% N	N	d15N (3pts	%C	C	d13C	(Molar)	Date Run
216	2991.1	Acetanilide	0.448	10.36	3.550607	-0.239045	71.09	26.36792	-30.31311	7.426313	10/18/2011
418	2991.1	Acetanilide	0.498	10.36	4.324062	-0.613132	71.09	30.15268	-30.4599	6.97323	10/26/2011
526	2991.1	Acetanilide	0.591	10.36	4.358653	-0.303502	71.09	34.36939	-30.28857	7.885324	11/2/2011
628	2991.1	Acetanilide	0.45	10.36	3.39	-0.05	71.09	26.81	-30.20	7.92	11/8/2011
677	2991.1	Acetanilide	0.449	10.34057	3.314889	-0.061425	71.09	26.55638	-30.40882	8.011241	11/9/2011
236	2991.2	Acetanilide	0.454	9.678305	3.36139	-0.071045	71.92828	27.03602	-30.44277	8.043106	10/18/2011
426	2991.2	Acetanilide	0.567	8.925527	4.255765	-0.149712	68.85007	33.1007	-30.60033	7.777851	10/26/2011
648	2991.2	Acetanilide	0.51	10.16	3.74	-0.08	71.11	30.21	-30.46	8.08	11/8/2011
697	2991.2	Acetanilide	0.426	10.59707	3.223101	-0.082298	71.73948	25.4261	-30.5247	7.888708	11/9/2011
260	2991.3	Acetanilide	0.437	9.66306	3.230409	-0.17731	71.43939	25.84703	-30.13888	8.001164	10/18/2011
462	2991.3	Acetanilide	0.416	7.921677	3.032817	-0.032573	68.01972	24.38924	-30.31842	8.041778	10/26/2011
570	2991.3	Acetanilide	0.572	10.26701	4.180656	-0.250918	72.64927	33.99384	-30.23336	8.131221	11/2/2011
672	2991.3	Acetanilide	0.52	9.90	3.70	-0.33	68.95	29.69	-30.36	8.03	11/8/2011
722	2991.3	Acetanilide	0.433	10.29398	3.182362	-0.230395	70.62894	25.44364	-31.87254	7.995206	11/9/2011
217	2992.1	Caffeine	0.294	26.66885	5.99811	-11.88159	48.07622	11.70228	-30.79123	1.950995	10/18/2011
419	2992.1	Caffeine	0.287	25.49933	5.819727	-11.60265	42.07562	11.23454	-30.82919	1.930424	10/26/2011
527	2992.1	Caffeine	0.216	29.276	4.501561	-12.35132	51.3524	9.074021	-31.0534	2.01575	11/2/2011
629	2992.1	Caffeine	0.28	28.38	5.84	-12.24	48.83	11.60	-30.93	1.99	11/8/2011
678	2992.1	Caffeine	0.251	27.94116	5.007217	-12.30673	47.81459	9.984878	-30.9262	1.994097	11/9/2011
237	2992.2	Caffeine	0.206	26.91742	4.241887	-12.47262	49.98357	8.52476	-30.9533	2.009662	10/18/2011
427	2992.2	Caffeine	0.232	23.90917	4.592546	-12.54593	41.6391	9.275434	-31.23177	2.019672	10/26/2011
649	2992.2	Caffeine	0.29	28.05	5.98	-12.23	48.99	12.05	-31.26	2.01	11/8/2011
698	2992.2	Caffeine	0.275	27.52405	5.404099	-12.30673	46.85313	10.7198	-30.64159	1.983641	11/9/2011
261	2992.3	Caffeine	0.286	26.02734	5.694507	-12.56472	48.04042	11.37537	-30.47518	1.997604	10/18/2011
463	2992.3	Caffeine	0.2	22.60705	3.882107	-12.6045	39.70281	7.880791	-30.82919	2.030029	10/26/2011
571	2992.3	Caffeine	0.293	28.28492	5.899621	-12.28088	49.97408	11.97798	-31.3786	2.030296	11/2/2011
673	2992.3	Caffeine	0.22	27.28	4.31	-12.47	46.80	8.53	-31.03	1.98	11/8/2011
723	2992.3	Caffeine	0.257	29.02739	5.326224	-12.40215	49.75281	10.63796	-42.87477	1.99728	11/9/2011
218	5676.1	Cod Standard	0.657	13.92301	6.997761	13.11082	46.79796	25.45563	-18.9841	3.637681	10/18/2011

		Sample	Mass		umoles			umoles		C/N	
Analysis	Sample ID	Type	(mg)	% N	N	d15N (3pts	%C	C	d13C	(Molar)	Date Run
420	5676.1	Cod Standard	0.673	14.20128	7.370989	13.15074	45.50989	26.28031	-18.83293	3.565371	10/26/2011
528	5676.1	Cod Standard	0.673	14.3874	6.892885	13.50045	46.89959	25.82031	-18.63645	3.745937	11/2/2011
630	5676.1	Cod Standard	0.75	14.26	7.72	13.55	45.91	28.68	-18.78	3.72	11/8/2011
679	5676.1	Cod Standard	0.693	14.45853	7.153782	13.43127	46.02584	26.53671	-18.88311	3.709466	11/9/2011
238	5676.2	Cod Standard	0.765	13.51345	7.90837	13.51968	46.61252	29.5223	-18.9294	3.733045	10/18/2011
428	5676.2	Cod Standard	0.726	13.40851	7.493754	13.74979	44.63965	27.72376	-18.80277	3.699582	10/26/2011
548	5676.2	Cod Standard	0.645	14.20443	6.522043	13.34468	47.09391	24.84821	-18.86731	3.809881	11/2/2011
650	5676.2	Cod Standard	0.80	14.06	8.16	13.35	45.62	30.56	-18.85	3.74	11/8/2011
699	5676.2	Cod Standard	0.779	14.69858	8.175065	13.2126	117.596	76.21507	-28.60358	9.32287	11/9/2011
262	5676.3	Cod Standard	0.619	13.29228	6.294358	13.57838	45.30916	23.21994	-18.58499	3.689008	10/18/2011
464	5676.3	Cod Standard	0.786	11.3676	6.939759	10.90043	48.49546	32.35384	-22.95028	4.662098	10/26/2011
572	5676.3	Cod Standard	0.6	13.83137	5.90766	13.33277	45.39637	22.28168	-19.01184	3.771659	11/2/2011
674	5676.3	Cod Standard	0.65	14.02	6.63	13.28	45.41	24.80	-18.85	3.74	11/8/2011
724	5676.3	Cod Standard	0.794	14.42373	8.176666	13.31299	45.44815	30.02265	-23.74182	3.671747	11/9/2011
430	8519	Brow2011_1 0.5-1.5	23.884	0.136426	3.007135	5.074291	2.20058	44.06558	-27.65328	14.65368	10/26/2011
431	8520	Brow2011_1:7-8	13.723	0.948146	13.52401	5.006659	1.107537	13.76698	-25.86196	1.017966	10/26/2011
221	8521	Brow2011_1:13.5-14.5	0	0	0.141118	-2.735755				0	10/18/2011
432	8522	Brow2011_1:14.5-15.5	11.347	0.076429	1.350605	3.248356	2.267015	22.30294	-27.96536	16.5133	10/26/2011
433	8523	Brow2011_1:18-19	12.72	0.17045	2.251823	2.94626	3.323289	35.72336	-27.92791	15.86419	10/26/2011
681	8524	Brow2011_1: 22-23	19.749	0.288857	4.072918	2.486035	3.850501	63.26608	-28.33828	15.53335	11/9/2011
682	8525	Brow2011_1: 23-24	19.658	0.241918	3.395367	2.642083	3.312219	54.17129	-27.86664	15.95447	11/9/2011
436	8526	Brow2011_1:24.5-25.5	10.379	0.068139	1.239693	2.525997	2.174617	19.74536	-27.8759	15.92762	10/26/2011
437	8527	Brow2011_1:25.5-26.5	14.452	0.014714	0.897079	2.396527	1.233362	15.89666	-28.37418	17.72046	10/26/2011
438	8528	Brow2011_1:27.5-28.5	16.807	0.072196	1.590397	2.371866	1.962485	28.19061	-28.29408	17.72552	10/26/2011
439	8530	Brow2011_1:29.5-30.5	11.159	0.004196	0.782216	2.177661	1.370849	13.84734	-28.31905	17.7027	10/26/2011
440	8531	Brow2011_1:30.5-31.5	14.677	0.053468	1.293409	3.069564	1.792145	22.77276	-27.77499	17.60678	10/26/2011
441	8532	Brow2011_1:32-33	12.391	0.031432	1.019562	3.195952	1.685014	18.37389	-27.54718	18.02135	10/26/2011
442	8533	Brow2011_1:34.5-35.5	11.122	0.018747	0.894257	2.788019	1.587866	15.76355	-27.65016	17.62754	10/26/2011

		Sample	Mass		umoles			umoles		C/N	
Analysis	Sample ID	Type	(mg)	% N	N	d15N (3pts	%C	C	d13C	(Molar)	Date Run
443	8534	Brow2011_1:35.5-36.5	13.816	0.040379	1.136307	2.74178	1.683417	20.30341	-27.55654	17.8679	10/26/2011
444	8535	Brow2011_1:43-44	9.635	0.787904	6.009002	1.977291	12.11775	22.83503	-27.66843	3.800137	10/26/2011
684	8536	Brow2011_1: 48-49	4.431	1.718248	5.43583	1.537819	25.23843	93.0411	-27.78634	17.11627	11/9/2011
631	8537	Brow2011_2:0-1	9.87	0.67	4.81	4.90	7.85	64.81	-28.08	13.46868	11/8/2011
447	8538	Brow2011_2:1-2	14.764	0.437468	5.224339	4.956124	5.791745	70.7881	-28.21814	13.54967	10/26/2011
639	8539	Brow2011_2:2.5-3-5	11.88	0.60	5.19	4.98	7.79	77.44	-27.44	14.92884	11/8/2011
449	8540	Brow2011_2:15-16	10.936	0.180502	2.117299	2.766441	4.029056	37.1747	-27.75107	17.5576	10/26/2011
450	8541	Brow2011_2:30-31	12.377	0.124571	1.817959	2.852754	3.157652	33.1362	-27.67721	18.22714	10/26/2011
640	8542	Brow2011_2:40-41	2.82	1.00	2.05	1.77	16.45	38.78	-28.40	18.88932	11/8/2011
452	8543	Brow2011_2:41-42	11.779	1.324712	11.55977	1.79439	19.88	29.32	-28.22	2.536707	10/26/2011
643	8544	Brow2011_2:50-51	2.71	1.71	3.36	1.36	25.37	57.59	-28.26	17.12978	11/8/2011
685	8545	Brow2011_2: 66-67	1.688	1.931783	2.32814	2.19183	28.67033	40.26366	-28.52938	17.29435	11/9/2011
686	8546	Brow2011_3: 0.5-1.5	3.414	1.014932	2.47388	4.6558	12.09237	34.3466	-27.45904	13.8837	11/9/2011
687	8547	Brow2011_3: 9-10	3.53	0.843885	2.126846	4.659775	11.87715	34.88171	-31.32669	16.40067	11/9/2011
457	8548	Brow2011_3: 15.75-16.7	16.466	0.19866	3.015978	3.169236	3.616167	49.73042	-27.60439	16.48899	10/26/2011
458	8549	Brow2011_3:16.75-17.75	15.662	0.119617	2.047685	3.004829	2.661414	35.24566	-27.47332	17.21244	10/26/2011
688	8550	Brow2011_3: 19-20	17.076	0.060673	0.739712	2.235563	0.882797	12.54194	-27.81378	16.95518	11/9/2011
689	8551	Brow2011_3: 20-21	9.421	0.61841	4.159602	1.651128	11.31286	88.67039	-28.59341	21.31704	11/9/2011
461	8552	Brow2011_3: 21-22	14.596	0.0683	1.440444	3.055179	2.20069	27.49107	-27.81556	19.08513	10/26/2011
257	8554	Brow2011_3: 29-30	0.44				1.996741	0.727177	-27.07567		10/18/2011
258	8555	Brow2011_3: 35-36	0.78				1.624471	1.049163	-27.73004		10/18/2011
259	8556	Brow2011_3: 36-37	0.554				7.20404	3.304052	-28.46951		10/18/2011
429	8557	Brow2011_3: 39-40	8.693	0.127215	1.515891	2.189992	4.090763	30.28085	-28.61448	19.97561	10/26/2011
690	8558	Brow2011_3: 43-44	2.001	1.895081	2.707405	0.441507	30.74713	51.18698	-27.42956	18.90629	11/9/2011
691	8559	Brow2011_3: 44-45	2.385	1.747734	2.976063	0.451446	27.6683	54.90089	-27.32181	18.44749	11/9/2011

		Sample	Mass		umoles			umoles		C/N	
Analysis	Sample ID	Type	(mg)	% N	N	d15N (3pts	%C	C	d13C	(Molar)	Date Run
692	8560	Brow2011_3: 57-58	2.671	1.539704	2.936225	0.404731	22.46533	49.9228	-27.79447	17.00238	11/9/2011
693	8561	Brow2011_3: 67-68	3.427	1.6973	4.152895	0.667131	26.18056	74.64533	-27.98252	17.97429	11/9/2011
1065	8732	Brow2011_3: 12	5.7	0.844167	3.560737	3.76191	11.88915	58.60481	-27.77781	16.45862	1/27/2012
1066	8733	Brow2011_3: 25	8.041	0.174533	1.038541	2.417186	2.765834	19.23298	-28.27681	18.51923	1/27/2012
1067	8734	Brow2011_3: 27	10.516	0.379988	2.957099	2.482513	6.067487	55.17824	-28.29388	18.65958	1/27/2012
1062	8729	Brow2011_3: 3	3.492	1.036862	2.679336	4.743819	13.07943	39.49754	-26.92641	14.74154	1/27/2012
1068	8735	Brow2011_3: 32	3.275	0.106199	0.257342	-0.42603	1.446393	4.096726	-27.69548	15.91937	1/27/2012
1069	8736	Brow2011_3: 34	2.54	0.231596	0.435249	1.935779	3.901269	8.569663	-28.43544	19.68909	1/27/2012
1070	8737	Brow2011_3: 37.5	2.57	0.915051	1.740305	1.791055	15.0963	33.55119	-28.45251	19.27891	1/27/2012
1071	8738	Brow2011_3: 42	2.132	1.071361	1.69029	0.826231	17.16046	31.6387	-27.86114	18.71791	1/27/2012
1072	8739	Brow2011_3: 47	2.931	1.809665	3.925204	0.446332	27.628	70.02795	-27.43343	17.84059	1/27/2012
1073	8740	Brow2011_3: 49	3.015	1.909991	4.261463	0.559899	26.74385	69.72938	-27.14227	16.36278	1/27/2012
1063	8730	Brow2011_3: 5	3.71	0.961314	2.639359	4.959899	12.53989	40.2324	-27.34408	15.24325	1/27/2012
1074	8741	Brow2011_3: 51	3.074	1.680509	3.822925	0.439296	26.5804	70.65928	-27.0991	18.48304	1/27/2012
1075	8742	Brow2011_3: 53	2.76	1.859827	3.798696	0.713668	24.06491	57.43828	-27.24869	15.12052	1/27/2012
1076	8743	Brow2011_3: 55	3.461	1.685677	4.317361	0.524724	22.9029	68.54898	-27.1744	15.87752	1/27/2012
1077	8744	Brow2011_3: 61	3.177	1.70434	4.007062	0.154874	25.10424	68.97141	-27.29789	17.21246	1/27/2012
1078	8745	Brow2011_3: 63	2.027	1.842148	2.76327	0.197085	20.29103	35.56812	-26.72359	12.87175	1/27/2012
1082	8746	Brow2011_3: 65	2.335	1.936096	3.345449	0.653367	21.76201	43.94367	-26.826	13.13536	1/27/2012
1064	8731	Brow2011_3: 7	2.85	0.847355	1.787204	4.482513	10.8427	26.723	-27.60512	14.9524	1/27/2012
694	8562	Brow2011_4: 0-1	3.385	1.483441	3.585149	4.888381	17.59756	49.55879	-28.11974	13.82336	11/9/2011
534	8563	Brow2011_4:6-7	7.477	0.822059	4.375488	4.919238	14.80927	90.58051	-27.74114	20.70181	11/2/2011
535	8564	Brow2011_4:11.5-12.5	12	0.634349	5.418878	2.421966	8.461434	83.06124	-27.40992	15.32812	11/2/2011
695	8565	Brow2011_4: 12.5-13.5	1.842	0.898648	1.181837	2.294205	11.07772	16.97642	-27.09412	14.36443	11/9/2011
696	8566	Brow2011_4: 18-19	1.707	0.952471	1.160817	2.038764	13.18835	18.73002	-27.09412	16.1352	11/9/2011
700	8567	Brow2011_4: 25-26	2.861	1.506839	3.077961	-0.095219	18.1621	43.23096	-27.87477	14.04532	11/9/2011
701	8568	Brow2011_4: 26-27	2.237	1.289978	2.060282	1.997018	19.68277	36.63212	-28.3149	17.78015	11/9/2011
702	8569	Brow2011_4: 36-37	2.55	0.781641	1.423069	0.176126	14.12189	29.95995	-18.69099	21.05305	11/9/2011

		Sample	Mass		umoles			umoles		C/N	
Analysis	Sample ID	Type	(mg)	% N	N	d15N (3pts	%C	C	d13C	(Molar)	Date Run
703	8570	Brow2011_4: 41-42	1.025	1.516456	1.109768	-0.4262	34.11522	29.09271	-28.33523	26.21514	11/9/2011
704	8571	Brow2011_4: 42-43	2.701	1.385052	2.67097	-0.051486	33.15602	74.50717	-28.03232	27.89518	11/9/2011
706	8572	Brow2011_4: 50-51	2.63	1.609657	3.022508	0.590597	20.79859	45.50904	-31.34296	15.05672	11/9/2011
544	8573	Brow2011_4:66-67	6.445	1.613411	7.40238	0.383074	18.8821	14.78283	-36.88168		11/2/2011
708	8574	Brow2011_4: 67-68	2.208	1.697861	2.676575	1.05079	20.17534	37.06202	-24.83554	13.84681	11/9/2011
709	8575	Brow2011_4: 72-73	2.704	1.526823	2.947636	0.757579	17.49352	39.35445	-30.28278	13.35119	11/9/2011
713	8576	Brow2011_4: 79-80	2.357	1.617712	2.722319	0.776464	19.21246	37.67472	-29.91889	13.8392	11/9/2011
551	8577	Brow2011_5: 0-1	16.152	0.721515	8.296053	4.24556	9.283124	122.658	-28.66356	14.7851	11/2/2011
552	8578	Brow2011_5: 8-9	11.974	0.560652	4.77896	4.651354	8.318511	81.48176	-27.63374	17.0501	11/2/2011
553	8579	Brow2011_5: 15-16	14.484	0.661203	6.817506	2.375335	10.66887	126.4099	-27.8114	18.54195	11/2/2011
554	8580	Brow2011_5: 16-17	17.839	0.06885	0.874379	2.10249	0.938959	13.70222	-27.88267	15.6708	11/2/2011
555	8581	Brow2011_5: 17-18	14.844	0.381539	4.031695	2.261236	5.985214	72.6782	-27.70501	18.02671	11/2/2011
556	8582	Brow2011_5: 18-19	14.258	0.055107	0.559338	1.494295	0.813108	9.483573	-28.1346	16.95501	11/2/2011
557	8583	Brow2011_5: 19-20	12.269				0.412497	4.139823	-28.18077		11/2/2011
558	8584	Brow2011_5: 20-21	14.577				0.551215	6.572921	-27.75218		11/2/2011
559	8585	Brow2011_5: 21-22	21.566	0.047247	0.725323	0.573569	0.643989	11.36133	-28.28214	15.66382	11/2/2011
560	8586	Brow2011_5: 22-23	16.25	0.50602	5.853561	1.009128	6.224273	82.7403	-27.69196	14.13504	11/2/2011
561	8587	Brow2011_5: 23-24	8.301	1.03912	6.140418	0.73033	12.15094	82.51157	-27.46612	13.43745	11/2/2011
710	8588	Brow2011_5: 27-28	2.899	1.719654	3.559324	0.642282	19.96385	48.1506	-31.51982	13.52802	11/9/2011
711	8589	Brow2011_5: 33-34	2.244	1.760463	2.820514	0.80827	21.16417	39.51227	-31.29518	14.00889	11/9/2011
712	8590	Brow2011_5: 43-44	2.614	2.042193	3.811367	0.636318	22.04004	47.9322	-28.11059	12.57612	11/9/2011

		Sample	Mass		umoles			umoles		C/N	
Analysis	Sample ID	Type	(mg)	% N	N	d15N (3pts	%C	C	d13C	(Molar)	Date Run
566	8592	Spiggie2011_1: 0-1	19.012	0.158326	2.142772	6.785495	1.661251	25.8368	-28.52906	12.05765	11/2/2011
567	8593	Spiggie2011_1: 1-2	22.663				0.116203	2.154397	-27.01546		11/2/2011
568	8594	Spiggie2011_1: 3-4	21.483				0.061804	1.085956	-25.04717		11/2/2011
569	8595	Spiggie2011_1: 5-6	16.868				0.063995	0.882984	-25.0271		11/2/2011
565	8596	Spiggie2011_1: 6-7	18.605				0.214411	3.263021	-24.78922		11/2/2011
632	8597	Spiggie2011_1: 8-9	16.75	0.02	0.22	1.24	0.16	2.19	-25.18	10.17	11/8/2011
633	8598	Spiggie2011_1: 10-11	14.85	0.04	0.38	4.58	0.45	5.59	-25.78	14.70	11/8/2011
634	8599	Spiggie2011_1: 11-12	19.62	0.06	0.82	3.71	0.82	13.52	-26.23	16.55	11/8/2011
635	8600	Spiggie2011_1: 19-20	7.42	0.06	0.34	2.81	0.91	5.62	-26.43	16.40	11/8/2011
636	8601	Spiggie2011_1: 26.5-27.5	12.93	0.02	0.15	2.61	0.23	2.53	-25.95	16.37	11/8/2011
637	8602	Spiggie2011_1: 27.5-28.5	14.35	0.02	0.17	3.18	0.29	3.44	-26.45	20.40	11/8/2011
638	8603	Spiggie2011_1: 28.5-29.5	17.58				0.10	1.53	-25.58		11/8/2011
642	8607	Spiggie2011_1: 36-37	19.35	0.04	0.57	4.79	0.61	9.82	-27.03	17.14	11/8/2011
644	8609	Spiggie2011_2:0-1	15.92	0.32	3.69	6.83	3.91	52.02	-27.84	14.11	11/8/2011
645	8610	Spiggie2011_2:7-8	14.70	0.15	1.63	6.67	2.09	25.67	-27.63	15.75	11/8/2011
646	8611	Spiggie2011_2:13.5-14.5	9.58	0.08	0.55	2.82	1.66	13.29	-28.46	24.17	11/8/2011
647	8612	Spiggie2011_2:14.5-15.5	16.63	0.16	1.90	3.25	2.34	32.55	-27.99	17.14	11/8/2011
651	8613	Spiggie2011_2:16-17	9.49	0.65	4.50	2.71	10.88	86.27	-29.83	19.19	11/8/2011
652	8614	Spiggie2011_2:19-20	6.79	0.38	1.87	2.31	8.30	47.16	-31.36	25.24	11/8/2011
653	8615	Spiggie2011_2:20-21	11.97	0.12	1.00	2.55	1.94	19.41	-27.72	19.37	11/8/2011
654	8616	Spiggie2011_2:27-28	9.88	0.37	2.64	2.35	6.11	50.52	-29.58	19.11	11/8/2011
655	8617	Spiggie2011_2:32-33	7.01	0.15	0.76	2.31	1.88	11.03	-26.86	14.44	11/8/2011
656	8618	Spiggie2011_2:33-34	6.06	0.35	1.53	3.11	4.27	21.62	-25.95	14.11	11/8/2011
657	8619	Spiggie2011_2:40-41	6.15	0.24	1.09	3.73	3.15	16.21	-25.11	14.88	11/8/2011
658	8620	Spiggie2011_2:49-50	7.32	0.22	1.18	2.66	3.13	19.17	-26.31	16.27	11/8/2011
659	8621	Spiggie2011_2:50-51	9.62	0.22	1.52	3.77	3.80	30.58	-26.53	20.16	11/8/2011
660	8622	Spiggie2011_2:67-68	9.96	0.46	3.31	2.56	7.36	61.27	-27.31	18.53	11/8/2011
661	8623	Spiggie2011_2:80-81	6.50	0.83	3.90	2.13	15.74	85.58	-27.43	21.96	11/8/2011

		Sample	Mass		umoles			umoles		C/N	
Analysis	Sample ID	Type	(mg)	% N	N	d15N (3pts	%C	C	d13C	(Molar)	Date Run
719	8624	Spiggie2011_3: 0.5-1.5	1.632	1.482724	1.727662	5.991651	15.24704	20.70202	-23.92986	11.98268	11/9/2011
663	8625	Spiggie2011_3: 6-7	8.07	0.92	5.38	5.90	13.41	90.49	-28.00	16.82	11/8/2011
664	8626	Spiggie2011_3: 11-12	8.18	0.85	5.06	4.78	11.97	81.89	-26.89	16.20	11/8/2011
665	8627	Spiggie2011_3: 12-13	6.05	0.75	3.28	4.15	10.31	52.14	-26.78	15.92	11/8/2011
666	8628	Spiggie2011_3: 17-18	5.92	0.87	3.71	4.17	12.06	59.66	-27.85	16.06	11/8/2011
667	8629	Spiggie2011_3: 25.5-26.5	5.96	0.18	0.78	3.68	2.51	12.52	-27.69	15.98	11/8/2011
668	8630	Spiggie2011_3: 26.5-27.5	9.99	0.05	0.35	3.48	0.58	4.85	-25.56	13.74	11/8/2011
715	8631	Spiggie2011_3: 35-36	19.741	0.082601	1.16422	2.755392	1.923593	31.59292	-25.28075	27.13655	11/9/2011
716	8632	Spiggie2011_3: 40-41	23.905	0.013917	0.237529	1.933406	0.167532	3.331835	-60.89571	14.0271	11/9/2011
717	8633	Spiggie2011_3: 41-42	25.448	0.026152	0.475157	2.403538	0.293246	6.208798	-23.90039	13.06683	11/9/2011
421	8634	Spiggie2011_3:43-44	17.436	0.214824	3.344668	3.62238	4.824916	69.66755	-28.45948	20.82944	10/26/2011
422	8635	Spiggie2011_3:45-46	12.539	0.092154	1.550322	3.898788	2.438533	26.23841	-28.29616	16.92449	10/26/2011
423	8636	Spiggie2011_3:46-47	17.864	0.062924	1.528497	3.479552	1.948201	29.66561	-28.33569	19.40836	10/26/2011
424	8637	Spiggie2011_3:56-57	12.473	-0.022554	0.554936	1.887896	0.574512	7.252734	-27.72818	13.06949	10/26/2011
425	8638	Spiggie2011_3:61-62	18.885	-0.028878	0.371964	2.461262	0.119514	3.271421	-26.91574	8.794985	10/26/2011